

TECHNO-ECONOMIC ASSESSMENT STUDY FOR ROGUN HYDROELECTRIC CONSTRUCTION PROJECT

PHASE II: PROJECT DEFINITION OPTIONS

Volume 3: Engineering and Design

Chapter 3: Alternatives design

Appendix 4 - Hydraulics of the Project Components

August 2014

Report No. P.002378 RP 47 rev. D

| | | | | | |
|-----------------|-------------|--------------------------------|----------------|----------------|-----------------|
| D | 07/08/2014 | Final Comments of GoT, WB, POE | Various | LCO | LCO |
| C | 31/03/2014 | Final | Various | LCO | NSA |
| B | 13 Nov 2013 | Comments of WB and POE | Various | PAR/LCO | LCO |
| A | 13 Jun 2013 | Draft | Various | PAR/ALA/LCO | LCO |
| Revision | Date | Subject of revision | Drafted | Checked | Approved |

CONTENTS

| | | |
|----------|--|-----------|
| 1 | INTRODUCTION | 1 |
| 1.1 | General Concepts Adopted for the Hydraulic Facilities Design | 1 |
| 1.1.1 | Diversion Tunnel N°3..... | 1 |
| 1.1.2 | Middle Level Outlet 1 | 4 |
| 1.1.3 | Middle Level Outlet 2 | 10 |
| 1.1.4 | High Level Tunnel Spillways | 11 |
| 1.1.5 | Provisions for Sediment Management | 13 |
| 1.1.6 | Surface Spillway | 21 |
| 2 | DIVERSION TUNNEL N 3 | 22 |
| 2.1 | Overview of the DT3 | 22 |
| 2.2 | Main Features and Hydraulics of the Diversion Tunnel | 24 |
| 2.3 | Operation modes and methodological approaches for the diversion tunnel | 26 |
| 2.3.1 | Pressure flow..... | 26 |
| 2.3.2 | Basic assumptions..... | 28 |
| 2.3.3 | Water surface profiles in steady flow conditions of operation | 29 |
| 2.3.4 | Scour due to impact of the falling jet in the plunge pool | 30 |
| 2.3.5 | Air Demand..... | 34 |
| 2.3.6 | Discharge capacity of the diversion tunnel..... | 37 |
| 2.3.7 | Behavior of the diversion tunnel in free flow condition..... | 38 |
| 2.4 | Flip bucket..... | 41 |
| 2.4.1 | Jet trajectories | 41 |
| 2.4.2 | Plunge Pool | 42 |
| 3 | MIDDLE LEVEL OUTLETS 1 AND 2 | 47 |
| 3.1 | Overview of the middle level outlets 1 and 2 | 47 |
| 3.2 | Main Features and Hydraulics of the Middle Level Outlets | 49 |
| 3.3 | Operation modes and methodological approaches for the Middle Level Outlet 1 and 2 | 52 |
| 3.3.1 | Discharge capacity of the Middle Level Outlet 1 and 2..... | 53 |
| 3.3.2 | Behavior of the middle level outlets in free flow condition | 54 |
| 3.4 | Vortex shaft..... | 55 |
| 3.4.1 | Inlet structure..... | 56 |
| 3.4.2 | Drop Shaft Diameter Theoretical Approach..... | 57 |

| | | |
|------------|---|------------|
| 3.4.3 | Design parameters used for Middle Level Outlet 2..... | 57 |
| 3.4.4 | Hydraulic conditions throughout the drop shaft segment..... | 59 |
| 3.4.5 | Cavitation induced by rotational flow..... | 60 |
| 3.5 | Flip bucket..... | 61 |
| 3.5.1 | Jet trajectories | 61 |
| 3.5.2 | Plunge Pool | 62 |
| 4 | HIGH LEVEL TUNNEL SPILLWAYS | 66 |
| 4.1 | Overview of the High level tunnel spillways | 66 |
| 4.1.1 | Alternative with FSL Elevation 1290 m a.s.l. | 66 |
| 4.1.2 | Alternative with FSL Elevation 1255 m a.s.l. | 67 |
| 4.1.3 | Alternative with FSL Elevation 1220 m a.s.l. | 68 |
| 4.2 | Main Features and Hydraulics of the High Level Tunnel Spillways | 69 |
| 4.2.1 | Lay-out and geometry for pressure and free flow operation tunnel stretches | 69 |
| 4.2.2 | Discharge capacity of the High Level Spillway Tunnels..... | 72 |
| 4.2.3 | Behavior of the high level tunnel spillways in free flow condition..... | 73 |
| 4.2.4 | Cascade System Verification Approach | 74 |
| 4.2.5 | Hydraulics performance of the cascade system..... | 76 |
| 4.3 | Flip bucket..... | 80 |
| 4.3.1 | Jet trajectories | 80 |
| 4.3.2 | Plunge Pool | 81 |
| 5 | SURFACE SPILLWAY | 86 |
| 5.1 | Design Criteria | 86 |
| 5.2 | Calculations | 87 |
| 5.2.1 | Pre-analysis..... | 87 |
| 5.2.2 | Analysis of the adopted configuration | 90 |
| 5.3 | Resulting Design | 105 |
| 5.4 | Conclusions and Recommendations | 105 |
| 6 | OPERATION OF THE HYDRAULIC FACILITES | 107 |
| 6.1 | Cofferdam..... | 107 |
| 6.2 | Stage 1..... | 108 |
| 6.3 | Dam Construction..... | 108 |
| 6.3.1 | Step A..... | 108 |
| 6.3.2 | Step B..... | 109 |

| | | |
|------------|---------------------------------------|------------|
| 6.3.3 | Step C | 109 |
| 6.4 | Operation Phase | 109 |
| 6.5 | Long-term Operation Phase..... | 110 |
| 7 | PHYSICAL MODELS | 112 |
| 8 | BIBLIOGRAPHY | 115 |

ANNEXES

| | |
|---------|--|
| Annex 1 | Drop Shaft Diameter Theoretical Approach |
| Annex 2 | Spillway Discharge Capacity |
| Annex 3 | Stilling Basins: Design Charts |
| Annex 4 | STEFLOW User's Manual (abstract) |

1 INTRODUCTION

This report deals with the analyses carried out in respect to the hydraulic behavior of the several hydraulic facilities designed for the different alternatives of dam height that are presented for optimization of the Project scheme in the frame of the TEAS.

The hydraulic facilities which are here analyzed are those proposed for the floods management, both during the construction phase and during the plant operation, as well as those envisaged for mitigating the effects of the sedimentation in the reservoir.

The required discharge capacity and elevations of each of them were discussed in Volume 3 - Chapter 3 – Appendix 5 “PMF Management” and in Volume 3 – Chapter 3 – Appendix 3 “Flood Management during Construction”.

According to the above documents, the number and hydraulic characteristics of the discharge facilities were defined for each proposed alternative.

Here in after the general concepts applied in designing the discharge provisions are firstly presented and subsequently the detailed analyses of the hydraulic behavior of the different components relevant to the selected solutions are reported.

1.1 General Concepts Adopted for the Hydraulic Facilities Design

According to the floods management studies carried out, the need for availing of discharge facilities at certain elevations arose as a consequence of the criteria proposed for assuring the safety of the works under construction or in the long term and of the limitations in operating the same facilities.

In fact, according to the construction time and the period during which the works are exposed to the risk of floods, the needed discharge capacities at different elevations have been established in the above mentioned documents.

In addition, the criteria that a discharge tunnel normally would not be operated under a head higher than 120 m and exceptionally up to 150 m, was set. This limitation is mainly linked to the maximum allowed water velocity in correspondence with the gates section and inside the tunnels, which was set following the agreed design criteria.

Also the aspects related to the sediment management have a considerable impact on the selection of the discharge facilities, leading eventually to propose a surface spillway as the only possibility to provide safety to the dam in the very long term, when the reservoir will be completely silted.

Here below the proposed hydraulic facilities and the general criteria based on which they have been designed are outlined.

1.1.1 Diversion Tunnel N°3

The Diversion Tunnel N°3, named Diversion Tunnel of 3rd Level in HPI Design, is required mainly during the construction of the cofferdam and the dam in Stage 1 configuration.

According to Volume 3 – Chapter 3 – Appendix 3 “Flood Management during Construction”, the tunnel should be ready to operate since the river diversion date, in consideration of the fact that the discharge capacity required to protect the cofferdam cannot be assured by the existing Diversion Tunnels N° 1 and 2 only. The analyses carried out by the TEAS consultant indicated the need for a cofferdam with a crest at 1,050 m a.s.l. Such elevation might be decreased whenever a higher discharge capacity of the existing DT1 and DT2 diversion tunnels, which has been indicated by the designer, would be proved through model studies; the actual construction situation shall be checked anyway.

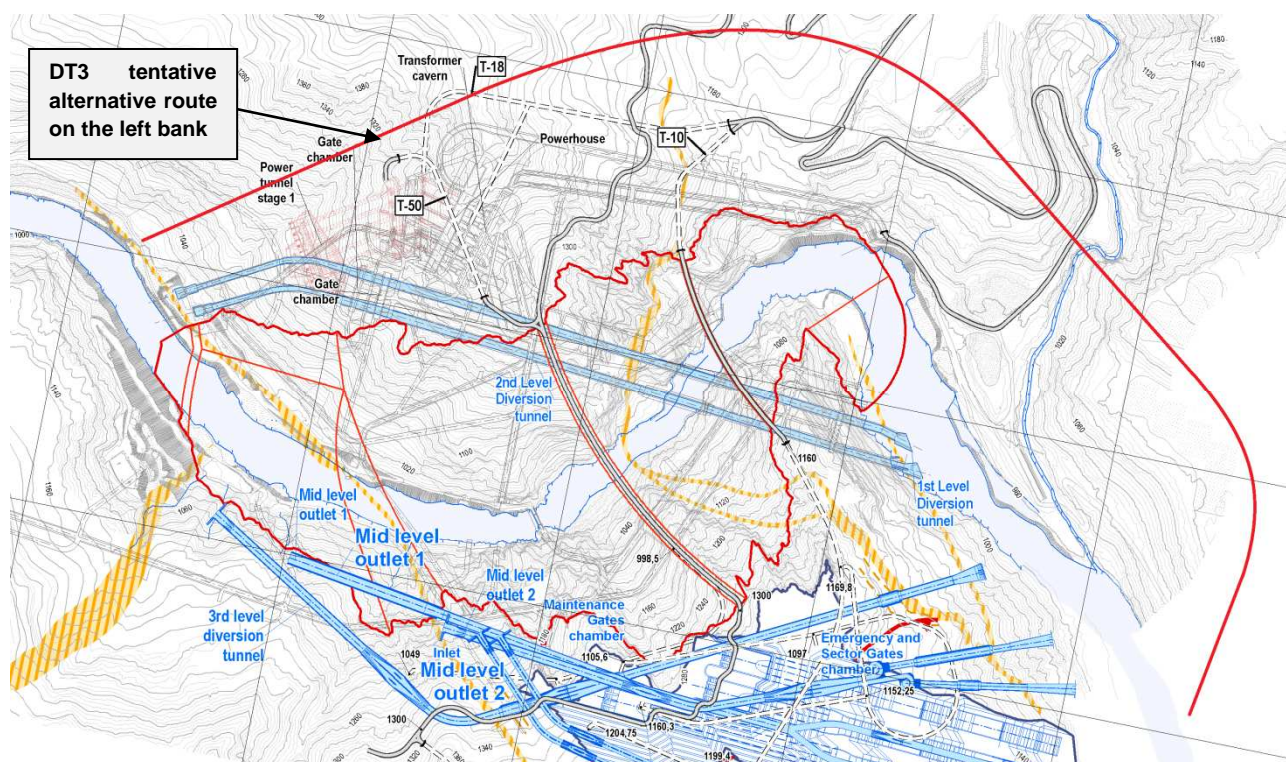
It is ought to recall that DT3 crosses Ionakhsh fault. Despite the fact that in designing the tunnel provisions have been made to mitigate the effect of large displacements in correspondence with the fault, the possibility of having an interruption or serious collapse in that section due to a strong earthquake cannot be disregarded. If this happens, it is assumed that only the Diversion Tunnels N° 1 and 2 will operate.

For considerations about the use of DT3 for protecting Stage 1 configuration dam, reference is made to the above mentioned report.

During the studies, the possibility to find an alternative route in the left bank of Vakhsh River for the diversion tunnel N. 3 was examined, with the aim to avoid the crossing of Ionakhsh fault.

Due to the presence of existing tunnels and facilities, the intake should have been placed upstream from the existing diversion tunnel 1 & 2 inlets, running in south-east direction to avoid interferences with the existing underground structures, then turning to the west so to reach the riverbed downstream from the junction between Obi Shur creek and Vakhsh River.

A tentative route alignment is shown in the sketch here below.



It should be noted that the tunnel outlet cannot be placed upstream from Obi Shur creek due to the presence of the powerhouse access tunnel and to the fact that in the same river reach, on the opposite bank, the outlets of DT1 and DT2 are present. DT3 outlet in this area would highly interfere with the above structures. In particular, for the higher dam alternative the outlet would be very close or within the dam footprint. Further, the morphology and geological conditions are not favorable for the construction of the outlet structure.

In any case, this solution has not been considered for further studies due to the following considerations:

Even if the crossing of Ionakhsh fault is avoided, the tunnel crosses several other faults (including fault 35), which in any case imply to implement adequate measures to face the possible differential displacements.

The tunnel route is passing below Obi Shur creek; riverbed elevation is only about 1030 m a.s.l. in the area where DT3 crosses it. Therefore, either the tunnel would be built with a cut and cover technique, in a highly instable area, or the route should be shifted considerably upstream, incrementing the tunnel length. In any case, this crossing would remain a very delicate point.

Even in the outlined configuration, the alternative tunnel route is about 80 % longer than the route in the right bank, which would imply a considerable increase in costs and in construction time. Any other alternative, as above indicated, would bring to even higher cost and larger construction time.

In consideration of all the above, a solution similar to that proposed by HPI was adopted for this tunnel. Taking also into account the present progress of the works, the diversion tunnel n° 3 upstream stretch was located on the same alignment proposed by HPI and the same intake elevation was adopted, i.e. 1,035 m a.s.l., while the downstream portion has been rerouted, due to the need of space for the remaining hydraulic facilities. The outlet is now placed somewhat downstream from Obi Shur creek training works at junction with Vakhsh River.

The main components are: the water intake, the maintenance/emergency gates chamber and the emergency and sector gates chamber, the pressure stretch of tunnel (up to the latter structure) with circular cross section 15.0 m diameter, the downstream free flow stretch with horseshoe cross section 14.5 m wide and 17.0 m high and the outlet structures. The stretches corresponding to the gates structures (rectangular conduits) and a portion of the transitions (5 m upstream and 10 m downstream) have been considered to be steel lined.

In consideration of the relatively low difference in elevation between the outlet portal (1,023.45) and the riverbed, a diverging chute with terminal flip bucket has been designed for restituting the water downstream from the dam.

The considerations relevant to the energy dissipation and need for plunge pool, as well as the possible scour effects, are contained in the detailed computations which follow.

At present, along the DT3 upstream stretch some 400 m of tunnel excavation works have been already carried out in correspondence with the crown, starting from the inlet portal and from the adit named TT-1. The heading of the tunnel has just reached the beginning of the upstream transition of the proposed maintenance/emergency gates chamber; all other special structures along the tunnel (gates chamber, fault crossing structures) are located more downstream. During

meetings held with the Client, the Consultant was assured that the improvements to the design proposed by him will be implemented while the construction progresses. It is deemed that the status of the works performed so far is such that any change can still be incorporated.

As for the sediments impact, it is recognized that after some years the silted material can start entering into the tunnel and may be cause of important damages. This might happen in just 7/10 years. The tunnel will remain in use until the sediments will reach the intake level or the tunnel will start be seriously damaged and stability will not be assured anymore. After the sediments will have reached the intake level, the tunnel should be put out of service, permanently plugging it in correspondence of the rectangular conduits of the emergency and sector gates.

The fact that starting from the lowest one upward the discharge facilities will progressively become inoperative is acknowledged, being the safety of the dam assured by the highest outlets and spillways.

The range in which the Diversion Tunnel N°3 would be operated is between el. 1035.0 and 1160.0 m a.s.l. for alternative with FSL = 1290 m a.s.l, which would be extended to el. 1170.0 and 1165.0 for alternative with FSL 1255 and 1220 m a.s.l. respectively. All features of Diversion Tunnel N°3 remain unchanged for all dam alternatives.

It is noted that in the upper range of operation DT3 tunnel would work under a gross head somewhat higher than 120 m, by 5, 15 and 10 m for the alternatives FSL 1290, 1255 and 1220 respectively. The above figures correspond to 4, 12.5 and 8.3 % of the head indicated as desirable for the normal operational conditions, being the maximum operation head equal to 135 m, which is below the 150 m accepted for exceptional conditions. It is noted that the tunnel will not operate for long periods under gross heads higher than the reference one; the actual net head at the gates section, due to the headlosses in the pressure stretch, will not be higher than 117 m.

For all the above expressed, it was considered acceptable to slightly exceed the theoretical maximum normal head, avoiding implementing additional discharge facilities.

1.1.2 Middle Level Outlet 1

The middle Level Outlet 1 is required for protecting the dam during its construction starting from water elevation 1,100.0 m a.s.l. This same elevation is considered as the limit of normal operation of Diversion Tunnels N°1 and 2, being the gross head above these tunnel 120 m in this situation. However, they will remain available for the case that an emergency (for instance DT3 out of service due to shearing at Ionakhsh fault section) obliges to make us of them for discharging floods.

Since the intake elevation of the MLO1 is set at 1085.0 m a.s.l., this structure has to be constructed at the same time as the Stage 1 configuration dam, for being used when the embankment is raised above 1,100 m a.s.l.

As far as the tunnel cross sections are concerned, the general features of the MLO1 are the same as those of Diversion Tunnel N°3; however, specific solutions had to be implemented for the intake and for the outlet structures.

In particular, a concrete culvert is foreseen through the dam embankment at intake elevation, so that the tunnel proper is starting shortly downstream from Ionakhsh fault. Such a culvert has an internal cross section D-shaped, 18 m wide and 18 m high, and has been conceived in such a way that possible displacements at Ionakhsh fault section can occur without interrupting the hydraulic route to the tunnel. The culvert is in fact constituted by short stretches with walls thickness of some 3.5 m; this robust structure would accept displacements and relative movements without collapsing, thus maintaining the tunnel operative.

The tunnel level at the outlet is about 1075 m a.s.l., thus there is a considerable difference in elevation with respect to the riverbed and the problem of restituting the flow, in the order of 3,700 m³/s, required proper consideration, to avoid undesirable large scouring effects which might also trigger bank instability.

As a first attempt the possibility to implement a chute with terminal flip bucket was examined. However this solution implied a very high water velocity at the chute end. In fact it has to be considered that the flow at the sector gates section exhibits a velocity in the order of 40 m/s and that along the short downstream stretch of the tunnel until the outlet it remains anyway very high. Therefore the flow would reach the chute top with a high energy, which is further increased in the sloped chute, resulting in a water velocity above 50 m/s in the terminal section. This figure, together with a specific discharge in the order of 105 m³/s/m (corresponding to a flip bucket width of 35 m) implies possible important scouring effects.

In consideration of the fact that the MLO1 is to be used mainly during the construction period, but during normal plant operation will remain closed, and on account of the high specific discharge, a solution with vortex chambers and drop shafts was subsequently analyzed.

In fact, this arrangement allows dissipating a large percentage of energy while keeping the water velocity within the ranges acceptable for hydraulic structures. Obviously the correctness of the predicted hydraulic behavior is to be confirmed through proper investigation on physical model.

The proposed solution differs from the one indicated by HPI since it is constituted by a upper vortex chamber, in which the twirling effect is imparted to the flow, followed by a drop shaft.

This configuration was proposed in view of the fact that the theoretical approach and model investigations are more familiar to the Consultant than the scheme anticipated by HPI; at any rate, for its final design, specific analyses and physical models should be implemented in order to verify the peculiarities of the hydraulic behavior and to optimize the structures both technically and economically.

Due to the large flow involved, the same was split into two streams, which allow bringing the maximum individual discharge of each shaft to about 1,850 m³/s; it shall be noted that splitting into two the total flow allows to discharge it with a lower specific impact and to better control the scouring effects, reducing thus the plunge pool dimensions.

Vortex shafts with the individual capacity above mentioned have been constructed at Tehri Dam Project, located in Uttarhand State in the North of India, located about 1 km from the confluence of the Bhagirathi and Bhilangana rivers.

The spillways system of the mentioned Project includes four vertical shaft spillways and a conventional chute spillway. The 220 m high vertical shaft spillways of Tehri Dam Project have been constructed utilizing the four diversion tunnels. The bottom outlet of the project also joins tangentially one of the vertical shafts at an intermediate level.

The spillways complex has been designed for a flood of 15,540 m³/s. The routed flow through the spillway structures is 13,200 m³/s at the maximum level of the reservoir.

Four diversion tunnels, two on the left bank (T-1 & T-2) and two on the right bank (T-3 & T-4) were constructed for diversion of river Bhagirathi during the construction of the project. After their plugging, these tunnels were used as sub-horizontal discharge tunnels for the shaft spillways system. Each shaft spillway comprises a 12 m dia vertical shaft joining the horizontal tunnel of 12 m dia tangentially, obtaining a swirling effect. The total transformation of the flow from vertical motion to the circular motion results into considerable energy dissipation.

The spillway configuration of the project consists of the following structures:

- Gated chute spillway on right bank designed for a discharge capacity of 5,490 m³/s;
- Two right bank un-gated shaft spillways designed for a global discharge capacity of 3,880 m³/s, having the inlet sill at el. 830.20 and intake structure in the form of morning glory;
- Two left bank gated shaft spillways designed for a discharge capacity of 3,680 m³/s. The intake structure is provided in the form of 10.5 m wide ogee crest having radial gates for regulation of flow, with sill at el. 815.0.
- An Intermediate Level Outlet at El. 700 which is the lowest level outlet for the Tehri reservoir having capacity of 1,080 m³/s at Full Reservoir Level.

To validate the structural design of the shaft spillways laboratory studies were conducted on a large-scale model, measuring the main parameters of the flow, vortex core formation conditions and movement of vortex flow lengthwise the tunnel to the outlet portal.

Source of above information: "Tehri Project Shaft Spillways – Example of an effective solution based on analytical and observational design approaches", Sharma, R.K, Mann, P.P.S & Vishnoi, R.K, Internal design reports of Design Dept. of THDC.

All the above spillway facilities were constructed at the Tehri HEP in 2006. The initial filling of the reservoir was started in October 2005 (after monsoon season) and continued till the end of monsoon season of 2007, when water level in the reservoir was gradually raised to El. 815.0 m.

The maximum discharge through the ILO in the monsoon season attained 600 – 800 m³/s. The Intermediate Level Outlet at El. 700 m was operated continuously for nine months during the Tehri reservoir impounding in year 2005-2006.

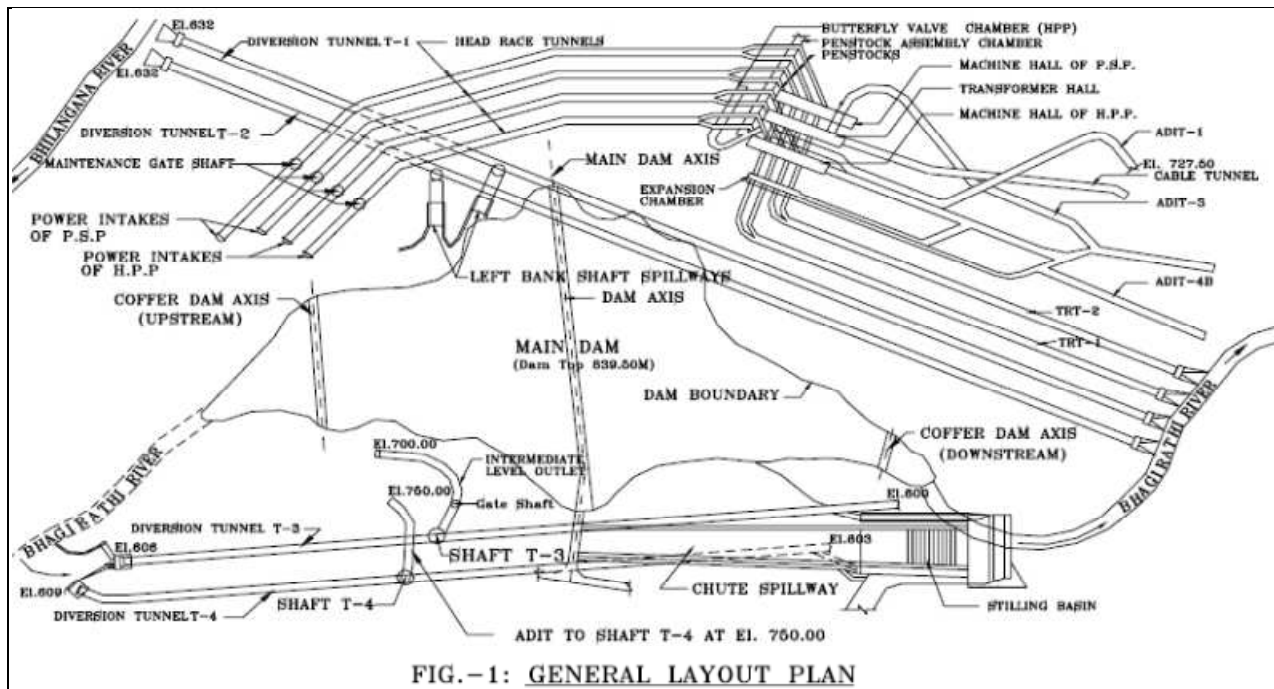
In September 2009 the water level in the reservoir rose to El. 832.0 m; the right-bank shaft spillways automatically started passing a discharge of 480 m³/s through each of them.

On completion of the spillways operation, the inspection of the tunnel surfaces was conducted, which showed satisfactory general conditions and lack of damages on the linings.

After that, the maximum outflow at right bank shaft spillway was 528 m³/s, recorded during flood in 2010.

According to information reported on the ICOLD homepage, heavy floods affected Uttarakhand in India, at the border with Tibet and Nepal, during the last month of June 2013. The water inflow from Bhagirathi and its tributaries reached about 7,000 m³/s. Though it was not possible to get confirmation about the flood actually discharged through the right bank shaft spillways, in consideration of the maximum discharge capacity of the chute spillway, one can infer that they would have discharged about 750 m³/s each.

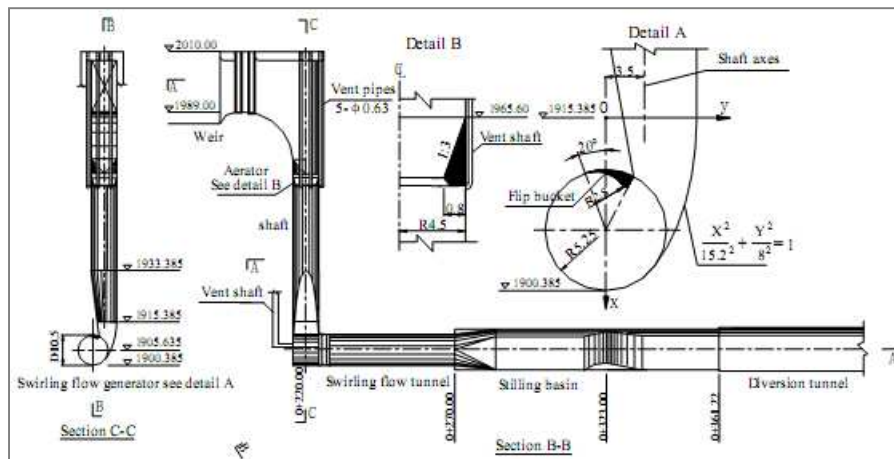
In the following figure a scheme indicating the general arrangement of Tehri project is shown.



Vortex drops shafts are being adopted in a number of projects in view of the advantages obtained in effectively controlling the water velocity and dissipating energy. Several applications can be found in Italy and France as well as other countries, even though in general the flows are not as high as proposed in Rogun project. Jain and Kennedy (1984) [15] reported the application of vortex drop shafts in the Milwaukee Metropolitan Sewerage District. Some of the drop structures carry a discharge of up to 90 m³/s over a drop height of 80 m. Vischer and Hager (1995) [26] reported the vortex drop of Curbans (Italy), 170 m high and 7.30 m in diameter, for a design discharge of 140 m³/s.

A vortex drop was built in china for Shapai Power Station with a drop height of about 110 m and a design discharge of about 250 m³/s (Dong and Gao 1995) [6]. Another vortex drop shaft was also proposed to convey water into an existing diversion tunnel so as to form a tunnel spillway in another power station of China (Zhao et al. 2001) [27].

Gongboxia horizontal vortex shaft spillway tunnel is the second application in China with the working head about 110 m and a discharge capacity up to 1000 m³/s, which was operated in 2006 at the design conditions, see following figure.



Applications of vortex shafts are becoming more and more frequent, and no drawbacks have been reported in respect to their behavior, even if it has to be recognized that so far the existing prototypes apparently have not been working under flows as high as that proposed for Rogun. The Consultant deems that with a proper investigation on model, this solution can be adopted for the Project.

As for the sedimentation problem, the same considerations expressed for DT3 remain valid also for the middle level outlet. It is acknowledged that by adopting the vortex shaft concept the risk of experiencing erosion due to the sediment transported by the flow would increase, due the twirling effect of the flow along the drop shafts and the outlet tunnels. However this risk was considered acceptable when the problem of dissipating the energy at the outlet is analyzed and the possible consequences recognized. As above mentioned, the Consultant considers that the owner of the plant should accept the fact that once the sediments will reach the inlet of the discharge facilities, these structures are to be put out of operation in a short time. For the case of MLO1, a lifespan in the order of 12/15 to 25/30 years can be envisaged, depending upon the FSL alternative. After the sediments will have reached the intake level, the tunnel should be put out of service, permanently plugging it in correspondence of the rectangular conduits of the emergency and sector gates.

The dam safety will not be affected, since the spillways located at upper elevations are in condition to manage the floods during the plant operation period.

In addition to the solution with vortex shafts, other possible alternatives have been analyzed, with the aim to reduce the number of outlets and therefore of the points of impact into the Vakhsh River. In particular, the possibility to make use of the cascade system envisaged at the outlet of the surface spillway, constituted by a sequence of chute and stilling basins, was evaluated.

This was found to be feasible for MLO1, being the elevation at the tunnel outlet some meters higher than the surface spillway bucket. The latter was somewhat modified, providing an additional stretch about 50 m long between the toe of the upstream chute and the final curve. This way the flow discharged by MLO1 can expand from the tunnel 12 m span to the whole canal width, and the specific flow becomes about 56 m³/s/m.

Since the water speed for the design flow of about 1,840 m³/s is substantially the same occurring when the surface spillway is operating, i.e. around 40 m/s, the hydraulic behavior is compatible

with the analysis carried out for the latter structure, being the impact in the riverbed even more favorable due to the lower specific discharge.

The tunnel pressure stretch, with inner section of 15 m diameter, is branching into two circular tunnels with 10.8 m inner diameter, each provided with an emergency and sector gates chamber, running along the same axes of the surface spillway and connected with two corresponding channels.

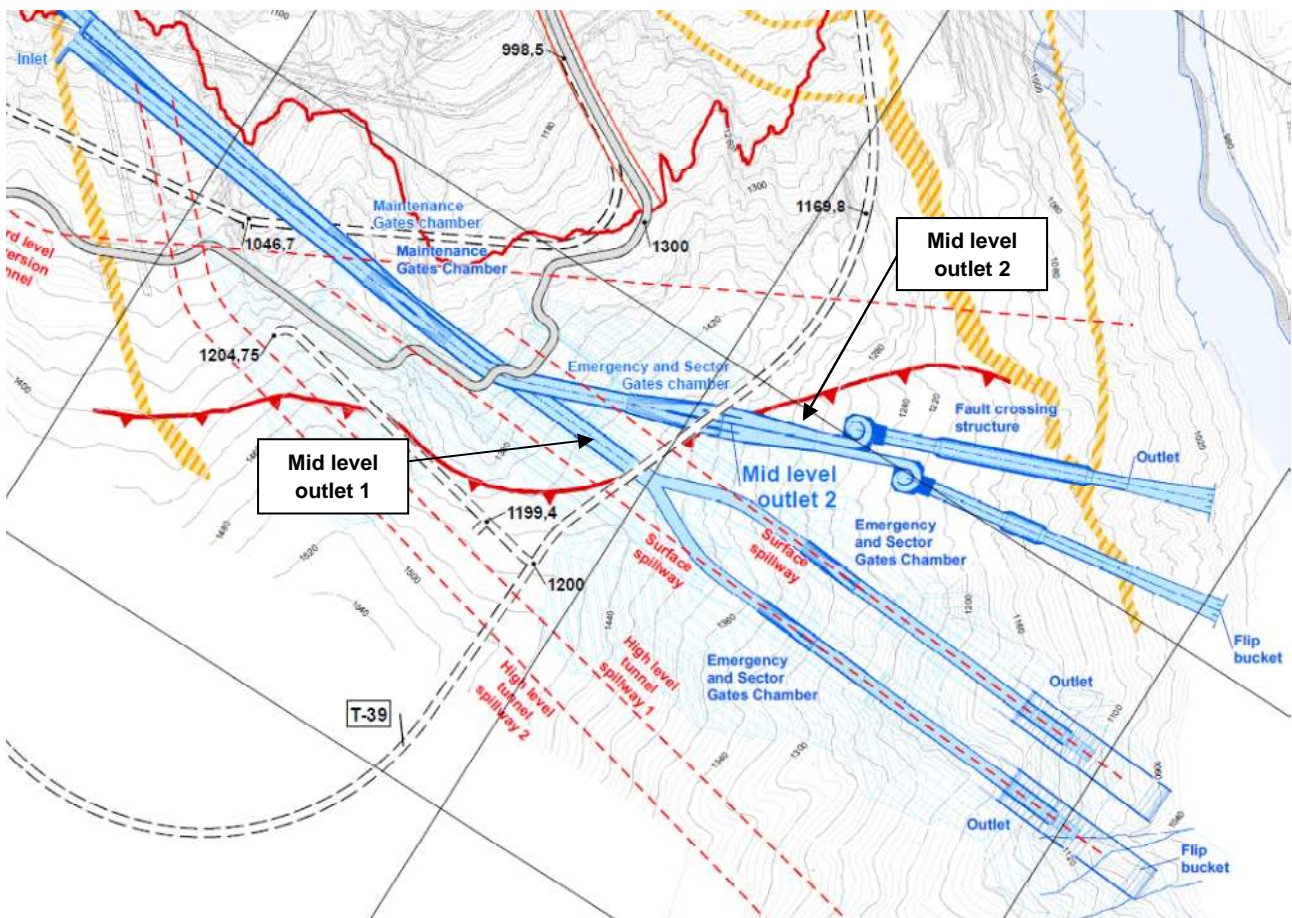
According to Volume 3 – Chapter 3 – Appendix 5 “PMF Management”, in the First Stage configuration of the surface spillway only one channel is envisaged to assure protection against floods for alternatives with FSL 1290 and 1255, whilst two channels are envisaged for alternative with FSL 1220. Thus, for the two highest alternatives it will be necessary to construct at least the last chute and flip bucket of the second channel, which will be incorporated later into the Final Stage of the complete surface spillway.

A layout of the proposed alternative is shown in the following sketch.

This alternative, which became feasible after having identified a suitable solution for the surface spillway, allows reducing the outlets to the river, fulfilling the requests expressed by the various involved parties. In addition, along the new alignments the crossing of the discharge tunnels with Fault 35 and other shearing zones are avoided. Eventually, by eliminating the two outlets of MLO1 corresponding to the previous solution, the distance between the points of jets impacts in the riverbed of the two upstream hydraulic facilities, i.e. between DT3 and the upstream outlet of MLO2, is considerably increased, thus the risk of interferences is strongly reduced.

It is therefore proposed to definitively adopt this alternative for MLO1, which remains valid for all FSL alternatives of the TEAS.

The ranges in which the MLO1 would be operated during construction are between water level 1100.0 and 1215.0 m a.s.l. for alternative with FSL = 1290, between water level 1100.0 and 1210.0 m a.s.l. for alternative with FSL = 1255 and up to maximum dam height for alternative with FSL = 1220. All features of MLO1 remain unchanged for all dam alternatives.



1.1.3 Middle Level Outlet 2

The middle Level Outlet 2 is required for dam protection during the construction of the alternative with FSL = 1290, starting from water elevation 1,160.0 m a.s.l.

The intake elevation of the MLO2 is set at 1,140.0 m a.s.l., which is the same elevation of the large berm envisaged on the upstream shoulder of the dam.

As far as the tunnel cross sections are concerned, the general features of the MLO2 are the same as those of Diversion Tunnel N°3 and MLO1.

Conversely, a common intake with rectangular cross section at the inlet and transition to the circular shape of the tunnel was adopted in this case, being the location selected for the inlet portal away from the dam footprint and downstream from Ionakhsh fault. Therefore no major problems are expected due to seismic events, even though a number of shearing zones and Fault 35 will be crossed in the vicinity of the discharge tunnels outlet portals.

The tunnel outlet level downstream from the sector gates chamber is about 1,132 m a.s.l., thus there is a difference in elevation with respect to the riverbed which is even higher than that of MLO1, therefore the same considerations made for the previous case are still applicable.

In this case the solution with vortex chambers and drop shafts firstly discussed for MLO1 was adopted, following the concept there indicated of splitting the flow into two equal streams.

Also all considerations and criteria expressed in the previous paragraph in respect to this specific solution remain valid.

The possibility to discharge the flow into the surface spillway was also analyzed for this hydraulic facility. This would have implied to split the tunnel into two branches, as for MLO1, bringing one of them to the third surface spillway channel, while the remaining would have needed an additional dedicated cascade discharge. However, being in this case the tunnel outlet elevation about 1,130 m a.s.l., the connection would have been possible only with the lower stilling basin. Taking into account the need for allowing the flow to expand and the conditions required for the hydraulic jump formation, it was found that the space available was insufficient. In the best case in fact, considering an expansion angle of some 12° at each side of the outlet, a minimum length of 135 m and a conjugated depth of 20.5 m would be needed, even accepting to dissipate only partially the energy in the stilling basin as done for the cases of surface spillway and high level tunnels.

Therefore, the solution with vortex shafts was maintained for MLO2.

Whenever this solution was found not convenient, it could be investigated the possibility to implement a solution similar to that of MLO1 but with a total discharge capacity of say 1,900 m³/s, to be divided between the third channel of the surface spillway and a further parallel stepped chute system; assuming that the total discharge need would still be around 3,600 m³/s, a third High Level Tunnel Spillway placed at an elevation of say 1,170 m a.s.l. for providing some additional 1,700 m³/s discharge capacity should be also envisaged. It is noted that this solution would oblige to construct at least partly the third channel of the Surface Spillway since the beginning, plus a similar additional chute for the second branch of MLO2, besides the third HLTS. In this case, the number of outlets will be even higher than that of the proposed solution.

In the case of MLO2, the indicative lifespan with regard to the sediment deposit would be about 50/55 years. This lifespan is evaluated without accounting for the possible beneficial effects of a provision allowing passing the sediments through to turbines; whenever implemented, this may have a significant impact on the lifespan. It is noted that MLO2, which is present only in the alternative with FSL 1290 m a.s.l., shall be maintained operative as long as possible, being required for floods control in the long term during the plant operation. Only once the sediments will prevent its use, it would be plugged in correspondence with the rectangular ducts of the sector gates.

The range in which the MLO2 would be operated during the dam construction is between water levels 1160.0 and 1270.0 m a.s.l.

1.1.4 High Level Tunnel Spillways

These structures have been proposed to evacuate the floods during the last stage of the dam construction and the subsequent operation period.

The basic components of these facilities are substantially the same of all other tunnels, cross section dimensions are the same for all alternatives, but their number has been defined case by case according to the requirements of the mentioned report on floods management. Completely different from those already described is the solution proposed for the controlling the problem of the very high energy at the outlet, which is discussed here in after.

Referring to the single spillway tunnel, the main components are the water intake, the maintenance gates chamber and the emergency and sector gates chamber, the pressure stretch of tunnel (up to the latter structure) with horseshoe cross section 10.0 m diameter and the downstream free flow stretch with D-shaped cross section 10.0 m wide and 12.0 m high, the outlet structures. The stretches corresponding to the gates structures (rectangular conduits) and a portion of the transitions (5 m upstream and 10 m downstream) have been considered to be steel lined.

The elevation and number of high level tunnel spillways for the different alternatives are as follows:

- Alternative with FSL 1290: two HLTS with intake at el. 1190.0 m a.s.l.
- Alternative with FSL 1255: three HLTS, out of which one with intake at el. 1145.0 m a.s.l. and the remaining two with intake at el. 1165.0 m a.s.l.
- Alternative with FSL 1220: one HLTS with intake at el. 1140.0 m a.s.l.

It is noted that the need for one high level tunnel spillway in alternative FSL 1220 arises out from the conclusions of Volume 3 – Chapter 3 – Appendix 5 “PMF Management”, in which it is recommended to adopt 1 HLTS and 2 modules of surface spillway, concurrently with a rise of the dam crest of 1.5 m, in order to protect Rogun. None of the other alternatives analyzed there can provide a reasonable protection to the cascade, being the more efficient for that purpose the option corresponding to a dam crest elevation at 1251 m a.s.l., which was not recommended. Also for the management of floods during construction 1 HLTS only is sufficient.

The noticeable difference of elevation between the tunnels outlets and the riverbed, between 150 and 200 m, and the consideration that the tunnels have to serve for controlling floods on permanent basis during the entire plant operation period, led to study a solution that had to effectively dissipate energy while keeping the hydraulic parameters (water velocity, cavitation index, specific flow) as close as possible to the ranges commonly accepted for long term structures.

It is therefore proposed a system combining in a cascade elements such as chutes, ogee crests and stilling basins, which according to the performed computations allows fulfilling the above requirements.

In general, at the tunnels outlets a chute with slope close to 45° is foreseen, widening progressively from 10.0 to 30.0 m, connected to a stilling basin with the same width, some 65 m long. A terminal sill 9.5 m high allows keeping the hydraulic jump inside the basin, dissipating the larger portion of the energy before the flow is spilled to the next chute. A further chute and stilling basin are then provided, being the cascade system concluded with the third and final chute with terminal flip bucket.

The above described sequence has been adopted for all HLTS proposed, just adapting to the morphological conditions and difference in total elevation the slopes and height of the chutes.

As in the case of other tunnels, the HLTS will remain operative until the sediments will reach their intakes and start damaging the lining and equipment, finally preventing the water discharge.

It is to be noted however that the HLTS intakes of each alternative are placed higher than the power intakes of the corresponding generating waterways.

The situation of intakes elevation is shown in the following table.

| | Alternative FSL 1290 | Alternative FSL 1255 | Alternative FSL 1220 |
|-------------------------|----------------------|----------------------|----------------------|
| HLTS 1 intake | 1,190 m a.s.l. | 1,145 m a.s.l. | 1,140 m a.s.l. |
| HLTS 2 intake | 1,190 m a.s.l. | 1,165 m a.s.l. | - |
| HLTS 3 intake | - | 1,165 m a.s.l. | - |
| Intake Units 3, 4 | 1,152 m a.s.l. | 1,130 m a.s.l. | 1,115 m a.s.l. |
| Intake Units 1, 2, 5, 6 | 1,167 m a.s.l. | 1,140 m a.s.l. | 1,115 m a.s.l. |

In consideration of the above, the lifespan of the HLTS would be longer than that of the generating plant of each alternative, in case no provision is made to mitigate the adverse impact of the reservoir siltation. Thus they would be still in operation when the sediments will have reached the power waterways inlets.

Their lifespan would range from 25/30 years for alt. FSL 1220 up to 70/75 years for alt. FSL 1290. Those periods have been estimated without considering the beneficial effects of any sediment flushing facility or other sediment management arrangement.

At this point the HLTSSs will also be put out of service and only the surface spillway, which will have to be implemented with its full discharge capacity, will be used for assuring safety to the dam.

1.1.5 Provisions for Sediment Management

In Volume 2 – Chapter 6 “Sedimentation”, the possible alternatives for mitigating the impact that the huge amount of sediments might have on Rogun plant operation and mainly on its useful lifespan have been examined, including:

- Watershed management
- Upstream check structures
- Reservoir by-pass
- Off-channel storage
- Adequate Operating Rules
- Tactical Dredging
- Reservoir flushing
- Mechanical Removal of Sediments

Most of the possible solutions analyzed have been considered not applicable, or very costly, or not adequate to the situation of Rogun.

During the development of the studies, the Consultant firstly proposed to implement facilities for performing at least the sediment flushing in the areas more sensitive to the problem of the silting, i.e. the area of the permanent power intakes.

Even though this solution did not represent the optimum, it was considered that it could at least provide protection to the equipment and to the power waterways during some time, allowing operating the plant for a longer period.

The flushing provision initially envisaged in the TEAS was constituted by a tunnel in the left bank, located just below the power intakes.

With the aim to cover an area as wide as possible, two intakes at some 50 m distance each other were proposed, located at few tens of meters below the power intakes invert.

The tunnel alignment was envisaged to remain away from the penstock shafts and any other permanent facility, being the only suitable discharge area the right bank of Obi Shur creek, some hundred meters downstream from the mud flow check dam.

The tunnel was provided with a terminal chute and stilling/sedimentation basin, with the aim of reducing the flow energy before discharging into the natural stream, as well as to provoke the deposit of the mud flow. Check cut-off were foreseen along the course of the creek in order to control possible bed erosion.

However, this solution was deemed not properly behaving, due to the fact that it should have worked under high head, say not less than 110 m for the alternative FSL 1290, being the inlet position located at least some 30 m below the power intakes. Some other drawbacks were noted, linked also to the nature of the Obi-Shur creek, which is the only possible point of discharge for a tunnel starting from the power intakes area.

Therefore, the possibility to implement a multi-level intakes arrangement, which would represent a possible solution for mitigating the sedimentation effects with a relatively low cost, was analyzed.

A system constituted by multi-level intakes allows the power waterways operation even after that the reservoir silting has reached their inlets elevation, making use of the openings at higher elevations while excluding those lower than the sediments deposit. They may also allow dragging turbidity currents which move at reservoir lower levels through the turbines, by means of the lower openings. The latter operation is given as an option that should be analyzed more in detail before accepting it, due to possible drawbacks on the electromechanical equipment. For the moment, the system has been designed so as to give the possibility to operate also under these conditions.

Other alternatives, like the operation of the bottom and middle level outlets, create operation and management problems. In the first case, if the bottom outlets (such could be considered the 3rd level diversion tunnel) are operated under heads higher than 150 m, safety problems could arise. Furthermore, possible obstructions due to the solid material in the bottom outlet could create an operation problem with the uncontrolled drawdown of the reservoir. Obviously this operation implies also a loss of water which cannot be used for generation.

On the other side, the position of middle level outlets intakes (such as MLO2) is not compatible with turbidity currents level. In fact the turbidity currents, having a higher density, move at lower

levels in the reservoir, thus a considerable time would elapse before the currents start passing through it. In any case, the problem of losing water which cannot be used for generation remains.

For the above, in case the venting of the turbidity currents would be considered acceptable, the most convenient solution was deemed that to pass them through the power waterways and the turbines, arrangement which avoids the water loss and is suitable to their management.

Other provisions discussed, such as curtain walls, are considered not suitable to be implemented in Rogun HPP, given the project layout.

Due to the general characteristics of the watershed, turbidity currents of cohesive nature with a particle diameter mainly around 20 micron could be expected in the reservoir. These particles, with a sedimentation velocity of 0.03 cm/s, could create an increase of the density of the turbidity currents, resulting in a strong stratification process. If good venting system solutions are adopted, it is possible to reduce the deposition process.

The expected velocities of the turbidity currents are around $0.1 \div 0.3$ m/s, being able to flow for some tens kilometers inside the reservoir. In order to create the venting effect, the withdrawal velocity of the intake structure should be higher than the turbidity currents velocity. Nevertheless, other than the intake withdrawal velocity, the dimensions of the intake mouth are important in improving the withdrawal effect. The final solution must be a compromise between the withdrawal velocity and the intake dimensions. The optimization of this structure at final stage requires an advanced mathematical modeling or/and a physical model.

Multi-level intakes are quite often used in domestic water supply structures, and were also proposed and implemented in mayor plants, such as in New Hope Dam and Glen Canyon Dam. This kind of intakes was reported having been implemented also in some hydro plants in Turkey.

The multiple intakes solution, with withdrawal velocities higher than the turbidity currents velocity, could result to be the adequate solution in the case of Rogun HPP. The multiple intakes are provided with steel elements for closure and an operational protocol is necessary for the optimal management of the turbidity currents. In principle the withdrawal intakes of the venting system should be located as low as possible in the reservoir.

It is to underline that the multi-level intakes, if used for venting the turbidity currents, are intended to drag suspended sediments only, particles would be in the field of clay-silt, ranging from 0 to 50 microns or exceptionally up to 75. Particles with these dimensions are usually considered not dangerous for the erosion / cavitation of turbines. It may be necessary to adopt a closed circuit solution for the units cooling system, avoiding the use of filters that could require frequent cleaning operations due to the presence of sediments in the water.

The multi-level intakes solution proposed for Rogun consists of an inclined concrete culvert, resting on the bank slope in correspondence with the power waterways inlets, provided with openings at various levels, spanning from elevation 1,090 m a.s.l. up to the dam crest elevation. Lower elevations would interfere with the already implemented stabilization works of the Stage 1 temporary power intake. On the other hand, until the units will be operated through the final waterways, it would not be possible to pass the turbidity currents through the turbines, which will occur not before 4-5 years after the river diversion for the first two units. On account of the

expected sediments volume, which was estimated of about 100 million m³ per year, and the fact that the reservoir storage volume at 1,100 m a.s.l. is about 610 Mm³, a considerable portion of the latter will be already filled by that time.

The preliminary design of the intakes considers a concrete culvert some 16.0 m wide and 12.0 m high. Even without considering the space occupied by the central concrete beam 3 m thick, the cross sectional area is 156 m² and the water velocity inside the duct for a 270 m³/s flow is about 1.73 m/s, which provides negligible headlosses. Water velocity through the intakes openings (preliminarily 6.50 m wide by 8.25 m high each, two openings each intake) is in the order of 2.52 m/s; even assuming a coefficient equal to 0.5, the headlosses would be about 0.16 m. Some other headlosses can be calculated in connection with the contractions given by the presence of the various gates, which have been evaluated equal to 0.2 m.

Summarizing, the total additional headlosses could be in the order of 0.40 m, which is a value surely lower than the range of precision that can be obtained when the whole power waterways headlosses are calculated. Model studies, involving the shape of the power inlet proper, which is envisaged to have elliptical contour, can allow improving the hydraulic behavior of the system and reducing the headlosses at a later stage of the studies.

The power waterways inlets proper would be provided with removable trashracks (2 openings 7.5 m wide by 42 m high, maximum water velocity on gross area 0.43 m/s) similar to those already foreseen at the power intakes of the solution proposed by HPI.

Further, the multi-level intakes would be provided with removable trashracks featuring widely spaced bars, the only purpose of which is that to avoid that large floating bodies can enter to the culvert. As above mentioned, the intakes would be provided with steel elements for closure, so to exclude those that will be progressively submerged by the sediments deposit. Those elements are not due to assure watertightness and will be operated under water pressure balanced conditions only. The fixed embedded parts shall be provided with adequate corrosion protection treatments, adopting if necessary corrosion resistant steel. Details will be defined at a later stage of the studies.

This solution allows catching the water from the most convenient elevation, which in principle would be the lowest one, since as mentioned before the turbidity currents normally move at lower reservoir elevation. The management of this kind of structures requires a proper monitoring of the sedimentation, since the closure of the intakes shall be decided before material starts occupying the opening, possibly preventing the operation of closing the steel elements.

It was already noted that by putting culvert intakes at elevations higher than the entrance of the power waterways inlets, it is possible to continue operating the plant even when the sediments are above their level. Thus the useful lifespan of the plant would be extended by several decades.

It is also highlighted that with the multi-level intakes solution the elevation of the power inlets can be lowered, if required, so to start early generation of the plant as soon as the dam construction has reached a sufficient elevation and the head on turbines allows to correctly operate the same.

As for the possible impact on the turbines, unless a very high concentration of sediments would occur, it is deemed that particles lower than 75 micron would not pose risk of cavitation or erosion.

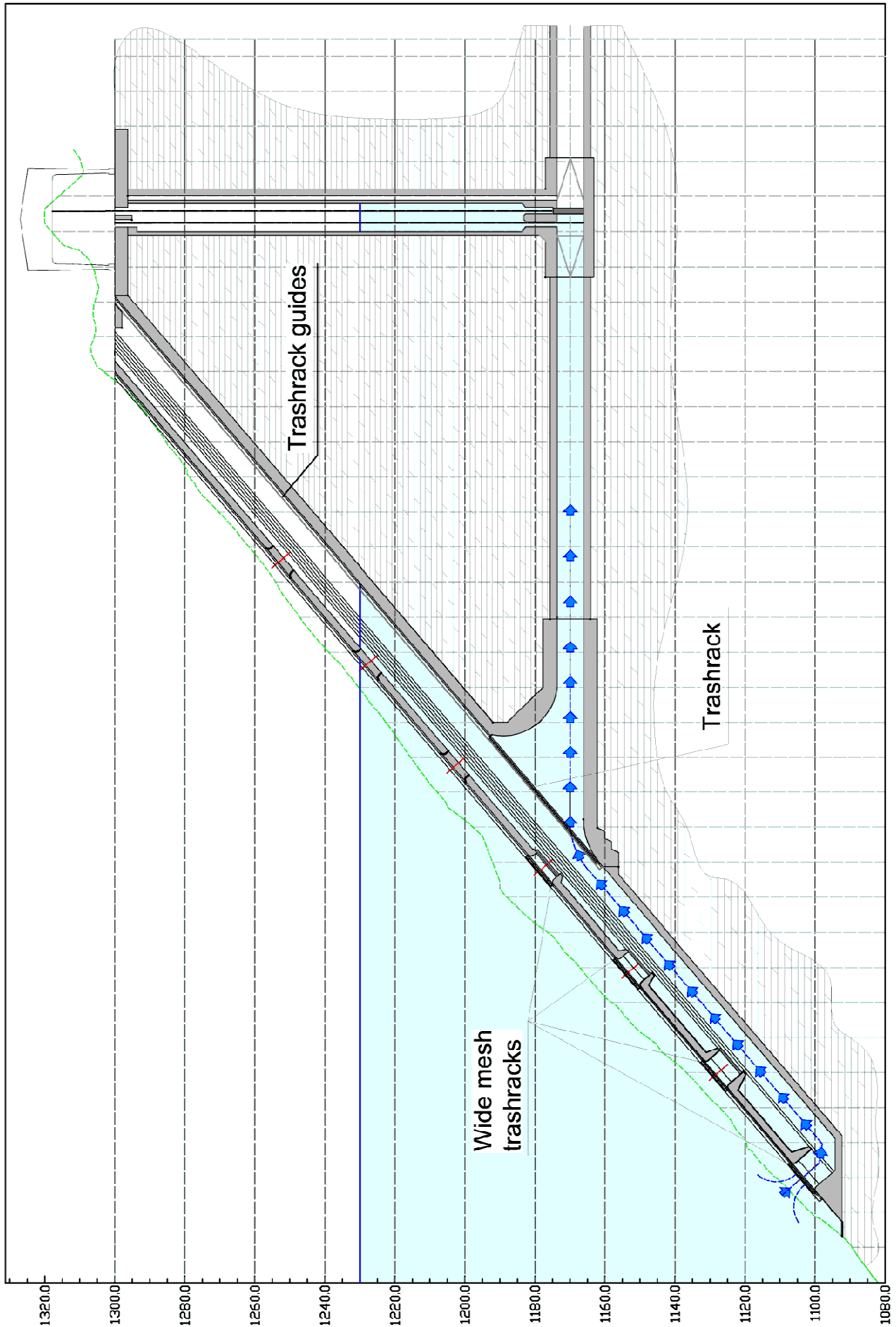
Anyway, in consideration of possible adverse impacts on the electromechanical equipment, it is recommended to analyze more in detail the topic before any final solution is taken in this respect.

In case it would be decided not to operate the multi-level intakes to pass turbidity currents through the turbines, the same can be implemented starting from the power waterways inlets up to the dam crest only.

It should be emphasized that the behavior of turbidity currents can be preliminarily predicted using numerical simulation based on experimental data on prototype. A campaign of observation and measures of sedimentation process and turbidity currents should be undertaken in the following phases of the project, as already conducted in Taiwan (Young and Lin 1991), Japan (Chikita 1989), Canada (Weirich 1984, 1986), Ecuador (Jervez 1985), and United States (Ford and Johnson 1981).

The density current venting and bypassing of high sediment loads through the turbines with a multiple intakes system can be implemented in the project, but an operational protocol for the management of the withdrawal systems must be adopted.

Here below a scheme of the proposed modified intakes is shown.



A schematic sequence of the different situations in which the multi-level intakes would operate is shown in the next figure:

Phase 1: the sediments are still lower than the bottom intake. Under this condition in principle only the lower intake would remain open, so to catch possible turbidity currents circulating at the reservoir lower elevations.

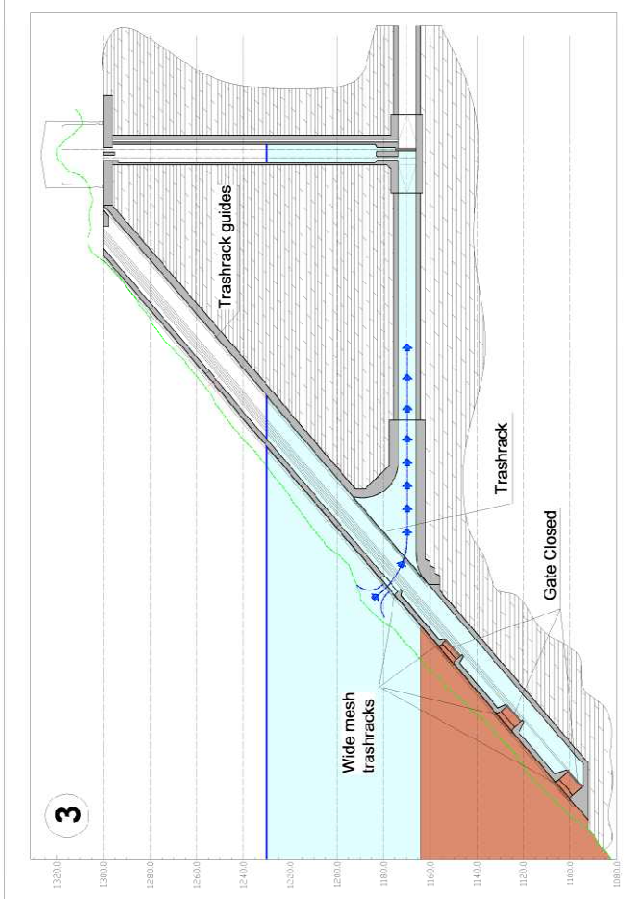
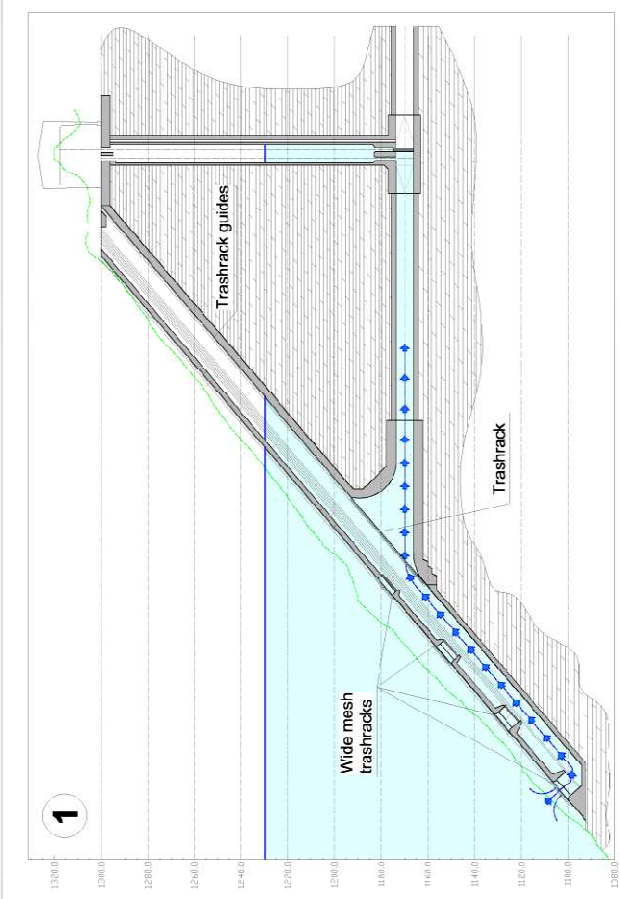
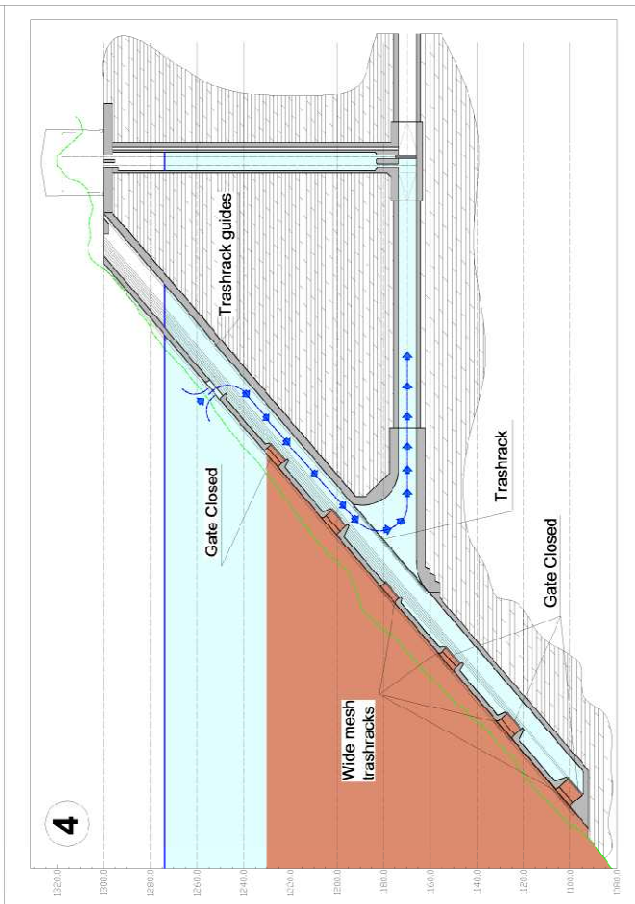
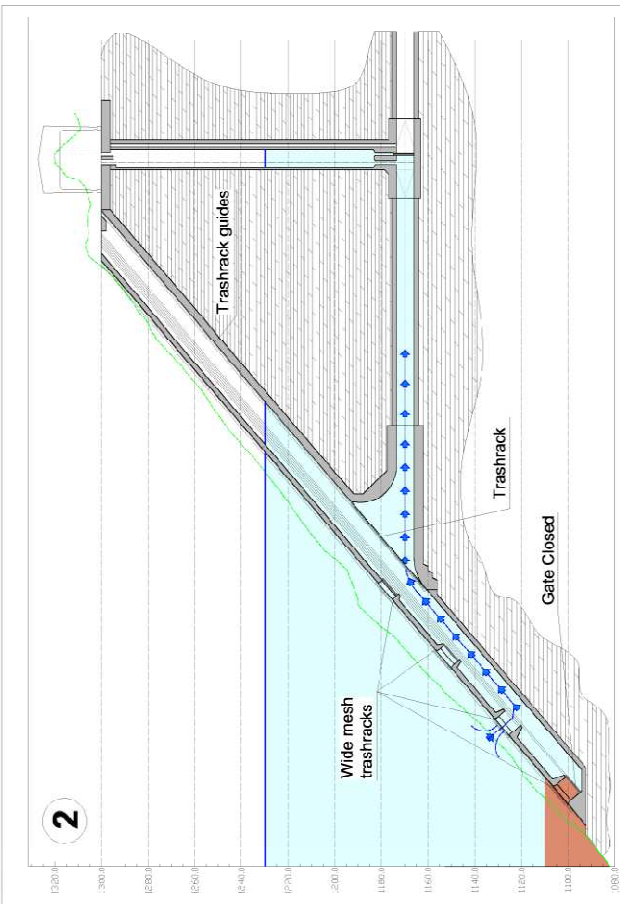
Phase 2: the sediments deposit has reached the lower portion of the culvert and the first intake has been already closed, whilst the next was opened. Similarly to phase 1, possible turbidity currents circulating at the reservoir lower elevations will be passed through the second intake and the power waterways.

Phase 3: the sediment deposit has reached the power waterways inlet elevation, but thanks to the multi-level intake structure, the plant operation can continue through the next higher intake, far enough from the silted material not to withdraw the larger elements but only the suspended particles of turbidity currents. It is noted that with a conventional intake at this point the plant should be already put out of service.

Phase 4: Notwithstanding the fact that the sediments deposit is higher than the power waterways inlet, the plant can continue operating through the higher culvert intakes in a situation in which it should have been already stopped since long.

It is highlighted that the proposed solution not only allows continuing operating the plant even in the above described situation, in which the silt has reached the highest reservoir levels, but can also impact on the useful life of the plant by passing part of the sediments downstream, thus increasing the time by which a certain reservoir elevation is filled by silted material.

It is sufficient to consider the value of the energy generated during one year to fully justify the additional cost of the multi-level intakes, which was evaluated in the order of 90 M\$, with respect to the conventional ones.



1.1.6 Surface Spillway

In the frame of the TEAS, the Consultant in charge must assess the existing design developed by Hydro-Project Institute of Moscow (HPI) and must also develop, at a feasibility level, the design of three alternative dam heights, proposing the most convenient alternative for further development.

HPI's design includes a 335 m high embankment dam with Full Supply Level (FSL) at 1290 m asl and dam crest at elevation 1300. Three organs for flood evacuation during the useful life of the project have been adopted. Two of them are tunnels, both with intakes at elevation 1145. The third one is an overflow structure with sill at El. 1288, connected to a vertical shaft and then to a sub-horizontal exit tunnel.

The Vakhsh River transports sediments with an annual volume estimated in the range of 60 hm³/yr to 100 hm³/yr.

The reservoir capacity at the above mentioned elevations of 1145 m asl and 1288 m asl is 1,500 hm³ and 13,000 hm³, respectively.

Those elevations would be reached in 50yr-80yr and 130-210yr, respectively. More accurate calculations could extend those periods of time, particularly for the lower elevations, because of the way in which depositions happens. But in any case those periods of time are too short (with respect to the useful life of the project) not to consider, since now, the way floods may be evacuated in the future.

HPI argues that in the future other reservoirs will be constructed upstream of Rogun, thus increasing the useful life of the flood evacuating organs.

The design of the evacuating organs in the three dam height alternatives of the TEAS considers intake elevations higher than those of the HPI's design. But in any case, the benefit in terms of useful life is just marginal.

Under these circumstances, the only way of ensuring a safe flood evacuation to protect the dam and the downstream population is introducing a surface spillway. Without such a structure the entire project is to be dismantled in a mid-term future or simply not constructed at all.

The surface spillway, design of which is discussed in the relevant section of the report at hands, at the final stage will be constituted by three modules, each composed by an intake/approach bay, a tunnel and a stepped chute discharging to the river. The complete configuration will be needed in the long term, once the reservoir sedimentation will prevent the discharge of the floods through other hydraulic facilities, in particular the high level tunnel spillways.

As indicated in Volume 3 – Chapter 3 – Appendix 5 “PMF Management”, only one “module” will be required in the initial stage of the project operation for alternatives with FSL 1290 and 1255, whilst two modules are envisaged for the alternative with FSL 1220. This arises out from the conclusions of the mentioned report, and, in the case of the two highest alternatives, is a consequence of the need of keeping the flow discharged from Rogun within values which assure that the safety of Nurek is not impaired.

2 DIVERSION TUNNEL N 3

2.1 Overview of the DT3

According to the results of the studies exposed in Volume 3 – Chapter 3 – Appendix 3 “Flood Management During Construction”, the need for a third level diversion tunnel in order to assure the safety of the works related with the dam construction, as already foreseen in the original HPI design, is confirmed. The aim of the diversion tunnel is to assure flood control and to avoid dam overtopping during the different construction phases, within the operating ranges summarized in paragraph 1.1.1.

The third level diversion tunnel remains the same for all the alternatives under study.

The proposed diversion tunnel consists basically of a pressure tunnel stretch, followed by a free flow tunnel stretch, and an outlet chute with terminal flip bucket.

The intake of the Third Level Diversion Tunnel is at el. 1,035, the pressure operation tunnel stretch, with circular cross-section 15.0 m diameter, is about 810 m long up to the sector and emergency gates chamber. The maintenance gates chamber is located at a distance of about 460 m from the intake. Downstream from the sector and emergency gates chamber, a horseshoe cross-section 14.5 m wide and 9.75 m to the springline with a circular arch roof reaching a maximum height of 17.0 m has been adopted.

The flip bucket is located at the downstream end of the free flow tunnel, at el. 1004.3 m a.s.l.

The layout can be seen in the following figure, for the alternative FSL 1,290 m a.s.l.

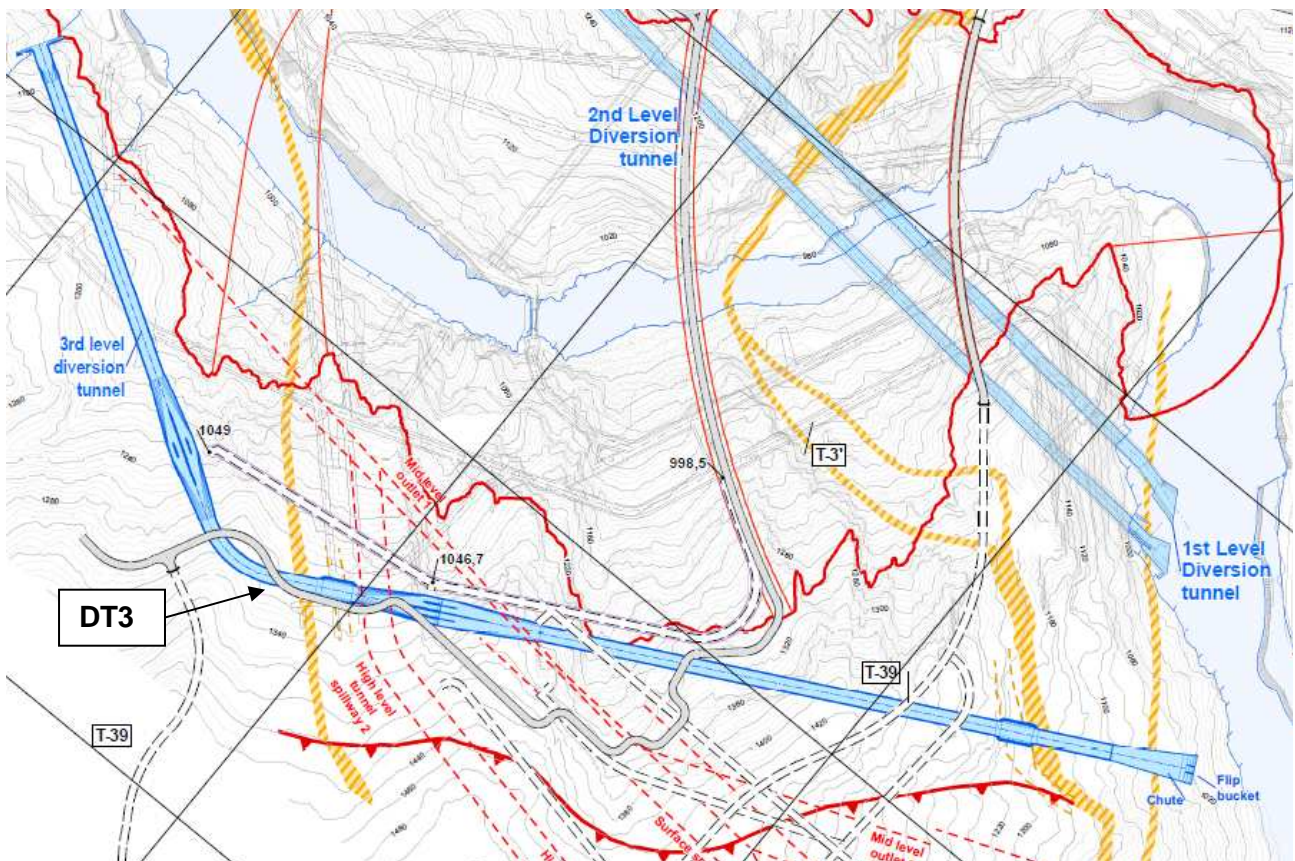


Figure 1. Layout of the third level diversion tunnel

The water discharge reaches 3,694 m³/s with water level in the reservoir at el. 1,185 m a.s.l, for an exceptional head of 150 m. For dam alternatives FSL 1255 and 1220 the maximum exceptional head is always 150 m, therefore the design discharge remains 3,694 m³/s. It is noted that the analyses have been conducted with the above mentioned head, corresponding to the maximum exceptional condition, notwithstanding the fact that, according to the criteria discussed in Volume 3 – Chapter 3 – Appendix 3 “Flood Management during Construction”, the actual maximum operating head would not be higher than 135 m.

In consideration of the fact that the tunnel will operate for a long period during the dam construction, measures were adopted to prevent cavitation and to provide adequate aeration around the control gates.

The diversion tunnel must operate in safe conditions with the discharge associated to the reservoir water level for all the dam alternatives with a maximum head of 150 m. The maximum velocity of the flow in the reach operating under pressure conditions must be in the order of 20 m/s, while the free board in the reach operating in free flow conditions must be at least 25% of the total height of the conduit and the water velocity in principle should not be higher than 20 m/s for the sections without aeration device. These design criteria have been adopted for this tunnel as well as for other hydraulic facilities.

A description of the tunnel features and the assessment of its hydraulic performance is provided in this chapter, explaining the degree of compliance to the design criteria.

2.2 Main Features and Hydraulics of the Diversion Tunnel

The investigation of the hydraulic behavior is focused on the water level 1185.00 m a.s.l.; however the results and criteria will be applicable to different situations of operation. It should be noted that the dimensions of the structures (intake, tunnel, gates, etc.) are the same for all the three dam alternatives, therefore only the situation related with the alternative FSL 1,290 was analyzed.

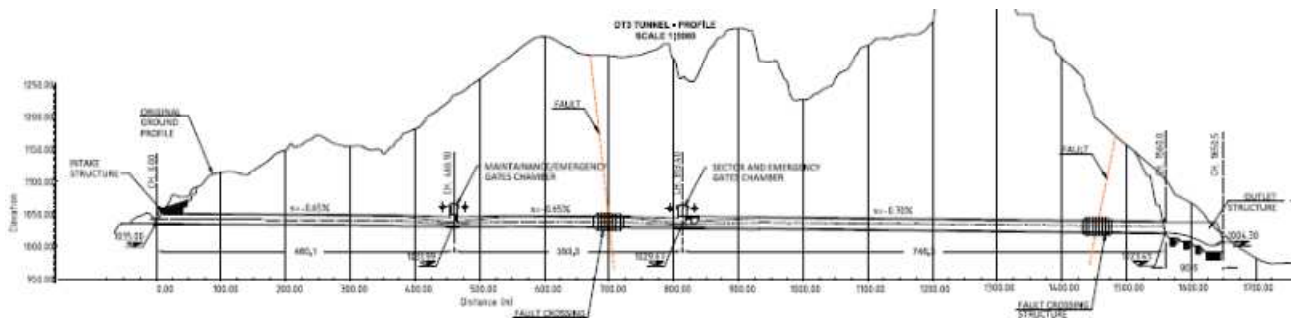


Figure 2. Profile of the diversion tunnel. See also Figure 9 for plan view.

Here below the main features and considerations involved in the design of the diversion tunnel n°3 are reported.

Intake structure.

The entrance to the tunnel has a rectangular cross section 15 m wide and 25 m high. The average velocity at the intake, around its axis, is about 10 m/s.

The maximum shear stress reached in the intake is approximately 2.0 kP. According to the velocity and pressure resulting from the theoretical analysis, conditions of local depression are always possible in the intake fillet between the different sections, due the high velocities and shear stress.

$$\lambda = \frac{P - P_0}{\rho \frac{u_0^2}{2}}$$

λ = degree of cavitation

ρ = absolute static pressure at the point of interest

P_0 = gas pressure (vapor pressure in a two-phase, one-component flow or sum of partial pressure of vapor and other gas in a multi-component system)

ρ = mass density of liquid

u_0 = reference velocity

The depressions decrease in intensity with increasing the length of the intake transition. It is known that for a given intake transition an elliptical contour produces lower depressions than the

circular ones and the depression height decreases with the transition length. However, being the tunnel a temporary structure, even though it has to operate during a relatively long period, the adoption of such a shape, which implies a somewhat higher cost than the circular one, is not a must. Therefore, the definition of the shape to be finally adopted is left to a more advanced phase of the studies, being its impact on the tunnel cost not substantial to the purpose of comparing alternatives.

It is possible to assume that the flow velocity distribution along and around the intake for high water levels is rather uniform. However the velocity gradient could be high and local velocities deviations may take place, being its occurrence closely associated to vortex formation.

Obviously when the intake is completely submerged, during normal exercise operation, the vortex formation on the free surface are unlikely to occur, but during the first filling of the reservoir when the tunnel is operated with low head, stationary waves on the free surface could appear, as the flow upper streamlines hit the intake upper boundary; these waves may contribute to inhibit vortex formation on the free surface, which would impact on the operation of tunnel. The experimental investigation on physical model could define the range of the reservoir level compatible with the operation of the diversion tunnel. In this phase of the design project a circular contour has been assumed for the bell mouth intake.

Tunnel Pressure Stretch.

From the station 00+000 to station 00+813.4 the slope of the tunnel is 0.65% and the tunnel cross section is circular with 15 m diameter. At the end of this reach the tunnel presents a 70 m long transition from circular cross section to a rectangular cross section 26.2 wide and 7.1 m high, where the sector and emergency gates are located. The bottom elevation is 1029.67 m a.s.l.

The total length of the sector gates chamber, including convergent, divergent and prismatic section, is approx. 201 m. Three piers with a nose 3 m thick each are used to split the section into four conduits, where four slide gates, 4.3 m wide and 7.1 m high, and four sector gates, 4.3 m wide and 5.2 m high, are located. The conduits are steel lined along gate chamber. Also steel lined are the adjacent stretches of the transitions (5 m upstream and 10 m downstream). Except for the maneuvers of opening and closure, the gates operate only fully open.

An air ducts system is located in the expansion area downstream from the gates. A 1.2 m aerated negative step was located in order to control the cavitation in the area of the impact of the lower nappe on the tunnel bottom.

The maintenance/emergency gates chamber is located at a distance of some 460 m from the intake of the tunnel. Four slide gates of 4.3 m wide by 7.0 m high are provided, capable to close the tunnel under flow. This solution was adopted in order to allow closure of the tunnel in case the gates at the downstream chamber remain stuck due to material proceeding from a collapse at the crossing of Ionakhsh fault, following the effects of a strong earthquake.

Also in this case steel lining is provided along the gates conduits and the adjacent stretches of transition (5 m upstream and 10 m downstream). Aeration is also provided, since the gates might be operated under flow, as above mentioned. However, the aeration ducts must remain closed to avoid flooding of the above cavern where operation devices are located. Devices which shall

automatically open in case the gates are operated under flow the and downstream pressure decreases to low values have been envisaged.

Immediately upstream from the gates chamber, a special structure for facing possible differential movements at Ionakhsh fault crossing has been provided. Such structure is basically constituted by a sequence of heavy reinforced concrete rings, some 3.5 m thick, with an inner diameter of 19 m, covering the area of the fault crossing. Being the diameter 4 m larger than the tunnel current section, a second concrete lining is provided, some 0.5 m thick, in order to restore the current tunnel section, avoiding disturbance to the flow. The space between the two linings, the external constituted by rings and the internal one, is filled by cellular concrete, which can absorb to some extent differential movements such those deriving from creeping effect, avoiding damaging the inner lining. In case of very large displacements the inner lining can even collapse, but the tunnel cavity will not be lost, thanks to the external structure, elements of which can displace each other without breaking. A detailed structural analysis will be required at a later stage of the studies.

Tunnel Free-flow stretch.

As above mentioned, downstream from the emergency and gates chamber the tunnel converges from a rectangular cross section 26.2 m wide to a horseshoe cross section 14.5 m wide and 9.75 m high to the springline with a circular arch roof, reaching a maximum height of 17.0 m. The tunnel was designed with a slope of 0.7 %.

At the outlet a chute with divergent cross section, between 14.5 and 30 m in width and 90 m long with terminal flip bucket system was provided, discharging into the Vakhsh River.

2.3 Operation modes and methodological approaches for the diversion tunnel

Flow conditions in the diversion tunnel are variable, depending upon the reservoir elevation and the geometrical features. In fact the tunnel may operate under partially free flow, pressure flow and free flow. The following flow conditions may occur in the tunnel.

Partially free flow – when the water level in the reservoir is between el. 1050 and 1060, pulsations may occur in the transition field between free and pressure flow operation.

Pressure flow – from the intake up to gate chamber the tunnel operates only under pressure flow conditions when the water level in the reservoir is higher than el. 1060 approximately. In this case the discharge is controlled by the head losses along the tunnel and through the gates openings.

Free flow – from the gates chamber to the outlet chute the flow is under free-flow conditions and in supercritical regime. In this reach the flow could be mixed (water and air). Formation of plugs of water-air mixture is possible. Therefore proper aeration system is required.

The theoretical concepts and methodological approaches adopted in the design are presented in the following paragraphs 2.3.1 to 2.3.5.

2.3.1 Pressure flow

The discharge capacity of a pressurized tunnel is given by the following equation:

$$Q = \frac{1}{\sqrt{K_L}} \cdot A \cdot \sqrt{2 \cdot g \cdot H}$$

where:

g: acceleration due to gravity [g=9.81 m/s²]

H: the total head to produce discharge [m]

K_L: the cumulative losses of the system [-]

A: outlet area [m²]

Q: discharge [m³/s]

The head of the tunnel is defined as:

$$H = h_e + \sum h_c + \sum h_{ex} + \sum h_f + h_v$$

where:

h_e: entrance losses [m]

∑h_c: contraction losses [m]

∑h_{ex}: expansion losses [m]

∑h_f: friction losses [m]

h_v: exit velocity head losses [m]

The various losses are related as follows:

$$H = k_e \cdot \left(\frac{V_1}{2g}\right)^2 + k_c \cdot \left(\frac{V_2^2}{2g} - \frac{V_1^2}{2g}\right) + k_{ex} \cdot \left(\frac{V_2 - V_3}{2g}\right)^2 + k_c \cdot \left(\frac{V_4^2}{2g} - \frac{V_3^2}{2g}\right) + k_v \cdot \left(\frac{V_4}{2g}\right)^2 + \frac{f \cdot L_1}{4R_h} \cdot \frac{V_1^2}{2g} + \frac{f \cdot L_2}{4R_h} \cdot \frac{V_2^2}{2g} + \frac{f \cdot L_3}{4R_h} \cdot \frac{V_3^2}{2g} + \frac{f \cdot L_4}{4R_h} \cdot \frac{V_4^2}{2g}$$

where:

k_e: entrance losses coefficient [-]

k_c: contraction losses coefficient [-]

k_{ex}: expansion losses coefficient [-]

k_v: exit velocity head coefficient [-]

L: length of the reach of the conduit [m]

$$f: \frac{8g \cdot n^2}{R_h^{1/3}}$$

n: Manning coefficient [s/m^{1/3}]

R_h: hydraulic radius [m]

From the continuity equation:

$$Q = A_1 \cdot V_1 = A_4 \cdot V_4 = A_x \cdot V_x$$

$$(A_4 \cdot V_4)^2 = (A_x \cdot V_x)^2$$

then:

$$\frac{V_x^2}{2g} = \left(\frac{A_4}{A_x} \right)^2 \cdot \frac{V_4^2}{2g}$$

It results:

$$H = \frac{V_4^2}{2g} \cdot K_L \cdot \left[\left(\frac{A_4}{A_x} \right)^2 \cdot k_e, \left(\frac{A_4}{A_x} \right)^2 \cdot k_c, \left(\frac{A_4}{A_x} \right)^2 \cdot k_{ex}, \sum_{i=1}^n \frac{f_i \cdot L_i}{4R_{hi}} \cdot \left(\frac{A_4}{A_i} \right) \right]$$

$$Q = \frac{1}{\sqrt{K_L}} \cdot A_4 \cdot \sqrt{2 \cdot g \cdot H}$$

2.3.2 Basic assumptions

Except for short stretches where steel lining is provided, the tunnel is concrete lined, Manning's coefficient values of 0.012 s/m^{1/3} has been adopted, according to literature [2]. Considerations relevant to Manning's coefficient values corresponding to higher lining roughness are reported in paragraph 2.3.6.

The head loss coefficient at the inlet, expansion and contraction singularities has been evaluated in accordance with USBR [2] and [16] and summarized here under:

$$\Delta h = k_{ex} \cdot \left(\frac{V_2 - V_3}{2g} \right)^2 = \left(\frac{A_3}{A_2} - 1 \right) \frac{V_3^2}{2g}$$

In general, the following coefficients are adopted.

$$k_e = 0.3$$

$$k_c = 0.5$$

$$k_{ex} = 0.5$$

However, according to the characteristics of the singularity, coefficients have been also evaluated making reference to the following publications:

A. Lencastre: Manuel d'Hydraulique Générale

H. King – E. Brater: Handbook of Hydraulics

L. Levin: Formulaire des Conduits Forcées, Oléoducs et Conduits d'Aération

2.3.3 Water surface profiles in steady flow conditions of operation

The water surface profiles in steady flow conditions downstream from the sector gates have been evaluated by implementing a hydraulic model based on the integration of the gradually varied flow equation. The software STEFLO has been adopted for the implementation of the model.

The mathematical model STEFLO - Steady Flow Computation in Rivers - was developed between 1990 and 1992 by the Laboratoire d'Hydraulique de France - CEFRHYG/SOGREAH, Grenoble and Centro di Ricerca Idraulica e Strutturale - ENEL, Milan.

STEFLO is a program for the computation of permanent flow profiles in non-branched river models. The computation of both supercritical and subcritical flow regimes are allowed, and the formation as well as the location of hydraulic jumps are considered. The program can take into account the effects of man-made or natural singularities which affect the flow behavior.

An abstract from the user's manual explaining the methodology is provided in Annex 4.

The main steps followed in order to carry out the hydraulic analysis are:

- modeling the geometry of the channel
- implementing head losses coefficients and boundary conditions
- defining discharges

As above mentioned, the basic computational procedure is based on integration of the gradually flow equation:

$$\frac{dh}{dx} = \frac{\beta \frac{Q^2}{g \cdot A^3} \frac{\partial A}{\partial x} + S_0 - S_f - \left(2 \cdot \beta \cdot \frac{Q}{A} - U_L \right) \cdot \frac{q}{g \cdot A} - \frac{Q^2}{g \cdot A} \frac{\partial \beta}{\partial x}}{1 - Fr^2}$$

h water depth

x longitudinal abscissa

| | |
|---------|---|
| Q | discharge |
| β | momentum correction factor = $\beta(x,h)$ |
| A | wet cross-section area = $A(x,h)$ |
| g | gravity acceleration |
| S_0 | bottom slope = $-dz_f/dx$ |
| z_f | bottom elevation |
| S_f | friction slope |
| Fr | Froude number |
| Q | lateral inflow = dQ/dx |
| U_L | velocity component along x of lateral inflow (neglected by the program) |

The Froude number is defined as:

$$Fr^2 = \frac{\beta \cdot B \cdot Q^2}{g \cdot A^3} - \frac{Q^2}{g \cdot A^2} \cdot \frac{\partial \beta}{\partial h}$$

It is of current use in modeling applications to calculate S_f by a uniform flow formula

$$S_f = Q^2 / K^2$$

where:

$$K = K(h,x) = \text{conveyance}$$

The above equation is an ordinary differential equation of the first order. It is integrated by using either a fourth order Runge-Kutta method or a parabola approximation on successive space intervals Δx .

2.3.4 Scour due to impact of the falling jet in the plunge pool

The estimation of scour due to the impact of the falling jet in the plunge pool will be conducted both by means of empirical formulae and through the theoretical evaluation of plunge pool bottom dynamic pressures approach as proposed by Hartung and Häusler [14].

The empirical formulae are a common tool for hydraulic design criteria because they are easy to apply. Nevertheless, the accuracy of different formulae show substantial differences whether model or prototype results were used for setting the parameters. Furthermore, the difficulty to simulate geomechanical aspects in scale model tests, significantly affects the results yielded by the empirical formulae.

The application to prototype conditions of the theoretical approach presented in [14] to calculate the mean dynamic pressure makes it possible to identify the scour tendencies and to define a confidence interval of scour depth as a function of dynamic pressures.

Empirical equations

Different typologies of empirical formulae are proposed in literature. In some formulae, the scour depth D only depends on the specific discharge q , on head drop H and on empirical exponent coefficients. In other formulae, D is also a function of the river bed granulometric curve (d_{50} and d_{90} for example) and of the water cushion in the plunge pool.

The general form is of the type:

$$D = t + h = kq^x H^y h^w d^z$$

where:

- D: depth of scour measured from tailwater level (m)
- t: depth of scour below un-scoured bed level (m)
- h: tailwater depth above un-scoured bed level (water cushion) (m)
- K: empirical constant
- q: specific discharge (m^2/s)
- H: head drop from reservoir level to tailwater level (m)
- d: mean bed particle size (m)

As above mentioned, different investigations, mostly on physical models, have led to the adoption of sets of values for “k”, “x”, “y”, “w” and “z”. Here reference is made to the most commonly used formulae in international literature.

The limits, coefficients and power factors used in the adopted equations are:

| Author | Applicability [5] | K | x | y | w | z |
|---------------|--|-------|------|-------|------|------|
| Veronese (B) | Horiz. and Plunging jet, $d_m < 0.005$ m | 1,9 | 0,54 | 0,225 | 0 | 0 |
| Damle (A) | Ski jump | 0,652 | 0,5 | 0,5 | 0 | 0 |
| Damle (B) | Ski jump | 0,543 | 0,5 | 0,5 | 0 | 0 |
| Damle (C) | Ski jump | 0,362 | 0,5 | 0,5 | 0 | 0 |
| Martins A | Plunging jet and rock chutes | 1,9 | 0,6 | 0,1 | 0 | 0 |
| Martins B | Ski jump | 1,4 | 0,5 | 0,1 | 0 | 0 |
| Mason | Plunging jet | 3,27 | 0,6 | 0,05 | 0,15 | -0,1 |
| Taraimovich | Ski jump | 0,633 | 0,67 | 0,25 | 0 | 0 |
| INCYTH* | Plunging jet and rock chutes | 1,413 | 0,5 | 0,25 | 0 | 0 |
| Pinto | Plunging jet and rock chutes | 1,2 | 0,54 | 0,225 | 0 | 0 |
| Chee and Kung | Plunging jet | 1,663 | 0,6 | 0,2 | 0 | -0,1 |

*INCYTH, Laboratorio de Hidraulica Aplicada, Ezeiza, Argentina

Table 1 Empirical equations proposed in literature

In fact, the variation field of scour depth induces uncertainty in the application of empirical equations to practical cases. It should be emphasized, for example, that the original Veronese equation provided scour depth values compatible with prototype conditions, in the case of the plunge pool located downstream of the spillway of Itaipu. The prototype measures after that the morphological condition of equilibrium was reached in the plunge pool of Itaipu dam showed that the maximum scour depth of 30 m approximately corresponded to that foreseen by Veronese equation (Electroconsult, 1972).

The same equations, applied to the case of Kariba Dam on the river Zambesi, somewhat underestimated the scour depth. The scour depth under the dam foundation reached 60 m after operation of the spillway. The scour depth mostly depends on the mode of operation of the spillway.

In the case of Karaiba Dam on the river Euphrates, the Veronese formula applied to the prototype conditions overestimated the measured scour depth. A discharge of about 8,000 m³/s after one year of operation of the HPP produced a scour depth lower than was foreseen by Veronese formula (Electroconsult, 1990).

Several studies have used the behavior of a plunging jet to derive the possible extent of scour caused by a free falling jet. In order to validate the scour depth calculated with the empirical formulae, a theoretical approach based upon the dynamic pressure of the underwater jet was used to identify the "pressure bulb" as proposed in [14].

Pressure bulb theory

The mean dynamic pressure is expressed as function of the hydrodynamic pressure variation with the depth:

$$\frac{P}{P_u} = \frac{y_k}{y} \cdot e^{-\frac{\pi}{16} \left(\frac{10x}{y} \right)^2}$$

which yields:

$$x = \sqrt{-0.05 y^2 (\ln P \cdot y - \ln P_u \cdot y_k)}$$

Substituting values of P_u and y_k for each case, and selecting arbitrary values of y and P , the values of x can be calculated along the impact axis, under the free water surface, as shown in the following figures.

P is the hydrodynamic pressure within the "pressure bulb" (t/m²)

P_u is the hydrodynamic pressure at the impact zone (t/m²)

y_k is the core jet length (m)

x, y are the coordinates in the pressure bulb (m)

The method allows calculating and consequently drawing up the "pressure bulbs" produced by the impingement jet and defining the distribution of pressure for different elevations under the impact area.

| | | |
|-------------------|-------------------|---|
| Q | m ³ /s | Discharge |
| Z _{res} | m a.s.l. | Reservoir Water Level or absolute energy in the ski jump |
| Z _{ds} | m a.s.l. | Tailwater |
| H | m | Total Head (Z _{res} - Z _{ds}) |
| Z _{flip} | m a.s.l. | Flip elevation |
| B | m | Chute width |
| q | m ² /s | Specific discharge q = Q/B |
| H ₀ | m | Drop Head between Z _{res} and the jet in the flip bucket (take off), minus head losses in this section / Or the energy in the flip bucket Z _{res} - Z _{flip} |
| H ₁ | m | Drop Head between the flip bucket and the Tailwater level. Z _{flip} - Z _{ds} |
| V ₁ | m/s | Jet velocity at take off |
| dl | m | Water depth at take off dl=q/V1 |
| α | ° | Take off angle |
| V _u | m/s | Theoretical jet velocity at the point of impact in the river $V_u = (2g (H_0 + H_1))^{1/2}$ |
| B _u | m | Width of rectangular impact zone. $2B_u = q/V_u$ |
| y _k | m | Length of jet core. $y_k = B_u / \tan(\alpha_i)$, α_i = internal diffusion angle = 14° as proposed by Ervin and Falvey and reported by Annandale [2]) |
| P _u | t/m ² | Hydrodynamic pressure at the point of impact $P_u = V_u^2 / 2g$ |
| α _u | ° | Angle of impact of the falling jet trajectory calculated as $\left(\frac{dy}{dx} \Big _{x=x_0} \right) \quad y = x \cdot \tan(\alpha) - \frac{x^2}{K [4 \cdot (d + h_v) \cdot \cos^2(\alpha)]}$ |

K = coefficient allowing for the effects of air resistance on the jet trajectory

Table 2 Main parameters used for the application of the mean hydrodynamic pressure method.

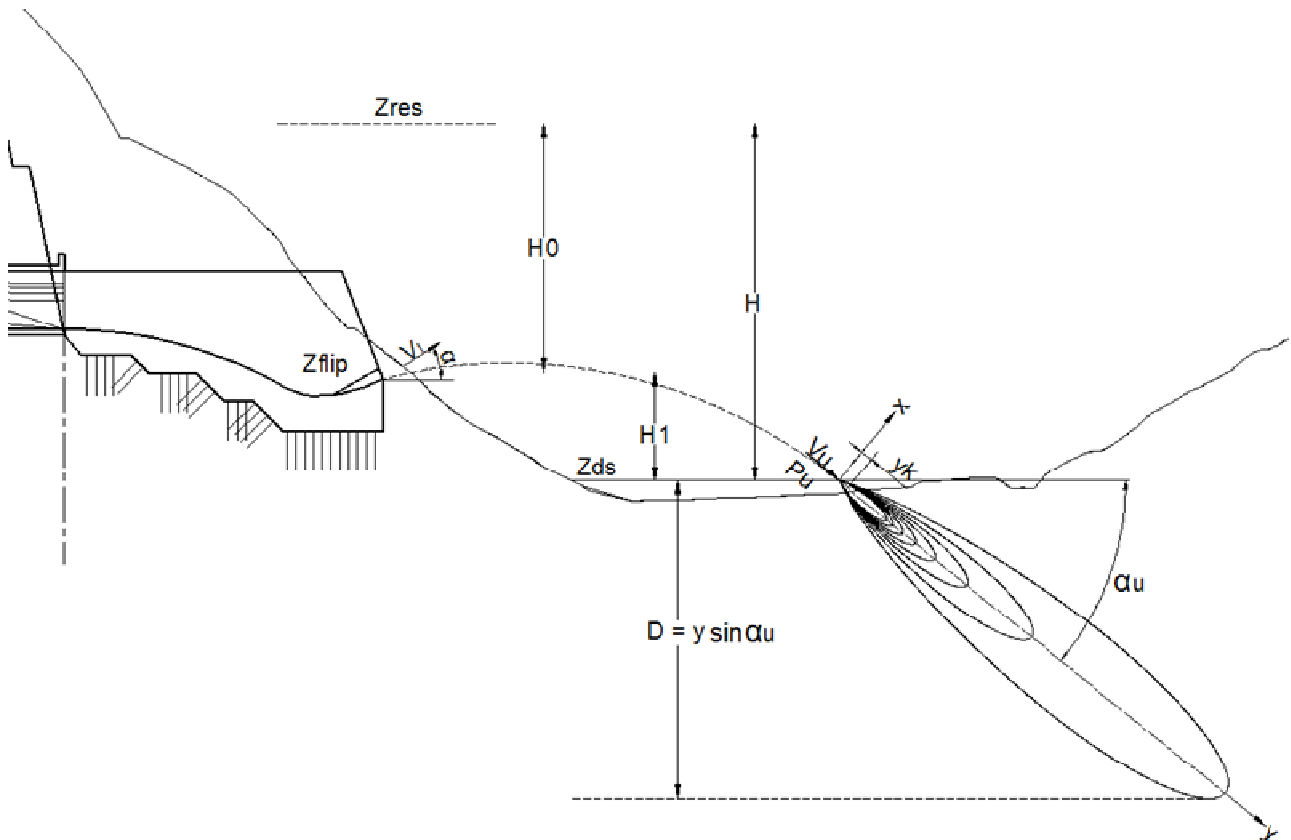


Figure 3 Main parameters used for the application of the mean hydrodynamic pressure method.

2.3.5 Air Demand

The following empirical equations can be found in the literature in order to predict air demand; they were applied in the case of aeration of the tunnel downstream from the gates chamber and at the inlet of the drop shafts.

$$\beta = 0.1 (F_r - 1)^{1.0} \quad (\text{U. S. Army Corp of Engineers "Hydraulic Design Criteria"})$$

$$\beta = 0.024 (F_r - 1)^{1.4} \quad (\text{Wisner Paul - Air demand and pulsatory pressure in bottom outlets})$$

$$\beta = 0.03 (F_r - 1)^{1.06} \quad (\text{A.Ghetti, G. Da Silva: Investigation on the running of deep gated outlets works from reservoir. IX Congress ICOLD, Istanbul, 1967})$$

Where:

$$Fr = V_w / (g h_w)^{0.5}$$

and

$$\beta = Q_{air} / Q_{water}$$

The three above equations are similar because they are based only on the Froude Number at the vena contract "Fr".

Usually the air demand is maximum when the gates are partially open. According to the criteria adopted in this case, the gates will be normally operated only with an opening ratio of 100 per cent. The contraction coefficient depends on the cross section downstream from the gate chamber; therefore the effective depth at vena contract for this case will be 80 per cent of the gate opening (hypothesis compatible with the deflection of the ceiling of the conduit at the gate section).

These criteria were applied in the case of the of the air shaft design for the gates chamber and for spillways aeration in the case of High level tunnel spillways, see paragraph 4.2.5.

Ventilation System Headlosses

The evaluation of the head losses has been carried out based on the classical equations of the fluid dynamics applied to the air inflow through the air ducts from outside atmosphere to the gates aeration ducts.

The energy equation in steady flow condition applied to the air inflow between two different points P1 and P2, assuming that there is no shaft work or heat-transfer effects, is the following:

$$z_1 \rho g + p_1 + \alpha_1 \frac{V_1^2 \rho}{2} - \sum_{i=1}^n \Delta P_{dist,i} - \sum_{j=1}^m \Delta P_{conc,j} = z_2 \rho g + p_2 + \alpha_2 \frac{V_2^2 \rho}{2}$$

Where:

- $\alpha_{1,2}$ = Kinetic energy correction factors
- $V_{1,2}$ = Cross sectional average flow velocity
- $z_{1,2}$ = Elevation
- $p_{1,2}$ = Static pressure
- ρ = Air density
- ΔP_{dist} = Distributed pressure losses (frictional head losses)
- ΔP_{conc} = Concentrated pressure losses (minor head losses)

The formulas adopted for determining the air density and the air kinematic viscosity as a function of the pressure and the temperature are the following:

$$\rho = 1.293 * \frac{p_b}{1.013} * \frac{273}{273 + t}$$

$$p_b = -0.1125 * H + 1011.5$$

$$\nu = \frac{1.53}{\rho} * 10^{-8} * \frac{(273 + t)^{1.5}}{413 + t}$$

Where:

ρ = air density [kg/m³]

t = air temperature [°C]

P_b = barometric pressure [mbar]

$H =$ altitude [m]

$\nu =$ air kinematic viscosity [m^2/s]

The head losses have been calculated with the Darcy Weisbach formulation and a simplification of the Colebrook White relationship has been used for the determination of the friction coefficient.

The Darcy Weisbach formulation applied to air flow can be written as follows:

$$\Delta P_{\text{dist},i} = \frac{L_i * \rho * f * V_i^2}{2 * D_i}$$

The friction coefficient f has been calculated with the simplification of the Colebrook White formulation.

$$f^* = 0.11 * \left(\frac{\varepsilon}{D} + \frac{68}{Re} \right)^{0.25} \quad \text{Simplification of Colebrook White formulation}$$

$$f^* < 0.018 \rightarrow f = 0.085 * f^* + 0.0028$$

$$f^* \geq 0.018 \rightarrow f = f^*$$

or

$$\frac{1}{\sqrt{f}} = -2 * \log \left(\frac{\varepsilon/D}{3.71} + \frac{2.51}{Re * \sqrt{f}} \right) \quad \text{Colebrook White formulation}$$

Where:

$L_{i=}$ Length of the pipe i-stretch [m]

$\rho =$ Air density [kg/m^3]

$V_1^2 =$ Average flow velocity in pipe i- stretch [m^2/s^2]

$D_i =$ Pipe diameter in the pipe i- stretch [m]

$\varepsilon =$ Absolute roughness coefficient [m]

The minor concentrated pressure losses have been calculated as a function of the dynamic pressure in the pipe stretch under examination.

$$\Delta P_{\text{conc},j} = k_j * \frac{\rho * V_j^2}{2}$$

The coefficients K_j depend on the specific type of discontinuity: bends, inlet, outlet, etc... The sum of the frictional pressure losses for each pipe stretch and the minor losses for each discontinuity represents the total pressure losses.

$$\Delta P_{\text{tot}} = \sum_{i=1}^n \Delta P_{\text{dist},i} + \sum_{j=1}^m \Delta P_{\text{conc},j}$$

The calculation of the frictional losses has been carried out also taking into account the following formulation:

$$\Delta P_{\text{dist},i} = \frac{L_i * \rho * V_i^2}{D_i} * \left(0.0036 + 0.305 * \left(\frac{v}{V_i * D_i} \right)^{0.35} \right)$$

that gives in general results less conservative than the more general formulation of fluid dynamics. For this reason the more general formulation of Colebrook White simplified has been taken into account.

2.3.6 Discharge capacity of the diversion tunnel

According to the above mentioned theoretical approach, the maximum discharge with the gates fully open for a reservoir water level of 1,185 m a.s.l., to which an exceptional design head of 150 m corresponds, is 3,694 m³/s.

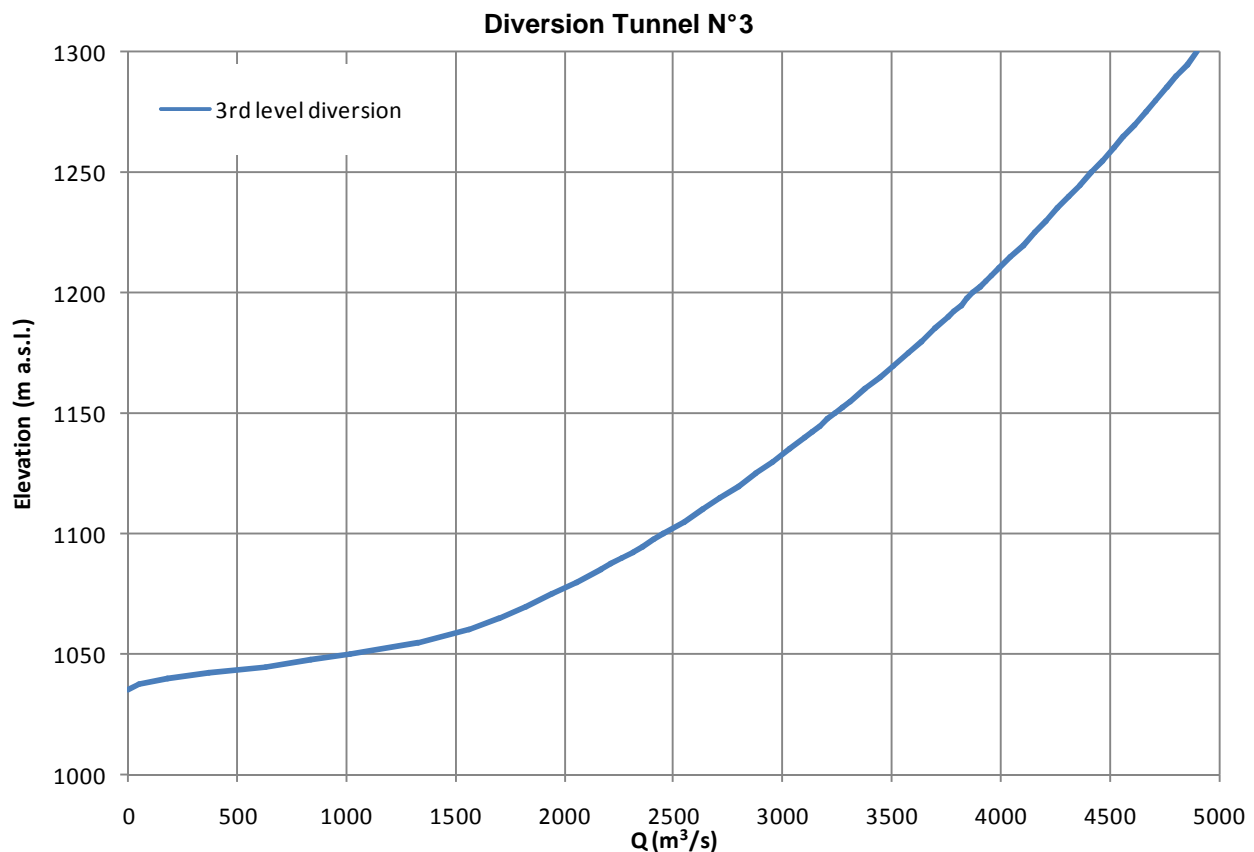


Figure 4 Head – Discharge Relationship. Tunnel under pressure conditions up to gates chamber

The computational approach adopted in order to define the Head – Discharge curve is conservative, in fact the theoretical analysis of the computation of the head losses has not taken into account various factors linked to complex physical phenomena: e.g. the losses of the gate chamber accounting for its actual shape (lower than those assumed) and the pressure reduction (equivalent to an increase in the head H) due to air suction in the downstream tunnel. Therefore it is reasonable to think that in the reality the Head-Discharge relationship will be somewhat greater

than the rating curve of the theoretical analysis. This increases the risk of plugs of water-air mixture formation in the downstream tunnel and higher air demand could be required.

The following considerations can be made in respect to the hydraulic behavior:

Q= 3694 m³/s.

Between the intake and the maintenance gates chamber, the tunnel is operating under pressure conditions with maximum velocity close to 21 m/s for 150 m gross head. At station 3+78 where the contraction towards the gates chamber starts, the area decreases progressively and the velocity increases up to 30 m/s in the conduits upstream of the gates.

The diversion tunnel is concrete lined and the average velocity of approximately 21 m/s is compatible theoretically with the structure and the dimensions of the conduit. In any case, in order to eliminate potential problems of cavitation and pulsations is necessary to avoid abrupt offsets of the bottom and sides of the lining. The specifications of the lining will be defined at detailed design stage.

In the area of the gates, where several changes of section and disturbances such as those due to the gates slots occur concurrently with the higher water velocity, a steel lining has been adopted.

Since after some time the tunnel lining may deteriorate, due to various factors, the impact of a higher roughness on the tunnel discharge capacity was analyzed, by repeating the computations with a Manning factor $n = 0.015$, which is a quite low value for a tunnel of 15 m diameter. In the computation the deterioration of the whole stretch up to the gates chambers was taken into account, except the steel lined portion. The coefficients of other losses which depend upon the tunnel general geometrical features (inlet, expansion, contraction and other singularities) have not been modified.

The results are here below compared with the outputs of the calculation done with $n = 0.012$.

| | | | |
|---|---------------------------|----------|----------|
| Manning friction factor | n (s/m ^{1/3}) | 0.012 | 0.015 |
| Friction headlosses in pressure stretch | h (m) | 7.56 | 13.18 |
| Net head at gates section | H (m) | 129.30 | 124.26 |
| Flow | Q (m ³ /s) | 3,693.91 | 3,621.30 |

The difference in flow discharge is somewhat higher than 70 m³/s, which is lower than the range of uncertainty of the calculation.

2.3.7 Behavior of the diversion tunnel in free flow condition

The main problems that could occur in the reach immediately downstream from the gates, where the flow is evacuated in free flow conditions, are the following:

- shock waves
- air –water mixture plugs
- air entrainment

Shock waves can occur when a high velocity flow is converging. In fact the water speed through the gates opening and immediately downstream is very high and there is a change of cross section between the gates section and the tunnel downstream cross section. Shock waves are characterized by strong differences in water depth for the cross section; their position is steady but they can propagate at long distance downstream, disturbing the flow far away from their origin. On the other hand, unstable water surface could lead to formation of plugs of air-water mixture.

The air mixture plugs occur in the tunnel at high discharges principally when the cross sectional area is too small for the discharge. The shock waves and unstable water surface could lead to the formation of the plugs and hydraulic jumps along the tunnel free-flow stretches.

The mechanism for formation of such a plug can be described as follows: in the upper part of the tunnel the air above the flowing water is circulating in the tunnel, the air near the water surface is carried downstream while the air near the ceiling is strained upstream. If the water surface, due to an instability, rises to the top of the tunnel, it will suddenly be slowed down by the reverse air current. This generates a plug, or a sort of hydraulic jump, which moves downstream like a piston. The normal air demand increases during this phenomena and causes the negative pressure.

Further to the above two phenomena, air entrainment in the flow with very high velocity (in the order of 41 m/s through gates opening) is expected.

Erosion due to cavitation might occur due to strong decrease in pressure downstream from the gates chamber. In order to avoid this risk, at this stage of the design an air ducts system was proposed and steel lining adopted along the gate chamber. The evaluation of air demand due to the carrying capacity can be computed according to the formulas taken from the references, see paragraph 2.3.5. According to those empirical indications, the air demand corresponds to approximately 25% of the water discharge when the velocity at the gates section is 41 m/s and the Froude number is 6.1. The maximum velocity in the ventilation ducts should be around 45 m/s, as proposed in "Air entrainment in free surface flows", IAHR, 1991. In these conditions, four air ducts with a diameter about 2.5 m are needed in order to obtain an air discharge equal to 25% of the water discharge.

The ventilation intakes would be placed in the tunnel roof immediately downstream from the sector gates and are envisaged to be connected with a ventilation gallery with a cross section of 22.5 m² and about 170 m long up the transportation tunnel T-3'. Calculations performed according with the methodology indicated in paragraph 2.3.5 showed that the global headlosses along the ventilation gallery and tunnels are in the order of 3.50 kPa.

Nevertheless, the results of physical model experimentation will be necessary in order to verify the hydraulic behavior and optimize the initial design, so to achieve the better hydraulic performance of the structure. The physical model must be to a scale compatible with the investigated phenomena, in order to have sufficient reliability concerning reproduction of air entrainment problems.

In consideration of all above, the following measures have been implemented:

- transition from the gates section to the tunnel cross section with an angle in the order of 4°;
- cross section area and slope of the downstream tunnel such that the filling rate is lower than 75%;

- an aeration system is foreseen downstream from the gates. An aerated negative step is also provided to control cavitation problems under the nappe. Ventilation can be also provided in correspondence with the step located downstream from the gates, through ventilation pipes developing in the concrete structures and reaching the vertical surface of such step.

The diversion tunnel operates in safe condition with the discharge associated to the reservoir water level for all the dam alternatives.

The head-discharge relationship curve for uniform flow is shown here in after. For the 3,694 m³/s discharge, the free board in the reach operating in free flow conditions would be about 25% of the total height of the tunnel.

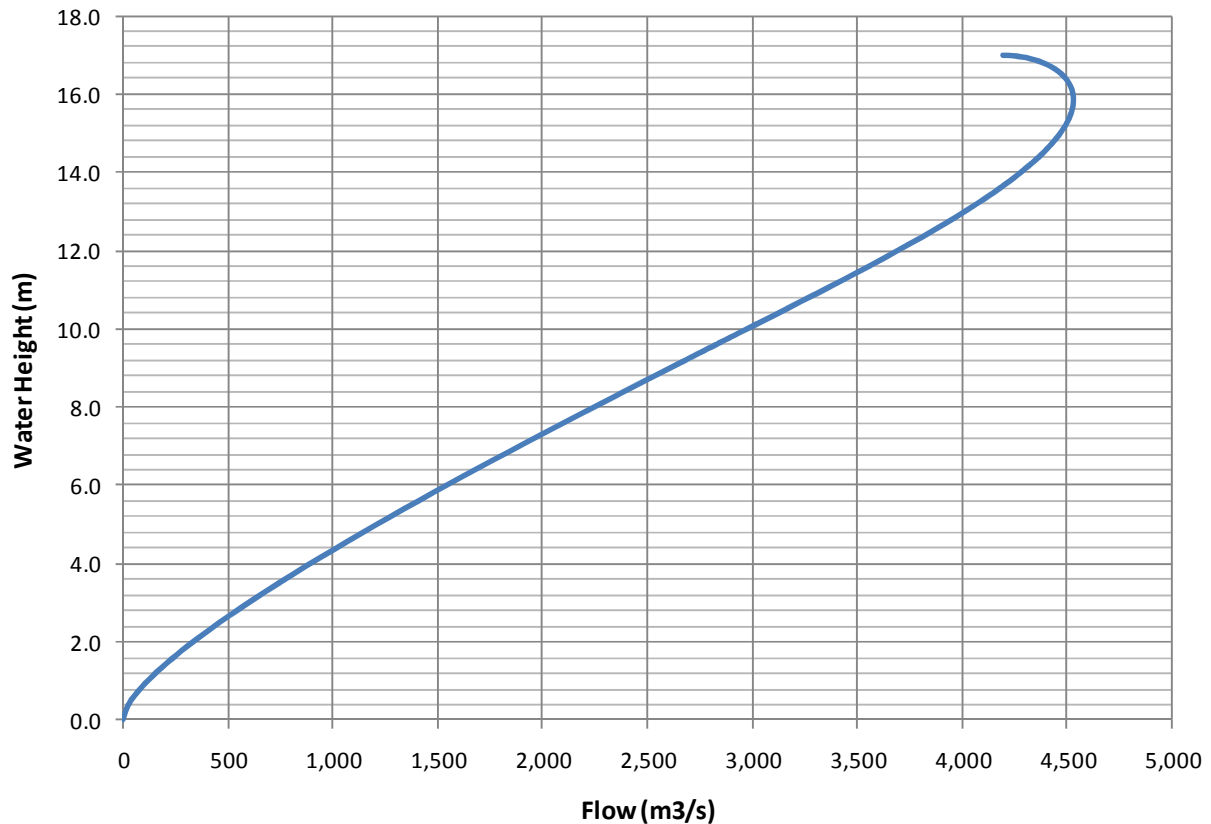
It should be noted that the flow immediately downstream from the gates is supercritical with water velocity values rather high and thus with free board higher than above indicated, then it progressively slow down towards the uniform flow for which the water velocity would be about 21 m/s.

However, given the length of the reach downstream from the gates to the tunnel outlet, the uniform flow condition is not achieved. The consequences of this situation are that from one side the free board is much higher than the theoretical one corresponding to the uniform flow, and that the water speed at the outlet is higher than the 21 m/s above mentioned: this fact has been taken into account for the computation of the chute profile, as well as of the jet trajectory and scour into the plunge pool.

Also in this case the effect of a Manning roughness factor of 0.015 has been analyzed.

With respect to the situation of $n = 0.012$, there is an increase of the water height of about 0.85 m at the end of the tunnel, but the free board remains largely sufficient, being the filling rate more than 50%, while the water speed results lower by about 2.0 m/s.

Diversion Tunnel N. 3 - Free Flow Stretch



2.4 Flip bucket

2.4.1 Jet trajectories

This section analyses the jet trajectories corresponding to the different angles examined: 30°, 25° and 20°.

The profile is calculated by applying the USBR formula [2], [16] that gives the trajectory of the lower nappe of the jet (the origin of the coordinates is taken at the end of the lip):

$$y = x \cdot \tan(\alpha) - \frac{x^2}{K[4 \cdot (d + h_v) \cdot \cos^2(\alpha)]}$$

where:

x = horizontal distance

y = vertical distance

α = angle of the edge of the lip with the horizontal

K = coefficient allowing for the effects of air resistance on the jet trajectory

d = thickness of the jet

$h_v = V_i^2 / (2g)$

g = acceleration due to gravity

The results are summarized in the next table:

| Z_{lip} [m a.s.l.] | Take off angle [°] | Impingement distance form lip [m] | Impingement angle $\left(\frac{dy}{dx}\right)_{X=X_0}$ [°] | Trajectory length $\left(\int_0^{x_0} \sqrt{1 + \left(\frac{dy}{dx}\right)^2} dx\right)$ [m] |
|----------------------|-----------------------|---|---|--|
| 1009.1 | 30 | 167 | 43 | 183 |
| 1009.1 | 25 | 158 | 40 | 171 |
| 1009.1 | 20 | 147 | 37 | 157 |

Table 3 – Summary Results of jet trajectories with different take off angles

The above computation refers to the exceptional discharge of 3,694 m³/s.

In consideration of the trajectory length and the impact area in respect to the outlet location, 20° are selected as take-off angle of flip bucket.

2.4.2 Plunge Pool

In order to identify the scour depth with different empirical formulae, the following values are adopted in the case of DT-3:

- $q = 3,694 \text{ m}^3/\text{s} / 30 \text{ m} = 123.13 \text{ m}^3/\text{s}/\text{m}$,
- $H = 113 \text{ m}$ (corresponding to the energy above the flip bucket)
- $d = 1 \text{ m}$ (average diameter considering rock hydrofracturing by jet impact)

The coefficients and power factors used in the adopted equations and results are:

| Author | D (m) | K | x | y | w | z |
|---------------|-------|-------|------|-------|------|------|
| Veronese (B) | 74.1 | 1.9 | 0.54 | 0.225 | 0 | 0 |
| Veronese mod. | 54.6 | 1.9 | 0.54 | 0.225 | 0 | 0 |
| Damle (A) | 77.0 | 0.652 | 0.5 | 0.5 | 0 | 0 |
| Damle (B) | 64.2 | 0.543 | 0.5 | 0.5 | 0 | 0 |
| Damle (C) | 42.8 | 0.362 | 0.5 | 0.5 | 0 | 0 |
| Martins (A) | 54.8 | 1.9 | 0.6 | 0.1 | 0 | 0 |
| Martins (B) | 43.2 | 1.5 | 0.6 | 0.1 | 0 | 0 |
| Mason | 56.3 | 3.27 | 0.6 | 0.05 | 0.15 | -0.1 |
| Taraimovich | 52.0 | 0.633 | 0.67 | 0.25 | 0 | 0 |
| INCYTH | 51.2 | 1.413 | 0.5 | 0.25 | 0 | 0 |
| Pinto | 46.8 | 1.2 | 0.54 | 0.225 | 0 | 0 |
| Chee and Kung | 76.9 | 1.663 | 0.6 | 0.2 | 0 | -0.1 |

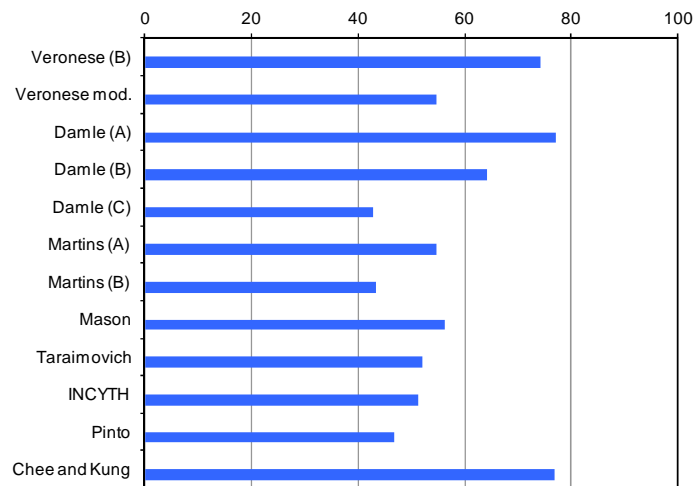


Figure 5 Scour depth (m) calculated by using different empirical formulae.

The field of variation of the scour depth $D = t + h$ obtained by the application of empirical formulae is between 42.8 and 77.0 m, while the average value is 58 m.

In order to verify the scour depth calculated with the empirical formulae, a theoretical approach, as above mentioned, was applied in the case of DT-3. The approach was based on the assessment of hydrodynamic pressure of the underwater jet, described in paragraph 2.3.4.

In this case, two falling jets were studied for 20° take-off angle, with the maximum discharge of 3,694 m³/s and with 1,697 m³/s, corresponding to water levels in the reservoir of 1,185 and 1,065 m a.s.l. The take-off velocities at the lip of flip bucket are 41.1 and 28.7 m/s respectively.

Figure 6 and Figure 7 show the pressure field on a plan where the origin "0.0" is the point of impact of the falling jet on the water surface. X, Y is the coordinate system with respect to the point of impact along the jet axis, as showed in Figure 3 of paragraph 2.3.4. The tailwater is assumed at elevation 980 m a.s.l.

Figure 8 shows the trajectory and the point of impact of the jet for the two design discharges.

The horizontal distance of the point of impact of the jet with respect to the flip bucket is 147 m for the discharge 3,694 m³/s and 84 m for 1,697 m³/s.

Figure 6 shows, for the discharge 3,694 m³/s, the pressure bulb with respect to the point of impact where $P_u = 114.9 \text{ T/m}^2$ (11.5 kg/cm²) with an impingement angle of 37°.

The Figure 7 shows, for the discharge of 1,697 m³/s, the pressure bulb with respect to the point of impact where $P_u = 67.5 \text{ T/m}^2$ (6.7 kg/cm²) with an impingement angle of 46°.

Considering a pressure value of 15 T/m² (1.5 kg/cm²) as an erodibility threshold, we can see from Figure 6 that this value is reached at a distance of 40 m along the axis of the bulb for the 3,694 m³/s case, while for the 1,697 m³/s case this happens at 14 m.

For the maximum discharge 3,694 m³/s, the theoretical scour depth obtained by the pressure bulb corresponds to about 30% less than the mean scour depth obtained by empirical formulae. The theoretical approach does not consider the head loss of the jet along the trajectory.

It is deemed that a pre-excavated pool is necessary in order to mitigate and control the scouring process.

The angle of impact is 37°, the pressure value of 1.5 kg/cm² assumed as design criterion is reached at 40 m along the jet axis (see Figure 6). In this situation, a pre-excavation of about 25 m from the tailwater level down to elevation 955 m a.s.l. could be adopted. A pre-excavation width of about 60 m (twice the take-off width) is assumed for a forecast of the volume of excavation and costing. However, this has to be checked by investigation on a movable bed physical model.

Experimental tests are necessary in order to more exactly define the local scouring at the left bank and the possible further mitigation measures, whenever required. In fact, the scouring process mostly depends on the frequency and instantaneous pressures induced by the falling jet and not on the mean dynamic pressure, calculated by the method proposed by Hartung and Hausler [14].

For the purpose of this study, a pre-excavation of the riverbed down to the elevation above indicated is assumed for controlling the scouring process. It is noted that the jet would impact the riverbed at a distance of some 50 m from the toe of the left bank slope. Therefore, the pre-excavation would also involve the slope of such bank, where a flat platform around elevation 1,100 m a.s.l. is present.

This situation allows carrying out the excavation without endangering the stability of the whole bank. In addition to the riverbed pre-excavation, some 0.4 x 10⁶ cubic meters of slope excavation would be necessary to provide sufficient space for the plunge pool.

It is noted that during the initial period of construction diversion tunnels 1 and 2 will be available, thus DT3 will be basically operated only when the floods will be higher than the DT1 and DT2 aggregate discharge capacity. Therefore the operation of DT3 in this situation will be relatively limited in time and discharged floods would not be very high.

This implies that the eventual scouring progress should be relatively low, allowing evaluating the process and implementing those measures deemed necessary to face more demanding operational conditions.

It is worth noting that model tests are presently being conducted in the Hydraulic Laboratory of Moscow, with the aim of optimizing the DT3 structures that are already under construction, including the outlet works.

Should any solution representing a substantial improvement of the design proposed in the report at hand found, it could be implemented for construction.

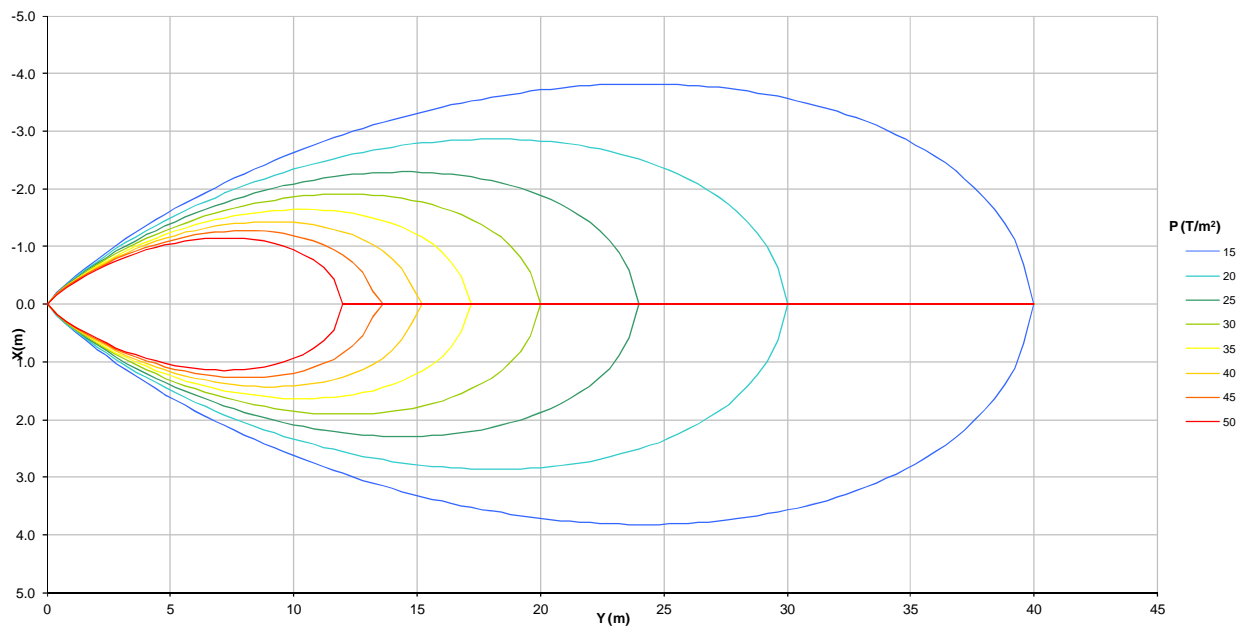


Figure 6 Hydrodynamic pressure bulb: $Q = 3694 \text{ m}^3/\text{s}$. Pressure in the point of impact $P_u(0,0) = 114.9 \text{ T/m}^2$. Angle of impact 37° .

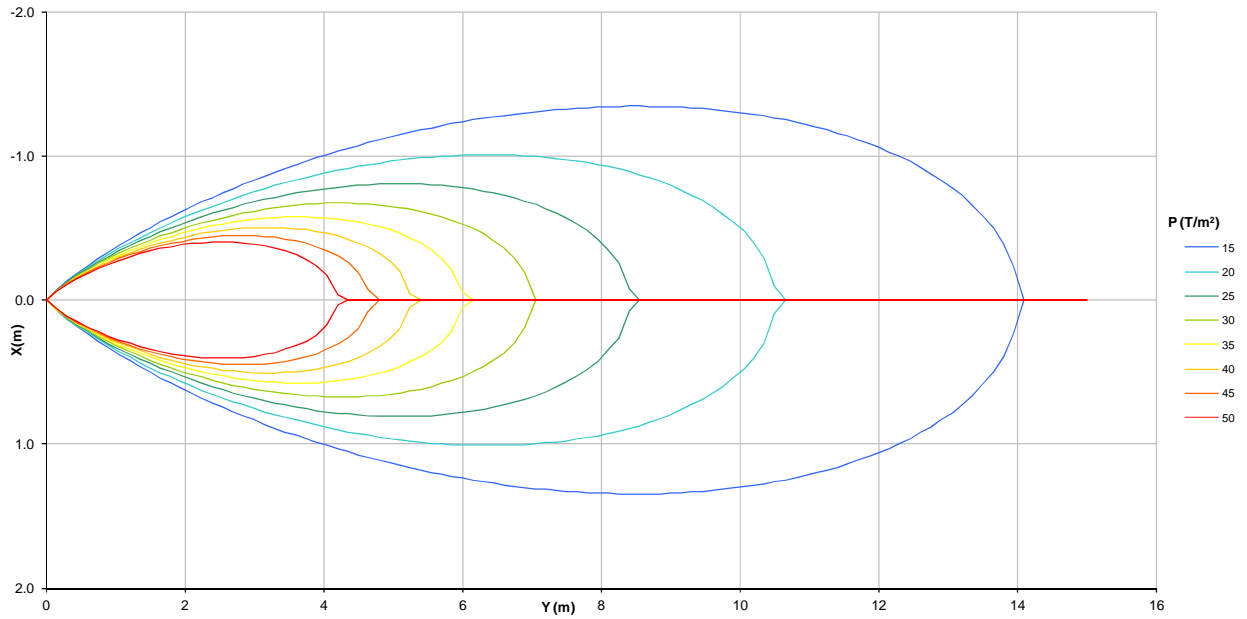


Figure 7 Hydrodynamic pressure bulb: $Q = 1697 \text{ m}^3/\text{s}$. Pressure in the point of impact $P_u(0,0) = 67.5 \text{ T/m}^2$. Angle of impact 46° .

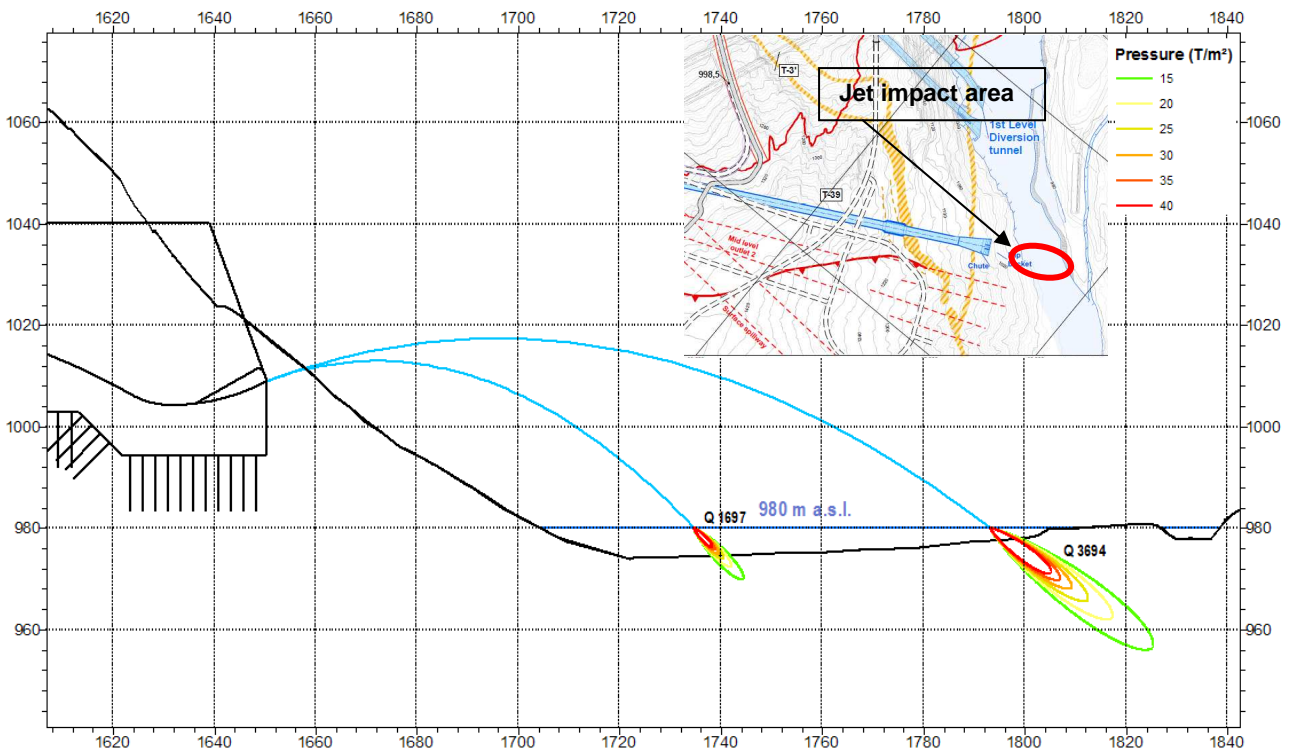


Figure 8 Hydrodynamic pressure bulb and jet trajectory: $Q = 3694$ and $1697 \text{ m}^3/\text{s}$

3 MIDDLE LEVEL OUTLETS 1 AND 2

3.1 Overview of the middle level outlets 1 and 2

According to the results of the studies presented in Volume 3 – Chapter 3 – Appendix 3 “Flood Management During Construction”, two Middle Level Outlets, numbered 1 and 2, are proposed for the alternative with the dam FSL 1290 m. For the other two alternatives, with FSL 1255 and el. 1220, the complex of hydraulic facilities includes the Middle Level Outlet n. 1 only.

Middle Level Outlet n. 1 (MLO1) is composed by a pressure tunnel, which branches into two smaller tunnels at some 1000 m from the intake, each followed by a free flow tunnel stretch discharging into a channel of the surface spillway at the flip bucket level.

The inlet of the MLO1 is set at El. 1,083.5, being constituted by the entrance to a 300 m long culvert, with D-shaped inner cross section of 18.0 m diameter. At the end of the culvert, there is a transition leading to a 15.0 m circular tunnel. The elevation of the tunnel invert in correspondence with its portal is 1085.0 m a.s.l. The cross section of each of the two tunnels after the branch is 10.8 m. The tunnel proper (excluding the culvert stretch) extends for about 880 m up to the sector and emergency gates chamber, measured along one branch. A maintenance gates chamber is located on the 15 m diameter tunnel at a distance of about 365 m from the tunnel portal.

Downstream from each sector and emergency gates chamber of the smaller tunnels, a D-shaped cross-section 12.0 m wide and 6.0 m high to the springline with a circular arch roof, reaching a total height of 12.0 m, has been adopted. The profile of the last reach of the tunnel shows a vertical bend and connects with the flip bucket floor.

Middle Level Outlet n. 2 (MLO2) consists of a pressure tunnel, followed by a free flow tunnel, two vortex shafts, two tailrace tunnels and relevant outlets with flip bucket downstream from each shaft.

The intake of MLO2 is set at El. 1,140.0, and the pressure tunnel exhibits circular cross-section of 15.0 m diameter. The tunnel extends for about 715 m between the intake and the sector and emergency gates chamber. The maintenance gates chamber is located at a distance of about 400 m from the intake. Downstream from the sector and emergency gates chamber, a rectangular cross-section 15.8 m wide and 9.1 m high to the springline with a circular arch roof, reaching a maximum height of 17.0, m has been adopted. The section is divided in two halves by a 1.80 m thick wall, each half flowing into a vortex shaft.

The distance between the chamber and the inlet of the first vortex shaft is approximately 130 m, while the inlet of the second vortex shaft is located at about 185 m downstream from the gates chamber.

The free flow tailrace tunnels, one for each shaft, with circular cross section of 12 m diameter, extend from the bottom of the shafts for about 215 m with a 3% slope down to el. 1026.8. Then a chute with terminal flip bucket is provided at the outlet of each tailrace tunnel, bringing the water down to el. 1000 m a.s.l. Deflector blocks are provided on the buckets in order to obtain a favorable jet trajectory and reduce scouring in the Vakhsh River.

The layout of the two middle level outlets can be seen in the following figure, for the alternative with FSL 1290 m a.s.l.

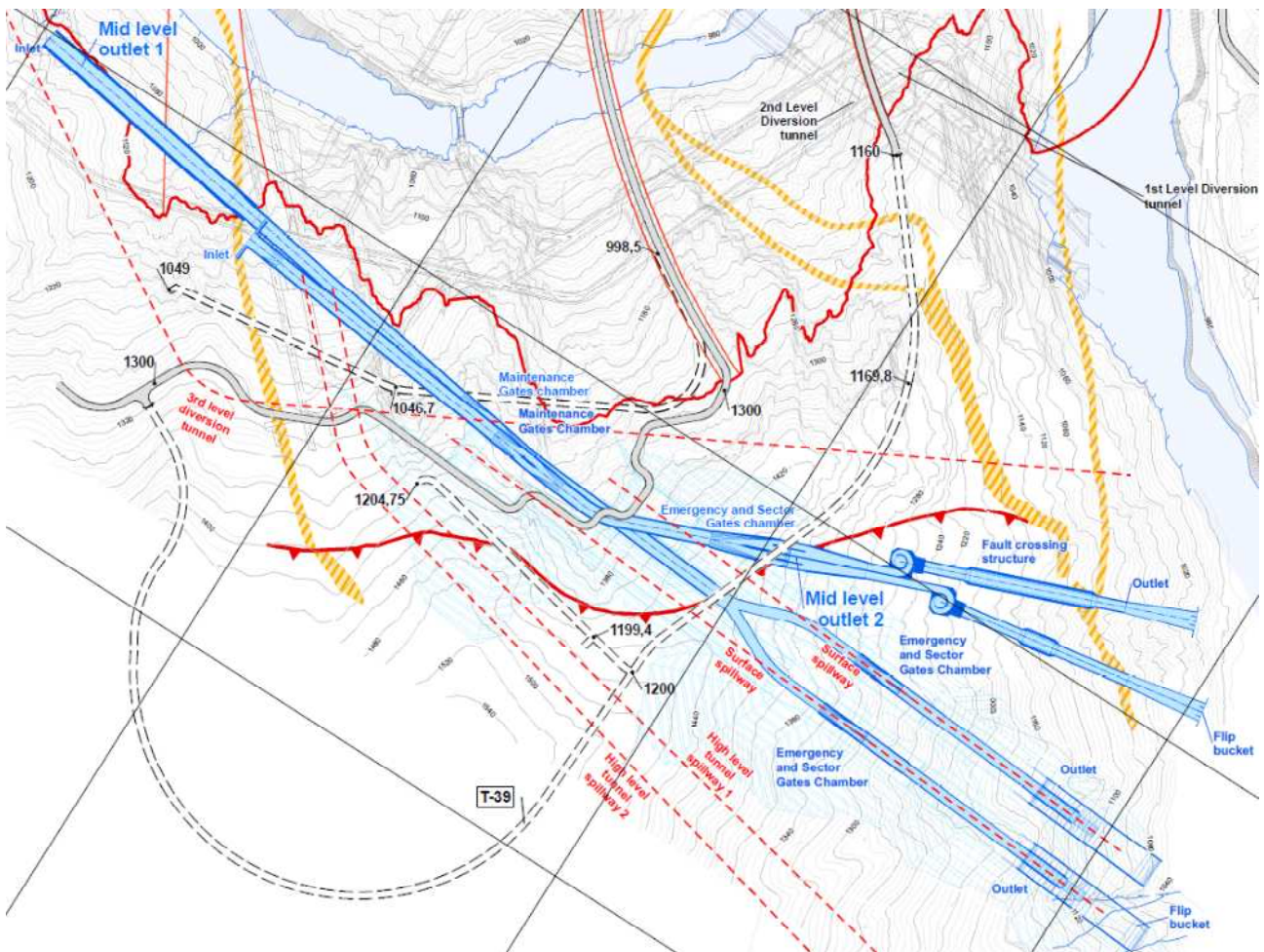


Figure 9. Layout of the middle level outlets

For MLO1 the water discharge reaches 3,685 m³/s for the exceptional head of 150 m, corresponding to a water level in the reservoir of 1,235 m a.s.l. For dam alternative with FSL 1,220, the maximum possible head is 140 m and the corresponding flow 3,562 m³/s. The flow is equally divided between the branches, corresponding to 1843 m³/s for each of them in the case of dam alternative with FSL 1290. This discharge value is the design discharge assumed for all the alternatives of FSL.

For MLO2, the water discharge reaches 3,710 m³/s for a head of 150 m. The flow is equally divided between the two vortex shafts, corresponding to 1855 m³/s each.

As explained in Volume 3 – Chapter 3 – Appendix 3 “Flood Management during Construction”, the aim of the middle level outlets is to assure flood control and to avoid overtopping during the different construction phases described in the mentioned document.

In consideration of the fact that the outlets will operate during several years during the dam construction, measures were adopted to prevent cavitation and to provide adequate aeration

around the control gates. It is noted that MLO2 will be used also as permanent discharge facility for high floods control during the plant operation.

The middle level outlets must operate in safety condition with the discharge associated to the reservoir water level for all the dam alternatives, with a maximum exceptional head of 150 m. The maximum velocity of the flow in the reach operating under pressure conditions must be in the order of 20 m/s. On the other hand, the free board in the reach operating in free flow conditions must be at least 25% of the total height of the tunnel and the velocity in principle should not exceed 20 m/s for the sections without aeration device.

A description of the tunnel design and the assessment of its hydraulic performance is described in this chapter, explaining the degree of compliance with the design criteria.

3.2 Main Features and Hydraulics of the Middle Level Outlets

The hydraulic behavior is analyzed focusing on the alternative with FSL 1,290 m a.s.l.; however the results and criteria will be applicable to different situations of operation. It should be noted that the dimensions of the structures (intake, tunnel, gates, etc.) and relevant elevation are the same for all the three dam alternatives, therefore only the situation related with FSL 1290 was analyzed.

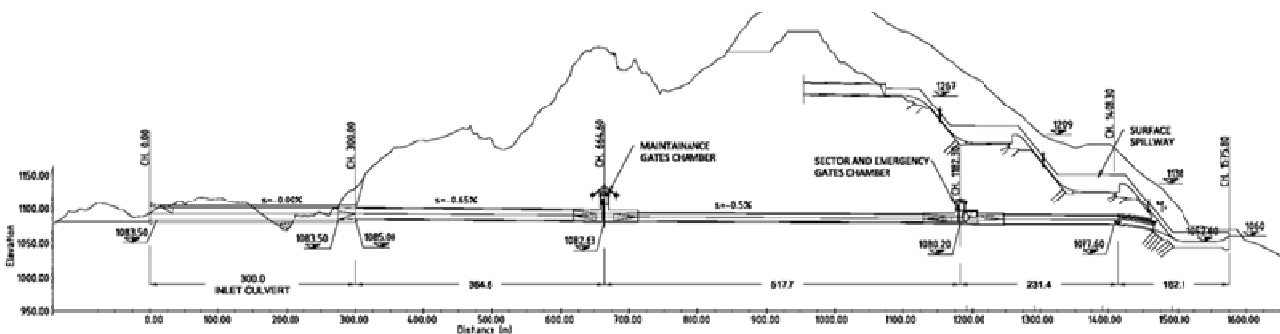


Figure 10. Profile of the MLO1. See also Figure 9 for plan view.

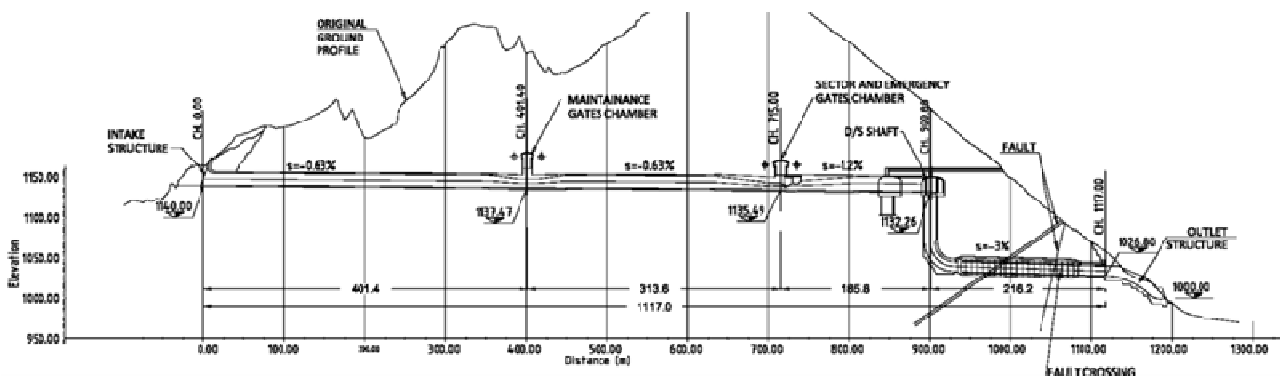


Figure 11. Profile of the MLO2. See also Figure 9 for plan view.

Some of the main features and considerations involved in the design of the MLO 1 and MLO 2 for alternative FSL 1,290 m are here in after commented.

Middle level outlet MLO1

Intake structure.

As shown in the drawings, the entrance to the culvert has a rectangular cross section 18 m wide and 25 m high. The average velocity at the intake is about 8.2 m/s. The culvert has a D-shaped cross section of 18 m diameter; average velocity is 13.2 m/s, and the maximum velocity around the axis is approximately 17.1 m/s.

The same criteria mentioned for the case of the Diversion N°3 in respect to the intake shape were adopted also in this case.

Tunnel Pressure Stretch.

As above mentioned, following the intake structure, from Station 0+00 to Station 0+300, the MLO1 is composed of a culvert with a D-shaped cross section of 18.0 m of diameter. The roof of the culvert is at elevation 1101.50 m a.s.l. Manning's coefficient for the concrete culvert is estimated as $0.012 \text{ s/m}^{1/3}$. This solution was adopted to avoid the crossing of Ionakhsh fault in underground. In fact the tunnel portal is located just downstream from the fault crossing. The culvert provides connection from the surface of the dam upstream shoulder to the portal of the tunnel and will be buried by the dam embankment. Thanks to its strong structure and being divided into independent short stretches, the culvert can accept relative displacements while keeping the hydraulic connection to the tunnel. It lays on a platform excavated into the right bank, except for a short stretch in which the foundation is provided by backfilling a gulley with RCC.

Just upstream the station 00+300 the culvert presents a contraction to the circular cross section of 15 m of the tunnel.

From the station 00+300 to station 00+664 the slope of the tunnel is 0.65 %. At the end of this reach the tunnel presents a contraction from the circular cross section of 15 m of diameter to a rectangular cross section 15.0 m x 10.0 m where the maintenance gates are located. The bottom elevation is 1082.63 m a.s.l.

In the maintenance gates chamber the tunnel is split into two conduits where two slide gates 6 m wide and 10 m high are located. The conduits are steel lined along the gates chamber. Also steel lined are the adjacent stretches of the transitions (5 m upstream and 10 m downstream). The maintenance gates are designed to operate only after the main gates have been closed.

From station 00+664 to station 0+999 the tunnel cross section is circular with 15 m diameter and slope of 0.5%. At this station the tunnel divides into two branches, constituted by tunnels with circular cross section with 10.8 m diameter. At station 01+182 of each tunnel the emergency and sector gates chamber is located. Each tunnel presents a 40 m long transition from circular cross section to rectangular cross section of 10.8 x 7.75 m. One pier with a nose 3 m thick is used to split the section into two conduits, where two slide gates, 3.9 m wide and 7.75 m high, and two sector gates, 3.90 m wide and 5.95 m high, are located.

Also in this case the conduits are steel lined along the gates chamber as well as on short stretches of the transitions. Except for the maneuvers of opening and closure, the gates operate only fully open. An aeration ducts system is located in the expansion area downstream from the gates.

Downstream from the sector gates, a 1.5 m negative step was located in order to control possible cavitation problems in the area of impact of the lower nappe on the tunnel bottom.

Tunnel Free-flow Stretch.

Downstream from the sector gates chambers, plan convergent transitions 40 m long were designed with a slope of 0.5%. The rectangular cross section in the gates chambers is connected with a conduit operating only under free-flow conditions, with the same above slope (station 01+182 to station 01+410). The conduit of each branch is 12.0 m wide and 6.0 m high to the spring line with a circular arch roof reaching a maximum height of 12.0 m. This way the design discharge is brought to the two outlets structures, each discharging into a channel of the surface spillway. The profile of the tunnel terminal reach, some 70 m long, shows a vertical curve connecting with the flip bucket of the surface spillway. The flip bucket structure was enlarged so to add a stretch some 50 m long which allows the flow outcoming from the tunnel to expand to the width of the channel before jumping to the riverbed.

Middle level outlet MLO2

Intake structure.

At the intake section at el. 1,140.0 the entrance to the tunnel has a rectangular cross section 15.0 m wide and 24.4 m high. The average velocity at the intake, around its axis, is about 13.2 m/s. The same approach above mentioned for the case of DT3 was considered in this case in order to avoid undesirable aspects of the flow behavior.

Tunnel Pressure Stretch.

From station 00+000 to station 00+715 the slope of the tunnel is 0.63% and the tunnel is prismatic with circular cross section of 15 m of diameter. At the end of this reach the tunnel presents a transition from said section to a rectangular cross section 26.2 m wide and 7.1 m where the emergency and sector gates are located. The bottom elevation is 1,135.49 m a.s.l.

The total length of the above chamber including transitions (convergent, divergent and prismatic section) is approx. 180 m. Three piers with a nose 3 m thick are used to split the section into four conduits, where four slide gates, 4.3 m wide and 7.1 m high, and four sector gates, 4.3 m wide and 5.2 m high, are located. Also in this case the conduits are steel lined along the gates chamber and short adjacent stretches of the transitions. In principle, except for the maneuvers of opening and closure, the gates operate only fully open.

An aeration ducts system is located in the expansion area downstream from the gates. A 1.0 m negative aerated step was located in order to control possible cavitation problems in the area of impact of the lower nappe on the tunnel bottom.

The maintenance gates chamber is located at a distance of about 400 m from the intake the tunnel. In the maintenance gates chamber the tunnel is split into two conduits where two slide gates 6 m wide and 10 m high are located. The conduits are steel lined along gate chamber and short adjacent stretches of the transitions. The maintenance gates are designed to operate only after the main gates have been closed.

Tunnel Free-flow Stretch.

As above mentioned, downstream from the sector gates chamber the tunnel converges from a rectangular cross section of 26.2 m span to a conduit with two barrels, each 7.0 m wide and 9.1 m high to the springline with a circular arch roof, reaching a maximum height of 17.0 m. The conduit profile was designed with a slope of 1.2 % up to the intake of the drop shaft. Between the approaching free flow tunnel and the vortex drop inlet there is a 6% steep slope transition zone which leads to the drop shaft. Each shaft is 14 m in diameter and about 99 m deep from intake to bottom, at el. 1033.29.

Intake structure of first vortex shaft. The intake structure, with plan spiral shape, is located at station 8+47.3 and elevation 1,132.90.

Intake structure of second vortex shaft. The intake structure, with plan spiral shape, is located at station 9+00.88 and elevation 1132.26.

Tailrace tunnels for both drop shafts. The free flow tailrace tunnels, one for each drop shaft, extend from the bottom of the shafts for about 215 m with 3% slope down to el. 1,126.8. The connection between the vertical shaft and the tailrace tunnel is constituted by a vertical curve with 28.9 m radius. A chute widening from 12 to 20 m is provided at the outlet of each tailrace tunnel, with a terminal flip bucket with 20° take-off angle set at el. 1,000 m a.s.l.

3.3 Operation modes and methodological approaches for the Middle Level Outlet 1 and 2

As for the case of DT3, flow conditions in the middle level outlets are variable, depending upon the reservoir elevation and the geometrical features. In fact the tunnels may operate under partially free flow, pressure flow and free flow. The following flow conditions may occur in the tunnel.

Partially free flow – When the water level in the reservoir is between el. 1,106.5 and 1,101.5, pulsations may occur in the transition field between free and pressure flow operation (for MLO2 the elevations are 1,164.5 and 1,155.0).

Pressure flow – from the intake up to the sector gates chambers the tunnel operates only under pressure flow conditions when the water level in the reservoir is higher than el. 1,106.5 approx. In this case the discharge is controlled by the head losses along the tunnel and the gates opening (for MLO2, the corresponding elevation is 1,164.5).

Free flow – from the gates chambers up to the outlet to the surface spillway channel for MLO1, or to the inlet of the drop vortex shaft for MLO2, the flow is under free-flow conditions and in supercritical regime. In this reach the flow could be mixed (water and air). Formation of plugs of water-air mixture is possible. Therefore aeration ducts are required.

Free flow in the drop shafts of MLO2 – In the drop shafts the flow is typically three dimensional. A tangential vortex intake produces a stable vortex flow in the drop shaft with sufficiently large air core. The flow is controlled by a tangential vortex and the free flow along the vertical drop shaft is under free flow conditions.

Tailrace Tunnels of MLO2 – Mixed flow could occur in case the tunnel would be operated under high heads. In this situation pulsations can be expected. The de-aeration of the flow is required anyway.

3.3.1 Discharge capacity of the Middle Level Outlet 1 and 2

According to the calculation methodology presented for the diversion tunnel N° 3, the maximum discharge with the gates fully open for a reservoir water level of 1,290 m a.s.l. would be 4,300 m³/s for MLO 1 and 3,710 m³/s for MLO 2.

According to the design criteria, the maximum exceptional design head was assumed 150 m, therefore the discharges are 3,685 m³/s for MLO 1 and 3,710 m³/s for MLO 2.

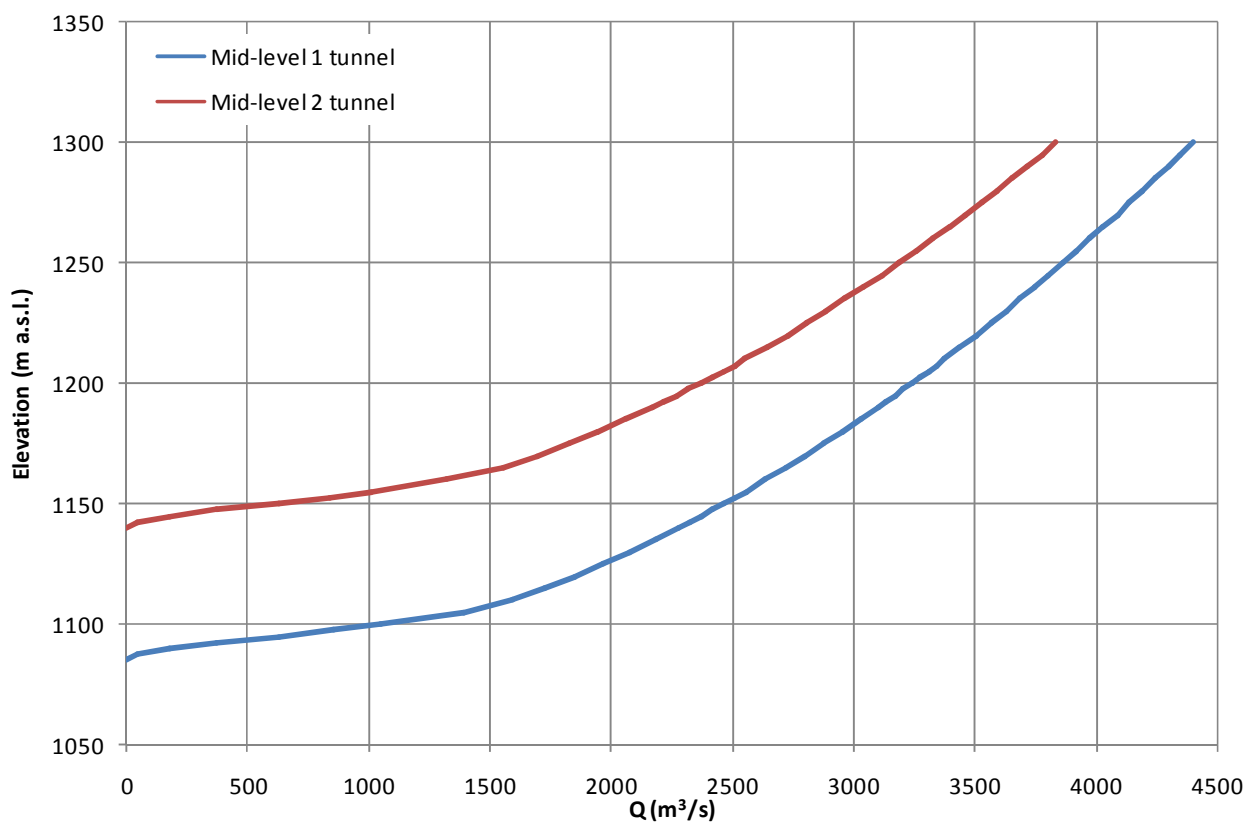


Figure 12 Head – Discharge Relationship. Pressure Tunnel up to gates chamber

As already mentioned for DT3, The computational approach adopted in order to define the Head – Discharge curve is conservative and it is reasonable to think that in reality the Head-Discharge relationship will be greater than the rating curves of the theoretical analysis. On the other hands, this increases the possibility of plugs of water-air mixture formation in the downstream tunnel and higher air demand could be required.

In the case of the alternatives with FSL 1255 and 1220, the design discharge for the Middle Level Outlet 1 is the same as in the alternative with highest dam, i.e. 3,685 m³/s.

The following considerations can be made in respect to the hydraulic behavior:

Q= 3685 m³/s. Middle level outlet 1

There is an increase in velocity around ch. 00+300 due to the fact that the cross-sectional area is decreasing in this region. The velocity changes from 17 m/s in the culvert to 21 m/s in the tunnel. Also, starting from station 01+130 at the beginning of the transition to the sector gates chamber the velocity varies, the area decreases between the piers and the velocity increases up to 30 m/s in the conduits of the gates and up to 40 m/s at the same gates section. The net static pressure in the gates chamber is about 120 m above the local elevation of the conduit bottom. It should be noted that in the reality the static pressure values are always determined by the local flow behavior; in fact, the actual pressure values can substantially differ from the average pressure values computed from the energy line. In this case problems of low static pressure could be recorded in the area where the gates are located, near to the gate slots, and pressure fluctuations would be encountered.

The middle level outlet is concrete lined and the average velocity of approximately 21 m/s in the tunnel is theoretically compatible with the structure and the dimensions of the conduit. In any case, in order to eliminate potential problems of cavitation and pulsations it is necessary to avoid abrupt offsets of the bottom and sides of the tunnel. The specifications of the lining will be defined at detailed design stage.

In the area of the gates, where several changes of section and disturbances such as those due to the gates slots occur concurrently with the higher water velocity, a steel lining has been adopted.

Q = 3710 m³/s. Middle level Outlet 2

In this case the average velocity is also approximately 21 m/s along the conduit and the velocity in the gate chamber is about 41.5 m/s. The hydraulic behavior is comparable with that of the middle level outlet 1.

3.3.2 Behavior of the middle level outlets in free flow condition

Being the conditions of the flow downstream from the gates essentially the same occurring in the diversion tunnel 3 (shock waves, air–water mixture plugs, air entrainment), similar considerations in respect of the possible problems and measures implemented in order to avoid or at least mitigate the same can be made for the middle level outlets.

In fact also in this case:

- For MLO2, the transition from the gates section to the tunnel cross section shows an angle in the order of 4°, while in MLO1 the transition is in the crown portion only, which is not interested by the flow;
- The cross section area and slope of the downstream tunnel are such that the filling rate is lower than 75%;
- An aeration duct system is foreseen downstream from the gates. An aerated negative step is also provided to control cavitation problems under the nappe. Ventilation can be also provided in correspondence with this step, through ventilation pipes developing in the concrete structures and reaching the vertical surface of such step.

The evaluation of air demand can be computed according to the formulas taken from the references, see paragraph 2.3.5. According to the relevant indications, the air demand corresponds to approximately 22% of the water discharge when the velocity in the gates chamber is 41 m/s and the Froude number is 6.2. The maximum velocity in the aeration duct should be around 45 m/s, as proposed in "Air entrainment in free surface flows", IAHR, 1991. In these conditions, four air ducts with a diameter about 2.5 m are needed in order to obtain an air discharge equal to 22% of the water discharge.

The ventilation intakes would be placed in the tunnel roof immediately downstream from the sector gates.

For MLO1, they are envisaged to be connected with a ventilation shaft some 95 m high up to the excavation platform of the higher stilling basin of the surface spillway. For MLO2, the ventilation gallery starts from the sector gates area and is brought to the vortex shafts, which also require ventilation. The total length is about 250 m. Cross areas are around 23.8 / 22.3 m² respectively. Calculations performed according with the methodology indicated in paragraph 2.3.5 showed that the global headlosses along the ventilation shaft or gallery are in the order of 2.78 kPa for MLO1 and 3.21 kPa for MLO2 respectively.

The tunnel water profile analysis was carried out with the design discharge of 3,685 m³/s (MLO 1), the upstream level water at the section of gate chamber was applied as boundary condition, based on the energy level at the gate section. Obviously, the value of the boundary condition depends on the head losses in the pressure conduit.

The supercritical flow downstream from the gate generates a water profile which remains supercritical along the whole tunnel.

The dimensions of the cross-sections for both tunnels guarantee a sufficient free board for a good aeration and for the shock waves control.

3.4 Vortex shaft

Extensive effort has been devoted in the present project to the investigation and design of structures which can operate effectively and simultaneously as a conveyance structure and energy dissipator, and yet are not prohibitively expensive.

Given the morphological features and the large volumes of excavation associated to steep channels solution, it was considered unfeasible to design a large conduit operating only under free-flow conditions that can be used to convey water from the tunnel outlet at high elevation down to an elevation close to riverbed in an area with limitation of space and not totally comfortable geology. Therefore, a spillway provided with vortex shaft was proposed for MLO2.

A vortex shaft spillway basically consists of the vortex inlet structure, the drop shaft and the tailrace tunnel. The geometry adopted for the vortex inlet in the present project is of the spiral shape, depending mainly on the shaft radius and on the width of the approaching channel. In the vortex drop shaft an angular momentum is applied to the flow through a special inlet design and the water spirals down clinging to the wall of the drop shaft.

The vortex drop structures are favorable as far as the stability of the fluid is concerned and the air transfer, and provide a significant energy dissipation that it is enhanced in the vortex flow occurring inside the drop shaft.

3.4.1 Inlet structure

The inlet was designed on the basis of a vortex drop inlet for supercritical approaching flow proposed by Hager [1].

The approach tunnel flow to the vortex drop must be supercritical, in order to obtain a correct operation of the inlet structure and the domain of Froude number between $1.5 < F_1 < 10$ must be respected.

A spiral vortex inlet generates extreme curvature effects resulting in a change of the cross-sectional area from the rectangular shape at the inlet to an almost triangular shape in the spiral inlet structure. The recommended inlet is based on model tests of an experimental investigation carried out in the Laboratory of Hydraulics, Hydrology and Glaciology (VAW) of the Swiss Federal Institute of Technology (ETH) in Zurich [1]. The inlet consists of an inner guiding wall up to $\alpha = 225^\circ$ and an outer wall. Along both walls, the respective radii of curvature change after $\alpha = 180^\circ$ where:

$$R_1 = 0.5 (a + R + t + c)$$

$$R_2 = 0.5 (2R + t + c)$$

$$R_3 = 0.5 (a + R + t - b)$$

$$R_4 = R + t$$

Herein R = shaft radius; a = distance of shaft axis to the outer approaching wall; t = wall thickness to be determined from static conditions; and c = channel width opposite to the inlet section. The centers of the circular arcs are:

$$e_1 = a - R_1$$

$$e_2 = R + t + c - R_2$$

$$e_3 = a - b - R_3$$

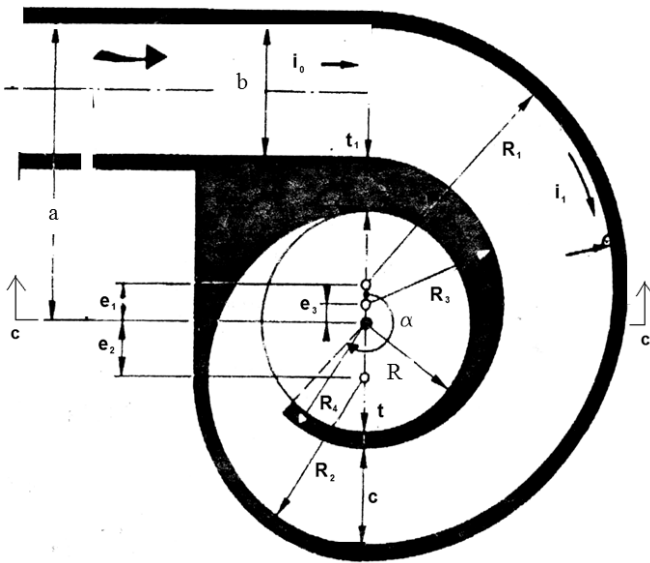


Figure 13 Geometry of Inlet Structure: Plan View

The thickness t_1 of the inner wall at the inlet section is:

$$t_1 = a - b - R$$

The slope at the inlet structure is between 5% and 30%. It should be anyway larger than the slope in the approaching channel.

3.4.2 Drop Shaft Diameter Theoretical Approach

In this case, given the importance of the phenomenon, a theoretical description is deemed pertinent.

Such a theoretical approach is described in Annex 1.

Based on it, the rate of discharge is:

$$Q = \frac{\varepsilon}{\sqrt{1 + \frac{4A^2\varepsilon^2}{(1 + \sqrt{1 - \varepsilon})^2}}} S_2 \sqrt{2gH}$$

Where A is a parameter characterizing the geometry of the "spillway vortex"

$$A = \frac{S_2 R'}{R S_1}$$

3.4.3 Design parameters used for Middle Level Outlet 2

On the basis of the theoretical description of the behavior of the vortex drop shaft, the diameter of the drop shaft was defined and the related design parameters were identified.

For each drop shaft, the design discharge is approximately 1800 m³/s. A first tentative value is found applying the Vischer and Hager empirical equation [26]:

$$D = \left(\frac{Q^2}{g} \right)^{\frac{1}{5}}$$

Based on the design discharge, the drop shaft diameter is 12.8 m. In fact, adopting the methodology described in Annex 1, a 14 m diameter (R = 7 m) was used.

The table shows the design parameters adopted.

| R | R ₁ | R ₂ | R ₃ | R ₄ | b | a | t | t ₁ | c |
|-----|----------------|----------------|----------------|----------------|-----|------|-----|----------------|-----|
| 7.0 | 16.0 | 11.25 | 9.0 | 8.5 | 7.0 | 16.5 | 1.0 | 2.5 | 7.0 |

Table 4. Parameters referring to Figure 13. Measures in meters.

Based on the approach channel characteristics, the values of area S(h) were calculated for several discharge values, being h the depth in the approaching channel. Furthermore this allows calculating the dimensionless parameter A:

$$A = \frac{R' S_2}{R S_{1(h)}}$$

Knowing A, it is possible to determine the discharge coefficient μ and the contraction coefficient ε . The discharge is calculated as a function of the energy "H" at the entrance of the drop shaft:

$$Q = \mu \cdot S_2 \cdot \sqrt{2g \cdot H}$$

The axial and radial velocity V_z and V_t are then calculated according to the above described model.

| S ₁ (h) [m ²] | H [m] | A [-] | μ [-] | ε [-] | Rv [m] | Q [m ³ /s] | V _z [m/s] | V _t [m/s] |
|---|----------|----------|--------------|----------------------|-----------|--------------------------|-------------------------|-------------------------|
| 18.8 | 20.6 | 13.47 | 0.07 | 0.25 | 6.05 | 214.3 | 5.5 | 20.1 |
| 25.3 | 26.6 | 9.98 | 0.09 | 0.30 | 5.85 | 322.5 | 6.9 | 22.8 |
| 31.6 | 31.6 | 8.01 | 0.11 | 0.34 | 5.67 | 431.8 | 8.2 | 24.8 |
| 37.6 | 35.9 | 6.73 | 0.13 | 0.38 | 5.52 | 539.2 | 9.3 | 26.4 |
| 43.5 | 39.7 | 5.81 | 0.15 | 0.41 | 5.38 | 647.4 | 10.3 | 27.7 |
| 49.3 | 43.1 | 5.13 | 0.17 | 0.44 | 5.25 | 753.9 | 11.2 | 28.7 |
| 55.0 | 46.1 | 4.59 | 0.19 | 0.46 | 5.12 | 858.7 | 12.0 | 29.6 |
| 60.7 | 48.8 | 4.16 | 0.20 | 0.49 | 5.01 | 962.5 | 12.8 | 30.4 |
| 66.3 | 51.4 | 3.81 | 0.22 | 0.51 | 4.89 | 1,065.1 | 13.5 | 31.0 |
| 71.9 | 53.7 | 3.51 | 0.23 | 0.53 | 4.79 | 1,165.9 | 14.2 | 31.6 |

| | | | | | | | | |
|-------|------|------|------|------|------|---------|------|------|
| 77.5 | 55.9 | 3.26 | 0.25 | 0.55 | 4.69 | 1,264.6 | 14.9 | 32.1 |
| 83.1 | 58.0 | 3.04 | 0.26 | 0.57 | 4.59 | 1,363.5 | 15.5 | 32.6 |
| 88.6 | 59.8 | 2.85 | 0.28 | 0.59 | 4.49 | 1,460.6 | 16.2 | 33.0 |
| 94.1 | 61.6 | 2.68 | 0.29 | 0.60 | 4.40 | 1,554.7 | 16.7 | 33.3 |
| 99.7 | 63.3 | 2.54 | 0.30 | 0.62 | 4.32 | 1,648.4 | 17.3 | 33.6 |
| 105.2 | 65.0 | 2.40 | 0.32 | 0.63 | 4.23 | 1,740.8 | 17.8 | 33.9 |
| 110.6 | 66.5 | 2.28 | 0.33 | 0.65 | 4.15 | 1,829.3 | 18.3 | 34.1 |
| 116.1 | 67.9 | 2.18 | 0.34 | 0.66 | 4.07 | 1,919.5 | 18.8 | 34.4 |
| 121.6 | 69.3 | 2.08 | 0.35 | 0.68 | 3.99 | 2,004.5 | 19.3 | 34.5 |

Table 5. Drop shaft design for several discharge values

The results show that the design discharge is compatible with the adopted geometry, that the diameter of the vortex is about 8 m, and that the axial and radial velocities are about 18 m/s and 34 m/s respectively.

Such dimensioning was adopted to design the drop shafts of Middle Level Outlet n. 2.

Anyway, an experimental validation in laboratory is obviously necessary.

3.4.4 Hydraulic conditions throughout the drop shaft segment

A helicoidal deflector was foreseen in the shaft, in order to avoid abrupt change in speed or direction of the flow; the energy dissipation occurs principally by friction distributed along the length of the drop shaft instead of being concentrated in a plunge pool at the bottom of the shaft. In these conditions the air entrainment is minimized, practically all the air that is entrained in the flow down the helicoidal stream is ejected from the swirling flow at the bottom of the shaft in the air shaft control.

With this arrangement, the need for a large underground energy dissipation structure, a de-aeration chamber and a large vent pipe are eliminated, and the drop shaft can be placed nearly adjacent to the conveyance tunnel and connected to it with a simple tunnel using only an air shaft of reduced size. Anyway, some air transport in vortex flow drop shafts is foreseen, thus de-aeration conduit is to be provided.

The amount of air entrained and transported in a drop shaft depends upon the type of flow and the water level in the drop shaft. A vortex-flow inlet imparts an angular momentum to the flow with an air core in the middle of the drop shaft. As the flow slides down into the drop shaft, its vertical velocity increases, the swirl attenuates, and the direction approaches the vertical. The flow, however, continues to hug the drop-shaft wall. In this case, a significant portion of the air bubbles converges, due to an inward pressure gradient toward the centre of the drop shaft, coalesced to form large bubbles, and then rises toward the surface. Nevertheless, a large number of air bubbles will be carried downstream.

The empirical equation proposed by Kalinske & Robertson [16] in order to assess the air entrainment through a hydraulic jump may be used in this case to determine the amount of air entrained into the flow through the annular undular hydraulic jump at the bottom of the drop shaft.

The equation proposed in [4] to estimate the volumetric amount of air Q_A entrained into the flow is used to determine the air demand:

$$\beta = \frac{Q_A}{Q_W} = 0.0066(F_R - 1)^{1.4}$$

The above equation derived from model tests in a 0.1494 m pipe seems to estimate β rather well also under prototype conditions. Falvey [4] presents the equation of Kalinske & Robertson [16] as a regression through prototype data from different projects. The following are the air flow data for the 14 m drop shaft.

| Q_W [m ³ /s] | V_z [m/s] | V_t [m/s] | Fr [-] | Beta [-] | Q_A [m ³ /s] |
|------------------------------|----------------|----------------|-----------|-------------|------------------------------|
| 214.3 | 5.5 | 20.1 | 1.80 | 0.005 | 1.0 |
| 322.5 | 6.9 | 22.8 | 2.06 | 0.007 | 2.3 |
| 431.8 | 8.2 | 24.8 | 2.27 | 0.009 | 4.0 |
| 539.2 | 9.3 | 26.4 | 2.43 | 0.011 | 5.9 |
| 647.4 | 10.3 | 27.7 | 2.57 | 0.012 | 8.1 |
| 753.9 | 11.2 | 28.7 | 2.69 | 0.014 | 10.4 |
| 858.7 | 12.0 | 29.6 | 2.80 | 0.015 | 12.9 |
| 962.5 | 12.8 | 30.4 | 2.89 | 0.016 | 15.5 |
| 1,065.1 | 13.5 | 31.0 | 2.98 | 0.017 | 18.3 |
| 1,165.9 | 14.2 | 31.6 | 3.06 | 0.018 | 21.1 |
| 1,264.6 | 14.9 | 32.1 | 3.13 | 0.019 | 24.1 |
| 1,363.5 | 15.5 | 32.6 | 3.20 | 0.020 | 27.1 |
| 1,460.6 | 16.2 | 33.0 | 3.26 | 0.021 | 30.2 |
| 1,554.7 | 16.7 | 33.3 | 3.31 | 0.021 | 33.2 |
| 1,648.4 | 17.3 | 33.6 | 3.37 | 0.022 | 36.4 |
| 1,740.8 | 17.8 | 33.9 | 3.42 | 0.023 | 39.6 |
| 1,829.3 | 18.3 | 34.1 | 3.46 | 0.023 | 42.7 |
| 1,919.5 | 18.8 | 34.4 | 3.51 | 0.024 | 45.9 |
| 2,004.5 | 19.3 | 34.5 | 3.55 | 0.024 | 49.1 |

Table 6. Air demand for the drop shaft

An air conduit with a diameter of 2.5 m was assumed, which is compatible with an air discharge of 50 m³/s, with an average velocity of 10 m/s.

3.4.5 Cavitation induced by rotational flow

The cavitation conditions which the elements of a spillway are subject to are usually estimated on the basis of the cavitation parameter K:

$$K = \frac{p_0 - p_{sat}}{\frac{\rho v^2}{2}}$$

Where p_0 and p_{sat} are the pressure at a characteristics point and the pressure of saturated water vapor, while v is the radial velocity.

The tangential flow rotation, see Table 5, represents a source of cavitation phenomena in vortex spillways of the type which is being considered here.

The steel lining in the bottom of the drop shaft is necessary, and adequate measures have to be implemented to improve the capability of the concrete lining to resist potential erosion phenomena.

3.5 Flip bucket

3.5.1 Jet trajectories

MLO1 discharges into the channels of the surface spillway, with a water speed comparable with the one occurring when the latter operates and with a maximum flow that is about 2/3 of the maximum under the PMF conditions. Thus the analyses presented for the surface spillway cover also the case of the discharge from MLO1.

Thus this section analyses only the jet trajectories relevant to the different angles examined: 30°, 25° and 20° for the case of MLO2.

As for the DT3, the impact of the impingement jets on the surface and their potential diffusion on the plunge pool bottom will be analyzed by applying the Hartung and Häusler method [11] that is indirectly based on the specific stream power of the plunging jet transmitted to the bed.

The distribution of the dynamic pressures on the plunge pool bottom, for different flip bucket angles alternatives, is examined and compared with the impact pressure.

The profile is calculated by applying the USBR formula [2] that gives the trajectory of the lower nappe of the jet (the origin of the coordinates is taken at the end of the lip):

$$y = x \cdot \tan(\alpha) - \frac{x^2}{K[4 \cdot (d + h_v) \cdot \cos^2(\alpha)]}$$

where:

x = horizontal distance

y = vertical distance

α = angle of the edge of the lip with the horizontal

K = coefficient allowing for the effects of air resistance on the jet trajectory

d = thickness of the jet

$$h_v = V_i^2 / (2g)$$

g = acceleration due to gravity

The results are summarized in the next table:

| Z_{lip} [m a.s.l.] | Take off angle [°] | Impingement distance form lip [m] | Impingement angle $\left(\frac{dy}{dx} \Big _{X=X_0} \right)$ [°] | Trajectory length $\left(\int_0^{x_0} \sqrt{1 + \left(\frac{dy}{dx} \right)^2} dx \right)$ [m] |
|----------------------|-----------------------|---|---|--|
| 1000.0 | 30 | 136 | 41 | 148 |
| 1000.0 | 25 | 128 | 38 | 137 |
| 1000.0 | 20 | 118 | 35 | 124 |

Table 7 – Summary Results of jet trajectories with different take off angles

The computation has been performed for the design discharge of each drop shaft, corresponding to 1850 m³/s.

In consideration of the trajectory length and the impact area in respect to the outlet location, 20° are selected as take-off angle of the flip buckets.

3.5.2 Plunge Pool

As described for Diversion Tunnel n°3, the scour depth for MLO2 is evaluated making use of the same methodology explained in Paragraph 2.3.4.

Two discharge values, 1850 m³/s and 1065 m³/s, were examined for each complex composed of vertical shaft and tunnel. The velocities adopted for the calculation of energy in the ski jump correspond to the vector resultant velocity of the axial and elicoidal motion downstream the vortex shaft. The velocity components are shown in Table 5. Drop shaft design for several discharge values.

- $q = 1850 \text{ m}^3/\text{s} / 20 \text{ m} = 92.5 \text{ m}^3/\text{s}/\text{m}$,
- $H = 95.4 \text{ m}$
- $d = 1 \text{ m}$

- $q = 1065 \text{ m}^3/\text{s} / 20 \text{ m} = 53.3 \text{ m}^3/\text{s}/\text{m}$,
- $H = 78.2 \text{ m}$
- $d = 1 \text{ m}$

| Author | D (m) 1850 m ³ /s | D (m) 1065 m ³ /s | K | x | y | w | z |
|---------------|---------------------------------|---------------------------------|-------|------|-------|------|------|
| Veronese (B) | 61.1 | 43.4 | 1.9 | 0.54 | 0.225 | 0 | 0 |
| Veronese mod. | 46.3 | 33.5 | 1.9 | 0.54 | 0.225 | 0 | 0 |
| Damle (A) | 61.3 | 42.1 | 0.652 | 0.5 | 0.5 | 0 | 0 |
| Damle (B) | 51.0 | 35.0 | 0.543 | 0.5 | 0.5 | 0 | 0 |
| Damle (C) | 34.0 | 23.4 | 0.362 | 0.5 | 0.5 | 0 | 0 |
| Martins (A) | 45.3 | 31.9 | 1.9 | 0.6 | 0.1 | 0 | 0 |
| Martins (B) | 35.8 | 25.2 | 1.5 | 0.6 | 0.1 | 0 | 0 |
| Mason | 47.0 | 33.4 | 3.27 | 0.6 | 0.05 | 0.15 | -0.1 |
| Taraimovich | 41.1 | 27.0 | 0.633 | 0.67 | 0.25 | 0 | 0 |
| INCYTH | 42.5 | 30.7 | 1.413 | 0.5 | 0.25 | 0 | 0 |
| Pinto | 38.6 | 27.4 | 1.2 | 0.54 | 0.225 | 0 | 0 |
| Chee and Kung | 62.6 | 43.2 | 1.663 | 0.6 | 0.2 | 0 | -0.1 |

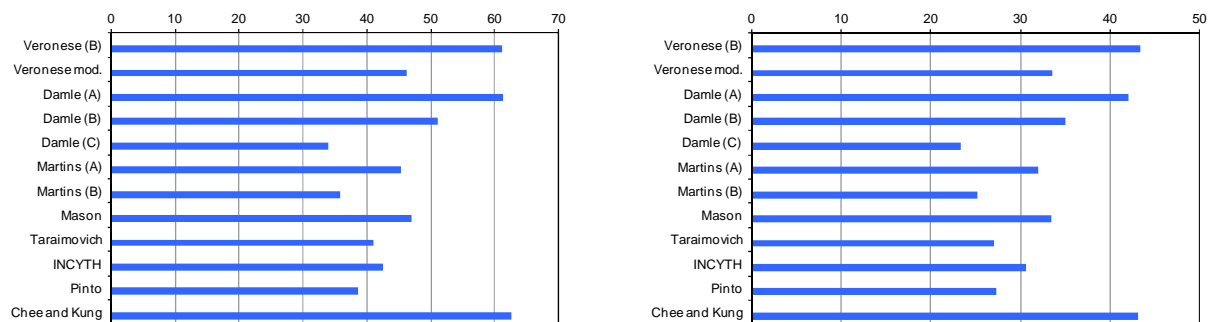


Figure 14 Scour depth (m) calculated by using different empirical formulae for 1850 and 1065 m³/s.

The field of variation of the scour depth $D = t + h$ obtained by application of empirical formulae, is between 34 and 62.6 m, while the average value is 47 m for the discharge 1850 m³/s. For the 1065 m³/s discharge, D is between 23.4 m and 43.4 m, with an average of 33 m.

Also in this case, applying the pressure bulb theory to the case of MLO 2 for the discharges of 1850 m³/s and 1065 m³/s and a take-off angle of 20°, in order to assess the results of the empirical formulae, we obtain:

The take-off velocities are of approximately 38.5 and 33.8 m/s respectively (without considering the head losses along the chute and water depth). The water energy levels at the flip bucket correspond to 1075.4 and 1058.2 m a.s.l. while the tailwater elevation is 980 m a.s.l.

For each tunnel, the average horizontal distance of the point of impact of the jet with respect to the flip bucket is approximately 118 m for the discharge 1850 m³/s and 97 m for 1065 m³/s.

Figure 15 shows, for the discharge of 1850 m³/s, the pressure bulb with respect to the point of impact, where the impact pressure is $P_u = 96.6 \text{ T/m}^2$ (9.7 kg/cm²) with an impingement angle of 35°, while the Figure 16 shows, for a discharge of 1065 m³/s, the pressure bulb with respect to the point of impact, where the impact pressure is $P_u = 79 \text{ T/m}^2$ (7.9 kg/cm²) with an impingement angle of 38°.

Considering a pressure value of 15 T/m^2 (1.5 kg/cm^2) as an erodibility threshold, Figure 15 and Figure 16 show that this value is reached at a distance of 27 m along the axis of the bulb for the $1850 \text{ m}^3/\text{s}$ case, while for the $1065 \text{ m}^3/\text{s}$ case this happens at 15 m.

The angle of impact for $1850 \text{ m}^3/\text{s}$ is 35° , the threshold pressure value assumed as design criterion is reached at 27 m along the jet axis (see Figure 15). In this situation, a pre-excavation of about 20 m from the tailwater level at elevation 980 m a.s.l. would be adopted. A pre-excavation width of about 40 m at each outlet (twice the take-off width) is assumed for a forecast of the volume of excavation and costing. However, this has to be checked by investigation on a movable bed physical model.

Also in this case, experimental tests are necessary in order to more exactly define the local scouring over the right and left banks and the possible further mitigation structures.

For the purpose of this study, a pre-excavation of the riverbed down to the elevation of 960 m a.s.l. is assumed for controlling the scouring process. As for the case of DT3, the jet would impact the riverbed at a distance of some 50 m from the toe of the right bank slope. Therefore, the pre-excavation would also involve the slope of the left bank, where a flat platform with elevation around 1,100 m a.s.l. is present.

This situation allows carrying out the excavation without endangering the stability of the whole bank. In addition to the riverbed pre-excavation, some 0.30×10^6 cubic meters of slope excavation might be necessary to provide sufficient space for the plunge pool at the outlets.

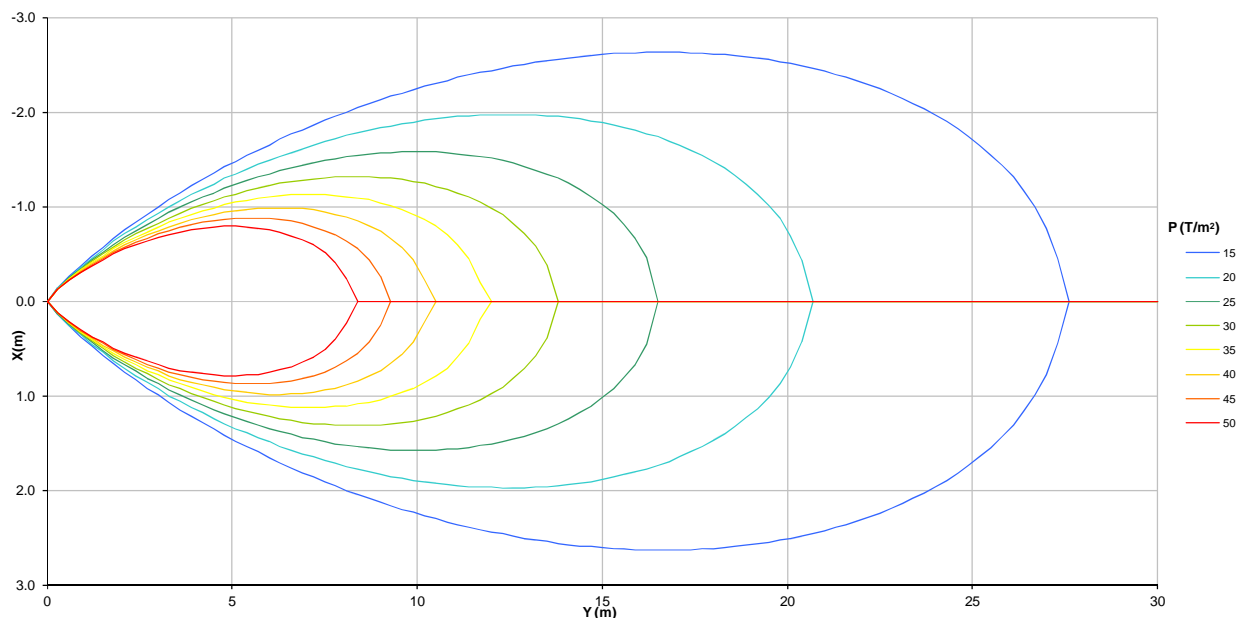


Figure 15 Hydrodynamic pressure bulb: $Q = 1850 \text{ m}^3/\text{s}$. Pressure in the point of impact $P_u(0,0) = 96.6 \text{ T/m}^2$. Angle of impact 35° .

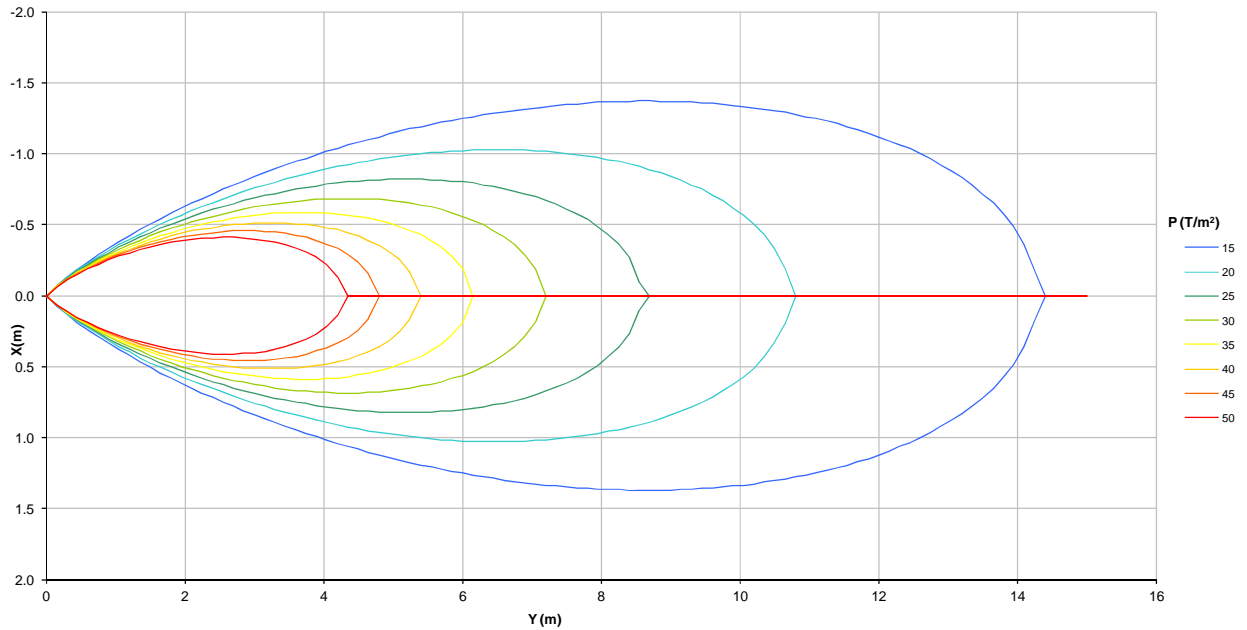


Figure 16 Hydrodynamic pressure bulb: $Q = 1065 \text{ m}^3/\text{s}$. Pressure in the point of impact $P_u(0,0) = 79 \text{ T/m}^2$. Angle of impact 38° .

Figure 17 shows the jet trajectory and pressure bulb for both discharges.

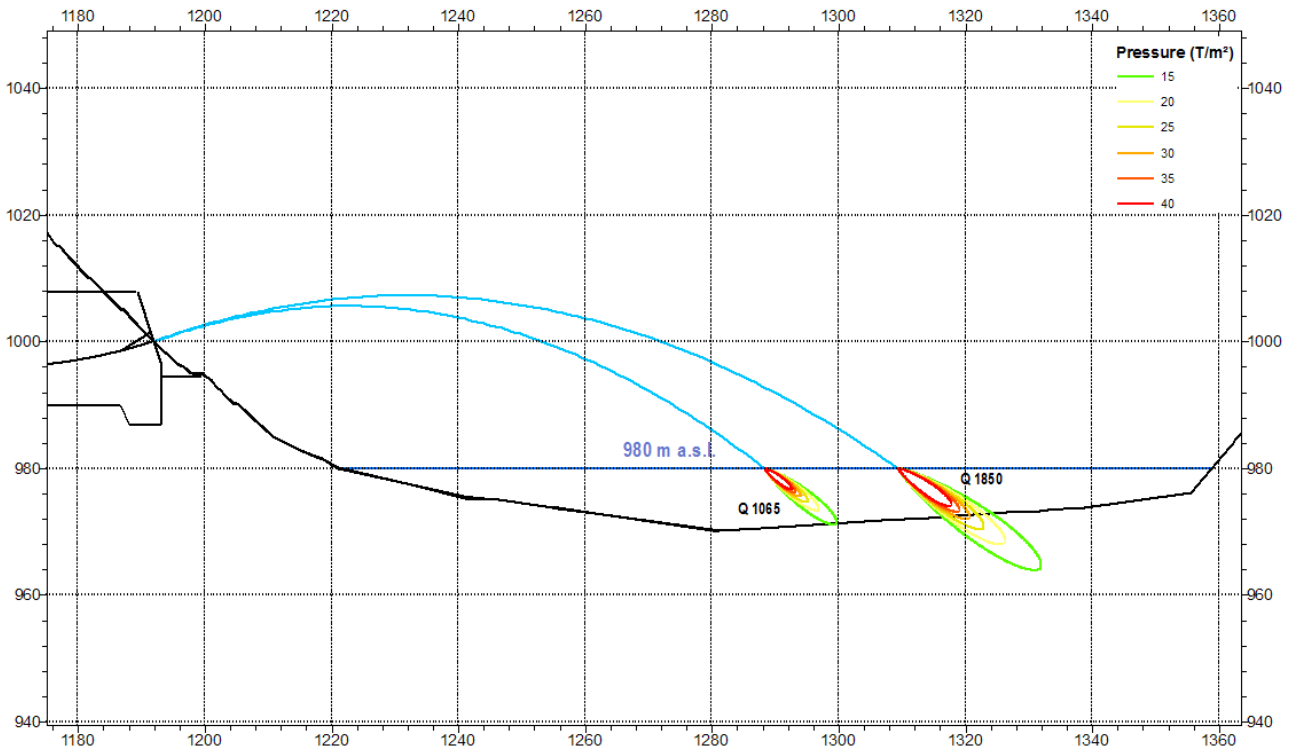


Figure 17. Jet trajectories for one tunnel of Mid level outlet 2; $Q = 1850$ and $1065 \text{ m}^3/\text{s}$

4 HIGH LEVEL TUNNEL SPILLWAYS

4.1 Overview of the High level tunnel spillways

According to the studies exposed in report Volume 3 – Chapter 3 – Appendix 3 “Flood Management during Construction”, two High Level Tunnel Spillways, numbered 1 and 2, are proposed for the alternative with FSL 1290 m. For the alternative with FSL 1255 the complex includes three High Level Tunnel Spillways, and for the alternative with FSL 1220 m there is one High Level Tunnel spillway only, as already indicated in paragraph 1.1.4.

Each of the proposed high level tunnel spillways basically consists of a pressure tunnel, followed by a free flow tunnel, a cascade system composed by chutes and stilling basins, and a terminal flip bucket.

4.1.1 *Alternative with FSL Elevation 1290 m a.s.l.*

The intake of the **High Level Tunnel Spillway n. 1 (HLTS1)** is set at el. 1190 m a.s.l.; the tunnel current cross section is horseshoe with 10.0 m diameter. The tunnel is about 510 m long from the intake to the sector and emergency gates chamber axis. The maintenance gates chamber is located at a distance of about 250 m from the intake. Downstream from the sector and emergency gates chamber, a rectangular cross-section 10 m wide and 7.0 m high to the springline with a circular arch roof reaching a maximum height of 12 m has been adopted.

The free flow tunnel extends until station 1+264.1. From its outlet portal, the cross section diverges to a width of 30 m through a chute with a slope of 45° between el. 1177.70 and 1130.00. The chute connects with a stilling basin, 30 m wide and 65 m long. At the end of the stilling basin a 9.5 m high sill is foreseen.

The second chute extends from el. 1139.50 down to el. 1055.00, with a slope of 45°, followed by the second stilling basin, 65 m long. Again, a sill 9.5 m high closes the stilling basin at el. 1064.50.

Downstream from the sill, a 30 m wide chute between el. 1064.50 and 1000.00, with a slope of 30°, flows towards a flip bucket, with a take-off angle of 30°.

The **High Level Tunnel Spillway n. 2 (HLTS2)** shows in the tunnel stretches under pressure and free flow operating conditions the same features and intake elevation as HLTS1, being the gates chambers located at distances from the intake somewhat different as a consequence of the slightly different route.

In this case the free flow tunnel extends until station 1+410.10. As for the previous spillway, the cascade system is composed of three chutes and two stilling basins. From the outlet portal, the cross section diverges to a width of 30 m through a chute with a slope of 45° between el. 1176.57 and 1120.00. The chute connects to a stilling basin, 30 m wide and 65 m long. At the end of the stilling basin a 9.5 m high sill is foreseen.

The second chute extends from el. 1129.5 to el. 1045.00, with a slope of 45°, followed by the second stilling basin, 65 m long. Again, a sill 9.5 m high closes the stilling basin at el. 1054.50.

Downstream from the sill, a 30 m wide chute between el. 1054.50 and 1000.00, with a slope of 36.5°, flows towards a flip bucket, with a take-off angle of 30°.

4.1.2 Alternative with FSL Elevation 1255 m a.s.l.

The intake of the **High Level Tunnel Spillway n. 1 (HLTS1)** is set at el. 1145; the tunnel current cross section is horseshoe with 10.0 m diameter. The tunnel is about 570 m long from the intake to the sector and emergency gates chamber. The maintenance gates chamber is located at a distance of about 317 m from the intake. Downstream from the sector and emergency gates the tunnel exhibits the same cross-section of HLTS for alternative with FSL 1290.

The free flow tunnel extends until station 1+385.7. The scheme of chutes and stilling basins is repeated with the following details, which can be found also on the relevant drawings:

- First chute: from el. 1131.74 to 1101.74, slope of 45°;
- Second chute crest at el. 1111.24, down to el. 1050.00, slope 45°;
- Third chute crest at el. 1059.50, down to 1000.00, slope of 45°;
- Terminal flip bucket with a take-off angle of 30°.

High Level Tunnel Spillway n. 2 (HLTS2): in the tunnel stretches with pressure and free flow operating conditions mostly the same features as HLTS1 were adopted, but its intake is located at el. 1165. The gates chambers are located at distances from the intake somewhat different from HLTS1 as a consequence of the slightly different route.

In this case the free flow tunnel extends until station 1+501.60. The scheme of chutes and stilling basins is repeated with the following details, which can be found also on the relevant drawings:

- First chute: from el. 1151.66 to 1102.4, slope of 45°;
- Second chute crest at el. 1111.90, down to el. 1040.0, slope 45°;
- Third chute crest at el. 1049.5, down to 1000.0, slope of 35°;
- Terminal flip bucket with a take-off angle of 30°.

High Level Tunnel Spillway n. 3 (HLTS3): in the tunnel stretches with pressure and free flow operating conditions mostly the same features as HLTS2 were adopted, including intake elevation. The gates chambers are located at distances from the intake somewhat different from HLTS2 as a consequence of the slightly different route.

In this case the free flow tunnel extends until station 1+585.1. The scheme of chutes and stilling basins is repeated with the following details, which can be found also on the relevant drawings:

- First chute: from el. 1149.85 to 1100.38, slope of 45°;
- Second chute crest at el. 1109.88, down to el. 1025.38, slope 45°;
- Third chute crest at el. 1034.88, down to 1000.0, slope of 39°;
- Terminal flip bucket with a take-off angle of 30°.

The layout of the HLTSS for the dam at El. 1265 m can be seen in the following figure.

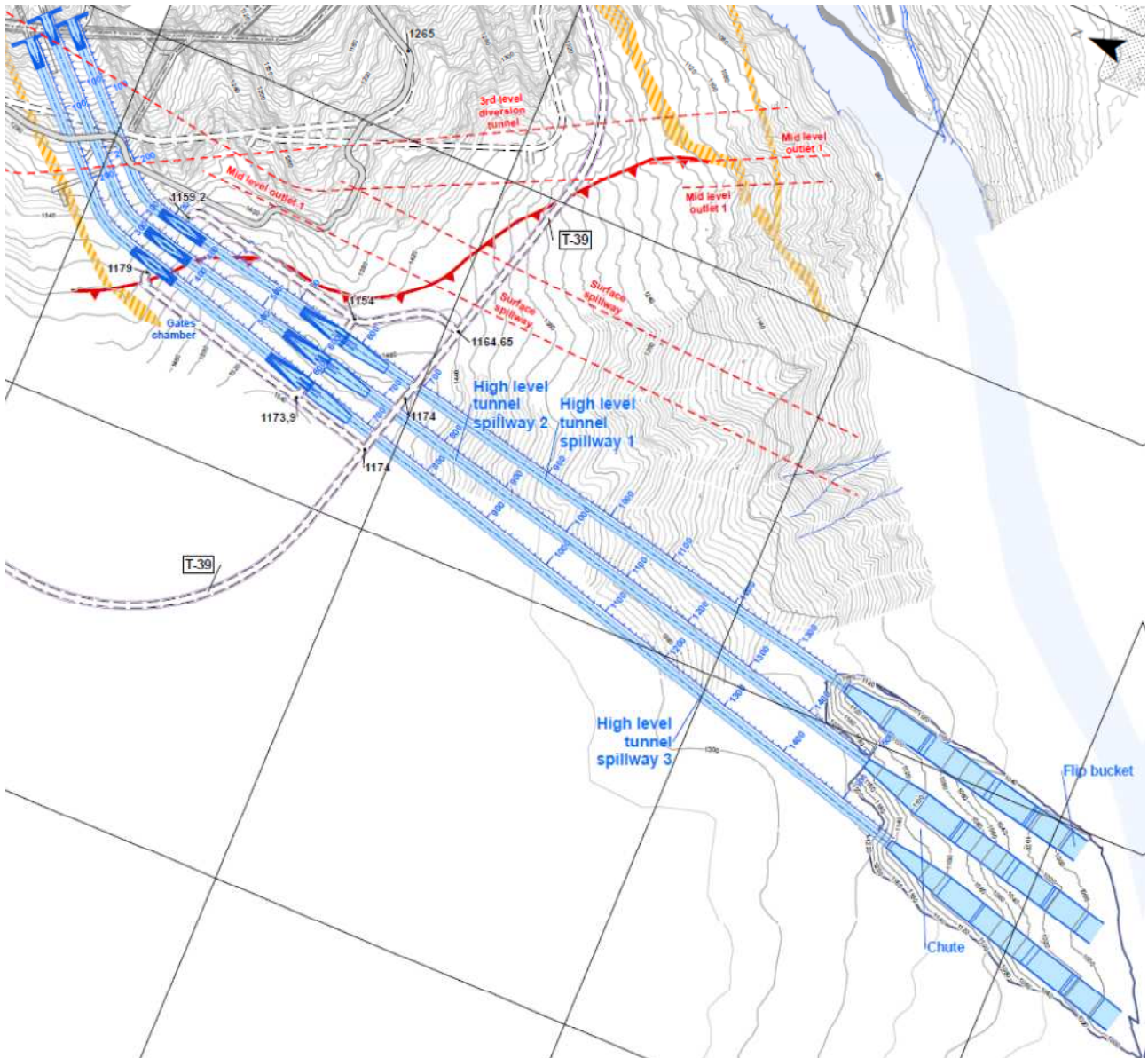


Figure 18. Layout of the high level tunnel spillways, alternative with dam crest el. 1265 ma.s.l.

4.1.3 Alternative with FSL Elevation 1220 m a.s.l.

The intake of the **High Level Tunnel Spillway n. 1 (HLTS1)** is set at El. 1140, the tunnel current cross section is horseshoe with 10.0 m diameter. The tunnel is about 580 m long from the intake to the sector and emergency gates chamber axis. The maintenance gates chamber is located at a distance of about 320 m from the intake. Downstream from the sector and emergency gates the tunnel exhibits the same cross-sections of HLTS for alternatives with FSL 1290 and 1265.

The free flow tunnel extends until station 1+416.8. The scheme of chutes and stilling basins is repeated with the following details, which can be found also on the relevant drawings. From the outlet portal, the cross section diverges to a width of 30 m through a 44.2 m long curved chute:

- First chute: from el. 1126.3 to 1106.3, terminal slope 45°;
- Second chute crest at el. 1115.8, down to el. 1050.00, slope 45°;
- Third chute crest at el. 1059.5, down to 1000.0, slope of 33°;
- Terminal flip bucket with a take-off angle of 30°.

4.2 Main Features and Hydraulics of the High Level Tunnel Spillways

The aim of the High Level Tunnel Spillways is that to assure flood control and to avoid dam overtopping during the last period of its construction as well as during the plant operation.

The maximum velocity of the flow in the reach operating under pressure conditions must be in the order of 20 m/s, while the free board in the reach operating in free flow conditions must be at least 25% of the total height of the tunnel and the velocity must not be higher than 20 m/s for the sections without aeration device. Such design criteria are the same adopted for all hydraulic facilities.

A description of the tunnels components and the assessment of its hydraulic performance are described in this chapter, commenting the degree of compliance with the design criteria.

4.2.1 Lay-out and geometry for pressure and free flow operation tunnel stretches

In this case, the hydraulic analyses are focused on the discharge 1570 m³/s and water level in the reservoir of 1290 m a.s.l., i.e. that of the alternative with FSL el. 1290 m; the results can be extrapolated to all the other situations of operation.

Here in after, the profiles of some of the above mentioned tunnels configurations are shown.

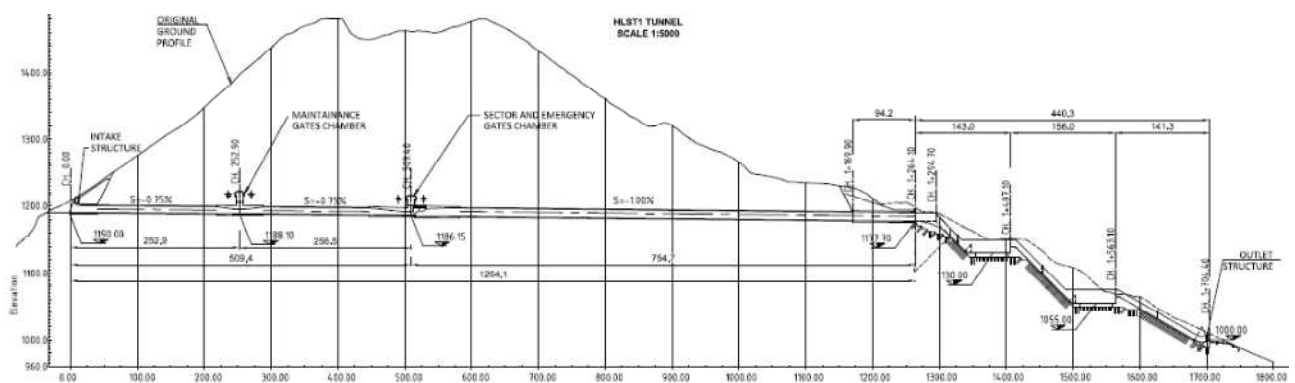


Figure 19. Profile of the High level tunnel spillway 1, for alternative with FSL at El. 1290 m

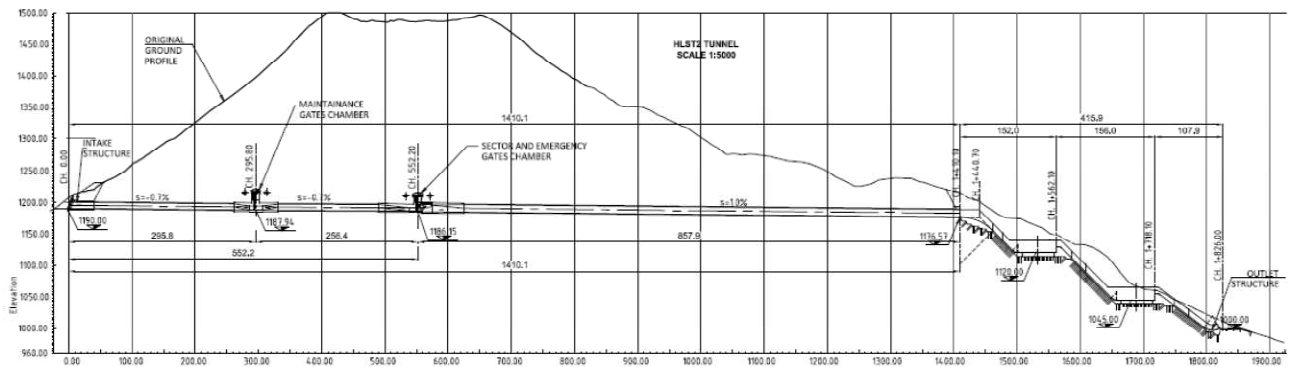


Figure 20. Profile of the High level tunnel spillway 2, for alternative with FSL at El. 1290 m

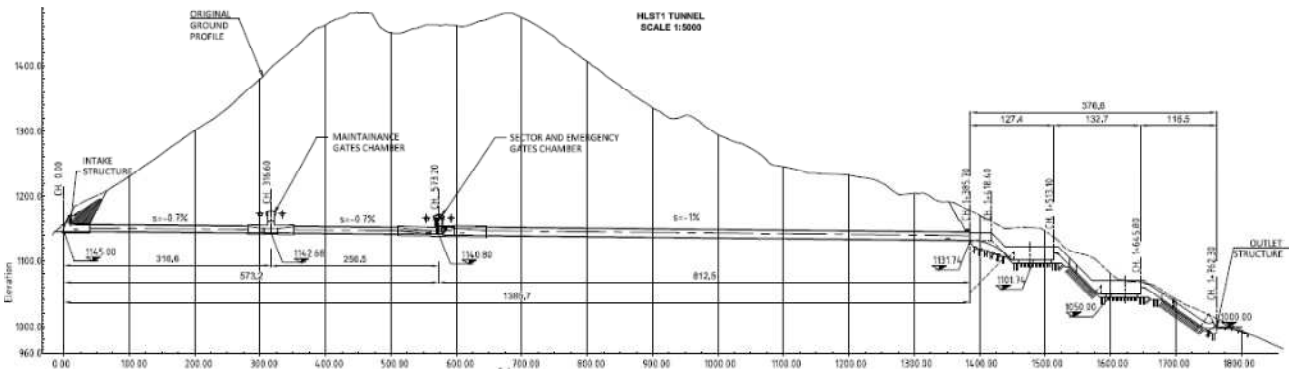


Figure 21. Profile of the High level tunnel spillway 1, for alternative with FSL at El. 1255 m.

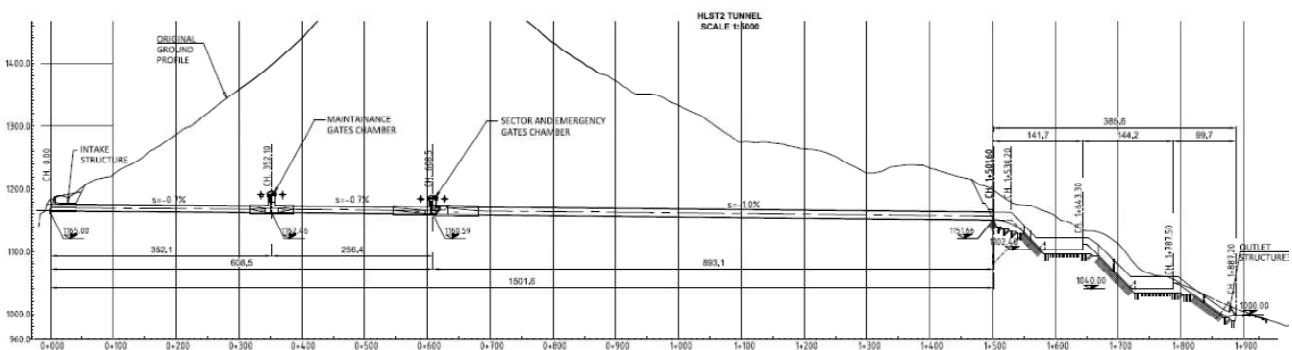


Figure 22. Profile of the High level tunnel spillway 2, for alternative with FSL at El. 1255 m.

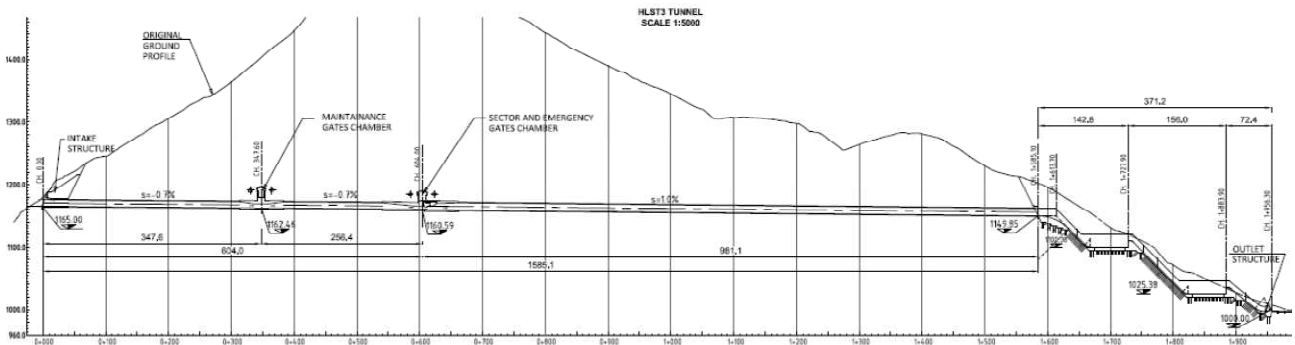


Figure 23. Profile of the High level tunnel spillway 3, for alternative with FSL at El. 1255 m.

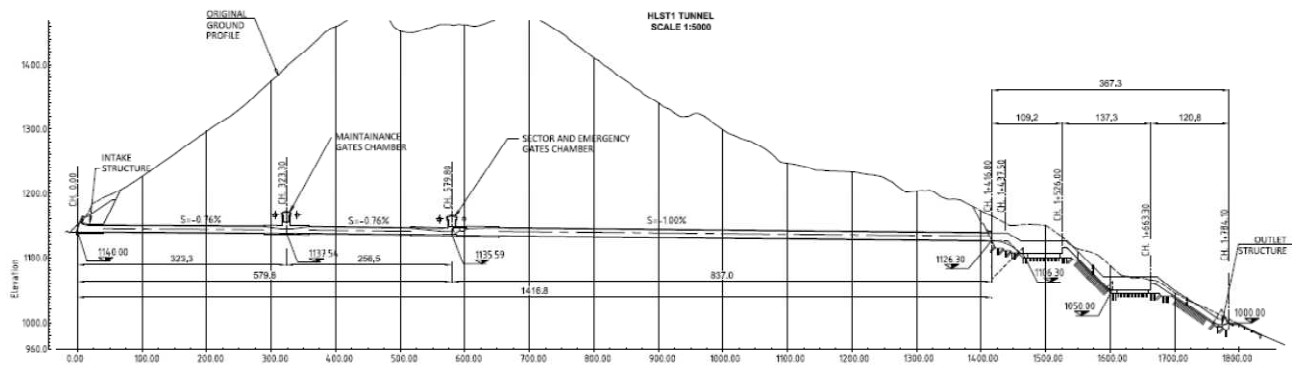


Figure 24. Profile of the High level tunnel spillway 1, for alternative with FSL at El. 1220 m.

The main features and considerations involved in the design of the HLTS1 and HLTS2 for alternatives with FSL at elevation 1290 m are reported here below. They remain valid for all alternatives examined.

Intake structure.

The intake is set at elev. 1190.0; the entrance to the tunnel has a rectangular cross section 18.5 m wide and 10 m high. The average velocity at the intake is about 8.7 m/s. The control of cavitation tendency depends on the length of the transition. In this case a length between 10 and 20 m can be considered conservative. A transition 20 m long has been adopted with a shape close to a elliptical contour, on account of the fact that this structure will operate as permanent discharge facility along the plant lifespan.

Tunnel pressure Stretch.

From the station 00+000 to station 00+509 the slope of the tunnel is 0.75 % and the tunnel is prismatic with horseshoe cross section with 10 m of diameter. Maximum water velocity is close to 20 m/s. At the end of this reach the tunnel presents a transition from the horseshoe cross section to a rectangular cross section 16.5 m wide and 5.15 m high, where the emergency and sector gates are located. The bottom elevation is 1186.15 m a.s.l.

The gates chamber total length including convergent, divergent and prismatic section is approx. 136 m. Two piers with a nose 3 m thick each are used to split the section into three conduits, where three slide gates, 3.5 m wide and 5.15 m high, and three sector gates, 3.5 m wide and 4.65 m high are located. Velocity in the gates conduits is 29.3 m/s and at gates section is 32 m/s. The conduits are steel lined along gate chamber. Also the adjacent stretches of the transitions, 5.0 m upstream and 10.0 m downstream, are steel lined. In principle, the gates operate fully open, but operation at partial openings higher than 50% can be accepted, in consideration of the head and speed on the same.

An air ducts system is located in the expansion area downstream from the gates. A 1.0 m negative aerated step was located in that zone in order to control the cavitation in the area of impact of the lower nappe on the tunnel bottom.

The maintenance gates chamber is located at a distance of about 250 m from the tunnel intake. The chamber is equipped with two slide gates 3.5 m wide and 6.7 m high. Upstream and downstream transitions from the tunnel current horseshoe cross section to the rectangular one (10 m wide and 6.7 m high) and vice versa are provided, each 25.0 m long; the total length of the maintenance gates chamber is 70 m including the gates conduits stretch. Steel lining is foreseen with the same configuration adopted for the emergency and sector gates chamber.

Tunnel free-flow Stretch.

As above mentioned, downstream from the emergency and sector gates chamber the tunnel converges from a rectangular cross section of 16.5 m to a tunnel 10 m wide and 7.0 m high to the springline with a circular arch roof reaching maximum height of 12 m. The tunnel was designed with a slope of 1.0 % up to the outlet portal.

Downstream from the outlet portal, the cascade system described in detail above starts.

4.2.2 Discharge capacity of the High Level Spillway Tunnels

According to the calculation methodology presented for the diversion tunnel N° 3, the maximum discharge with the gates fully open for the alternative FLS 1,290 m a.s.l. is 1,570 m³/s. The Head-discharge curves for various tunnel elevations are given in the following figure.

High Level Tunnels

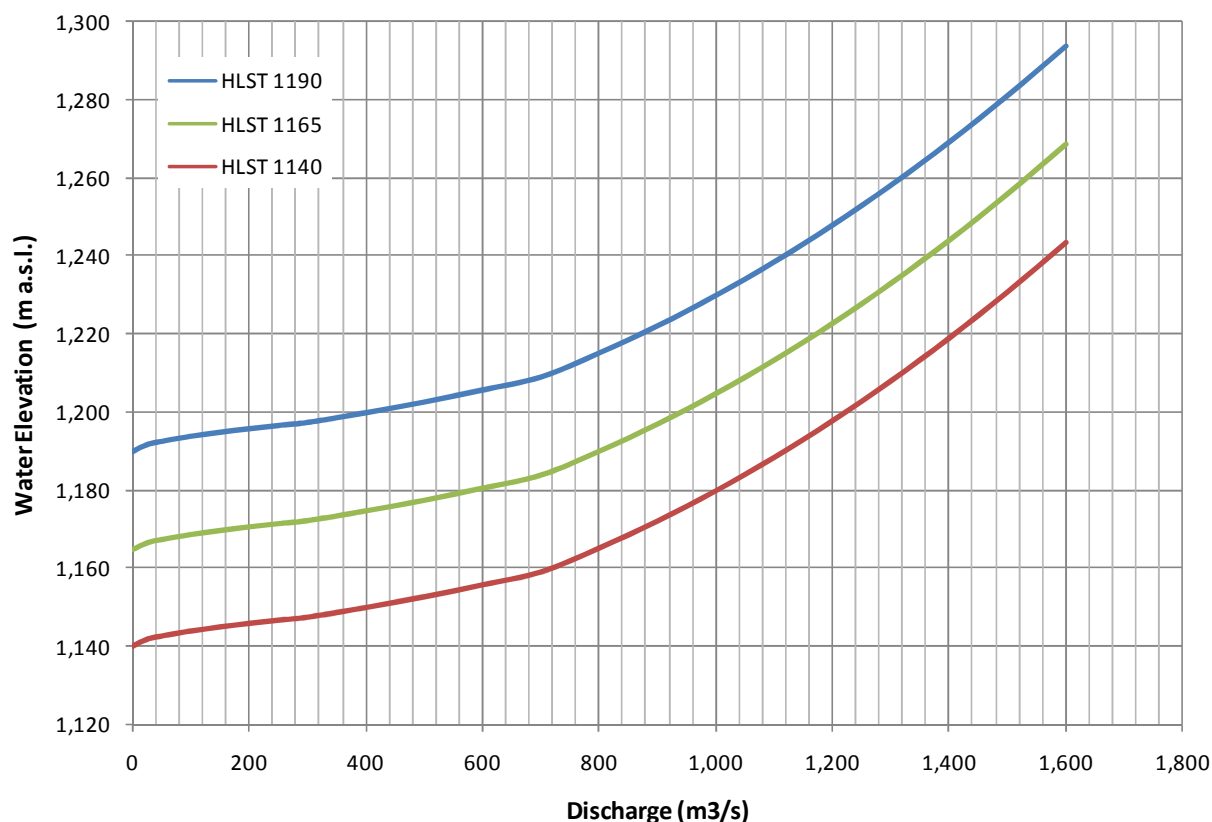


Figure 25. Head – Discharge Relationship. Pressure Tunnel up to gates chamber

4.2.3 Behavior of the high level tunnel spillways in free flow condition

The same problems that have been mentioned while analyzing the other hydraulic facilities are also taken into account here in order of decreasing importance as follows: shock waves, air –water mixture plugs, air entrainment.

In order to avoid or mitigate those possible problems, the measures already implemented in other tunnel were adopted, i.e.:

Upstream and downstream transitions with low deviation angles, normally lower than 4°, adequate free board and aeration system.

In the transition downstream from the gates, three conduits of 2.0 m diameter are adopted. The ventilation intakes would be placed in the tunnel roof immediately downstream from the sector gates.

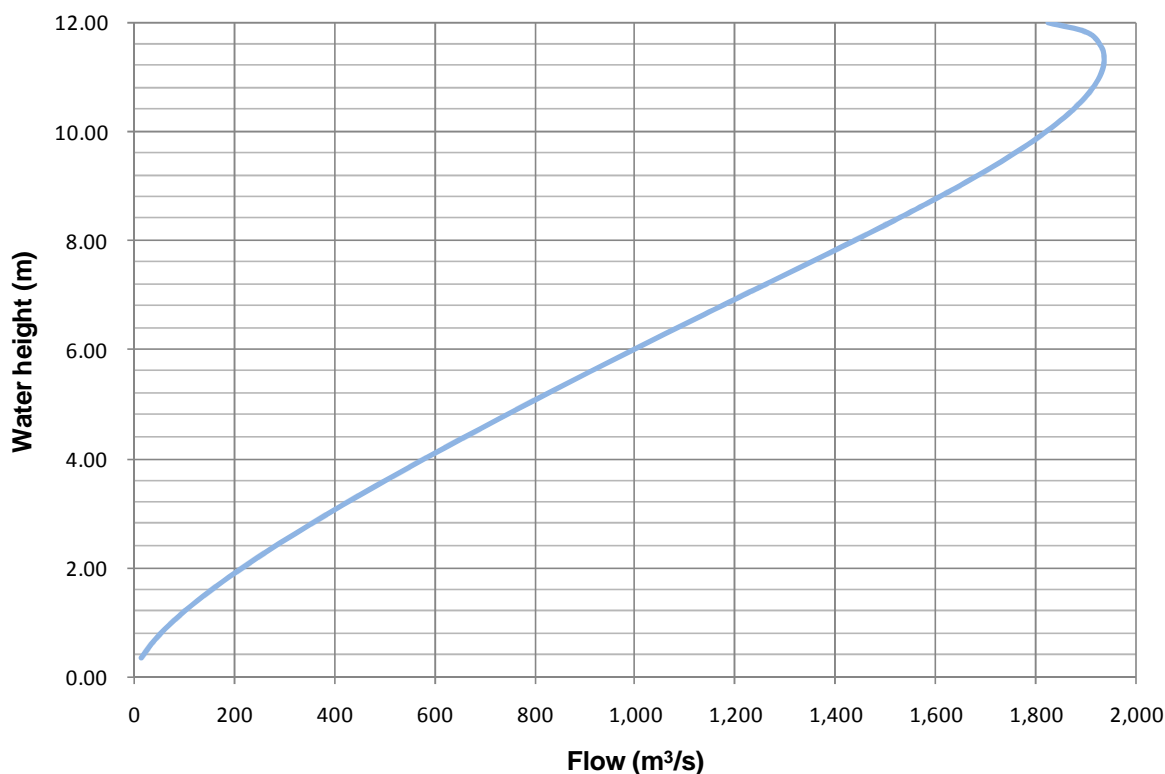
These air intakes are to be connected with a ventilation gallery some 100 m long, 22.3 m² cross section, up the Transportation Tunnel T-39. Calculations performed according with the methodology indicated in paragraph 2.3.5 showed that the global headlosses along the ventilation gallery and tunnel are in the order of 2.92 kPa.

For the design discharge, if the uniform flow condition is considered, the freeboard is about 35%, velocity is about 18 m/s.

It has to be noted that in fact the freeboard will be greater than above indicated, since the initial water velocity at the gates openings is much higher than the above indicated and is progressively decreasing along the free-flow stretch. The conditions of uniform flow are not achieved in the stretch downstream from the gates up to the tunnel outlet, thus the water speed remains higher than that of uniform flow and the freeboard is also higher than above mentioned. This has been taken into account when designing the profile of the chute and the following stilling basin.

The height-discharge relationship for the uniform flow is given in the figure which follows.

High Level Tunnel Spillway - Free flow stretch



4.2.4 Cascade System Verification Approach

The free flow cascade system was verified for three scenarios:

High level tunnel spillway 1, for alternative FSL 1290 m.

High level tunnel spillway 2, for alternative FSL 1290 m.

High level tunnel spillway 3, for alternative FSL 1255 m.

The cascade system consists of a series of chutes and stilling basins which allow dissipating energy while controlling the effect of erosion-cavitation on civil structures, as well as the scouring at the outlet.

In following paragraphs, the design criteria and the methodology adopted for the definition of the cascade system are reported.

4.2.4.1 Uncontrolled overflow ogee crest

The curves of the spillway are designed like those of the uncontrolled ogee crest in subcritical condition, as in the case of a Creager spillway.

$$Q = \alpha H^{\frac{3}{2}}$$

where H is the upstream head.

However, the profile shape for a crest with a vertical upstream face and high approach velocity must be investigated in laboratory in the next phases of the studies. In fact, the discharge coefficient, in this particular case, is strongly influenced by the approach velocity. The efficiency of the spillway depends on a correct assessment of the discharge coefficient.

4.2.4.2 Stilling basin

The stilling basins were used as energy dissipation device, designed in order to contain the hydraulic jump and to decrease the flow velocity at the exit so to reduce scouring downstream from the cascade system.

One of the most effective ways of controlling the hydraulic jump is by means of variations in the bottom profile of the canal. A step, either positive (sill) or negative (drop) is built into the stilling basin. The present project was carried out based on the US Bureau of Reclamation (USBR) criteria, as described by Peterka [24], and from the Saint Anthony Falls Hydraulics Laboratory (SAF), Blaisdell [4], Hager and Sinniger [25] and Hager and Bretz, [11].

Considering the case of a positive step as a design solution, it is important to underline that depending on the tailwater level, the jump could form entirely before the step or, by lowering the TW, the jump could be induced to form partly before and partly over the step. Hager and Bretz [11] proposed the **limit condition** to form a jump entirely before the positive step:

$$F_0^2 = \frac{q^2}{gy_0^3} = \frac{\frac{y_2}{y_0} \left[\left(\frac{y_2}{y_0} \right)^2 + \frac{2a}{y_0} \left(\frac{y_2}{y_0} \right) + 2 \left(\frac{a}{y_0} \right)^2 - 1 \right]}{2 \left(\frac{y_2}{y_0} \right) - 1}$$

The length of the jump can be calculated from the equation of the length of the uncontrolled jump recommend by Hager and Sinniger [25]:

$$\frac{L}{y_0} = 6 \left(\frac{y_2}{y_0} + \frac{1.2 a}{y_0} \right)$$

The design of the stilling basin is based on the above equations. The application of the **limit condition** and the calculation of jump length based on the equations proposed by Hager and Bretz [11] in the studied cases, for y_0 between 2 and 4 m and Froude numbers between 5 and 10, yield a maximum length of about 100 m. The design adopted 65 m long stilling basins, which corresponds to about two third of the maximum jump length, which is considered acceptable on

account of the fact that the strongest rate of energy dissipation occurs in the first half of the hydraulic jump length.

The basin dimensions were then verified with the mathematical model described in chapter 2.3.3 *Water surface profiles in steady flow conditions of operation*.

4.2.4.3 Sidewall height

The sidewalls must extend above the tailwater level at the end of the stilling basin by an amount sufficient to prevent overtopping. Rough water in the stilling basin requires a greater freeboard than is frequently used in open canals. The minimum height of the sidewalls above the water surface at the end of the stilling basin should be:

$$t = y_2/3$$

or greater. All the rules presented here are based on sidewalls extending above the tailwater level, even when submergence must be considered. Under submerged flow conditions, much higher sidewalls may be required; however the freeboard above the tailwater level may be safely reduced somewhat because the water surface would be smoother.

The flow depth and corresponding Froude number at the approach of the stilling basin that were estimated show that the thickness of the stilling basin slab could be between 1.0 and 1.5 m. Prudentially, a slab 2.0 m thick was adopted.

The magnitude of these phenomena cannot be reliably predicted by ordinary computations. Model test will be proposed as a means to confirm the design assumptions and with the aim to optimize the structures both from the technical and economical point of view.

4.2.5 Hydraulics performance of the cascade system

The cascade system must operate in safety condition with the design discharge for the three scenarios:

HLTS 1: $Q=1610 \text{ m}^3/\text{s}$, reservoir water level 1290 m, for alternative FSL 1290

HLTS 2: $Q=1610 \text{ m}^3/\text{s}$, reservoir water level 1290 m, for alternative FSL 1290

HLTS 3: $Q=1610 \text{ m}^3/\text{s}$, reservoir water level 1255 m, for alternative FSL 1255

The following criteria have been adopted in designing the structures of the discharge system: the velocity of the flow along the system must not be higher than 40 m/s adopting air shafts in any case. The maximum head of the chutes is 75 m and the slope is not higher than 45°. The maximum approaching Froude number in the stilling basins is approximately 10 and maximum exit velocity is around 8 m/s.

The length of the stilling basins is 65 m adopting the empirical approach described in 4.2.4.2.

Figure 26, Figure 27 and Figure 28 show the bed profile, water profiles, energy profile, water velocity, water depth and Froude number for the high level tunnel spillways above listed. The oscillating jumps are identified in the stilling basins for scenarios HLTS1 and HLTS2, alternative FSL 1290. The strong jump is reached in the stilling basin in scenario HLTS3.

The energy losses compared to potential energy are as follows:

| Scenario | Energy loss (m) | Potential energy (m) |
|---------------------------|-----------------|----------------------|
| HLTS 1, alt. FSL El. 1290 | 163 | 192 |
| HLTS 2, alt. FSL El. 1290 | 189 | 192 |
| HLTS 3, alt. FSL El. 1255 | 144 | 171 |

Table 8. Energy loss, compared to potential energy calculated as difference between water level at the entrance and on the flip bucket

The STEFLO mathematical model is a steady flow algorithm used to compute the flow-line based on the elementary principles stated by Molinas and Yang [17]. The computation of both supercritical and subcritical flow regimes is allowed. Hydraulic jumps occurrence and location are taken into account.

In fact, STEFLO is capable of treating transcritical flow with a generalized approach. In other words, it is not necessary to identify the control sections. The computation automatically identifies the hydraulic jumps and mixed flows. The application of STEFLO in the case of the cascade system allowed assessing the empirical design criteria adopted in the design of the stilling basins and of the spillways.

It is deemed that the ordinary computations performed for evaluating the hydraulic behavior of such a complex system cannot be considered totally reliable. Model tests will be required in order to confirm the design assumptions and for optimizing the structures both technically and economically.

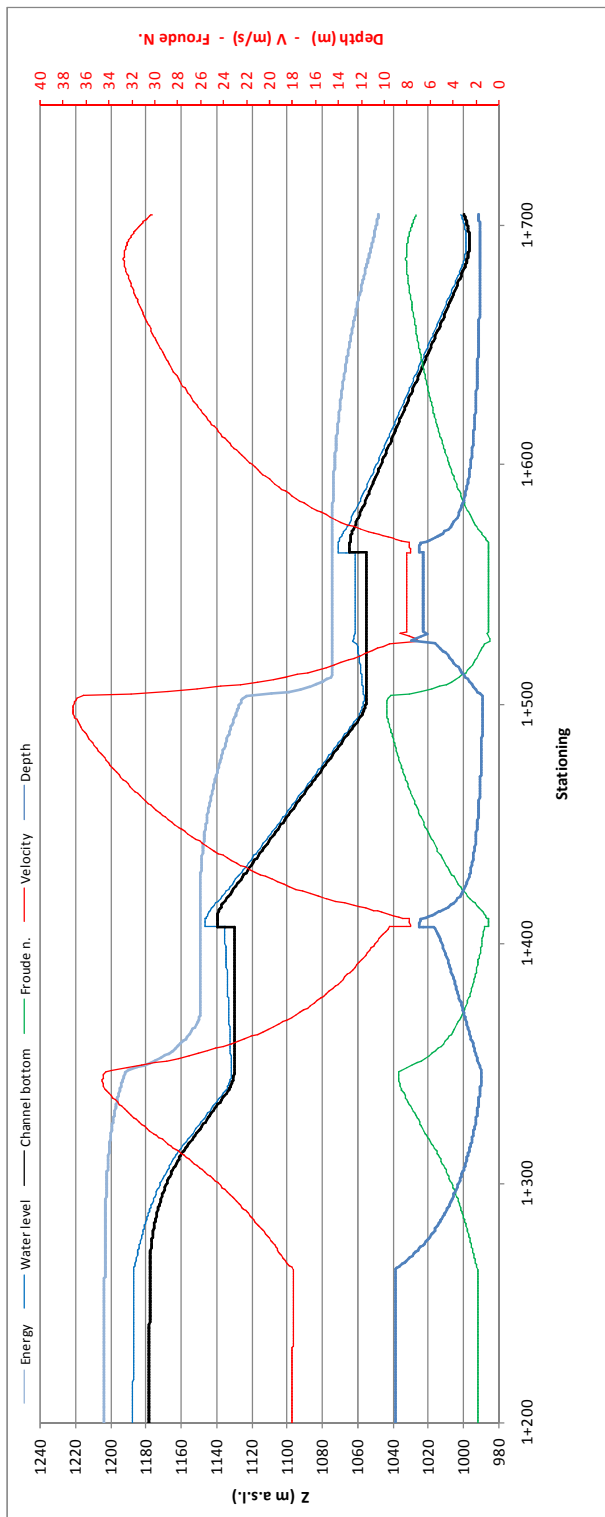


Figure 26. Water profile and hydraulic characteristics for High level tunnel spillway 1, FSL elevation 1290 m

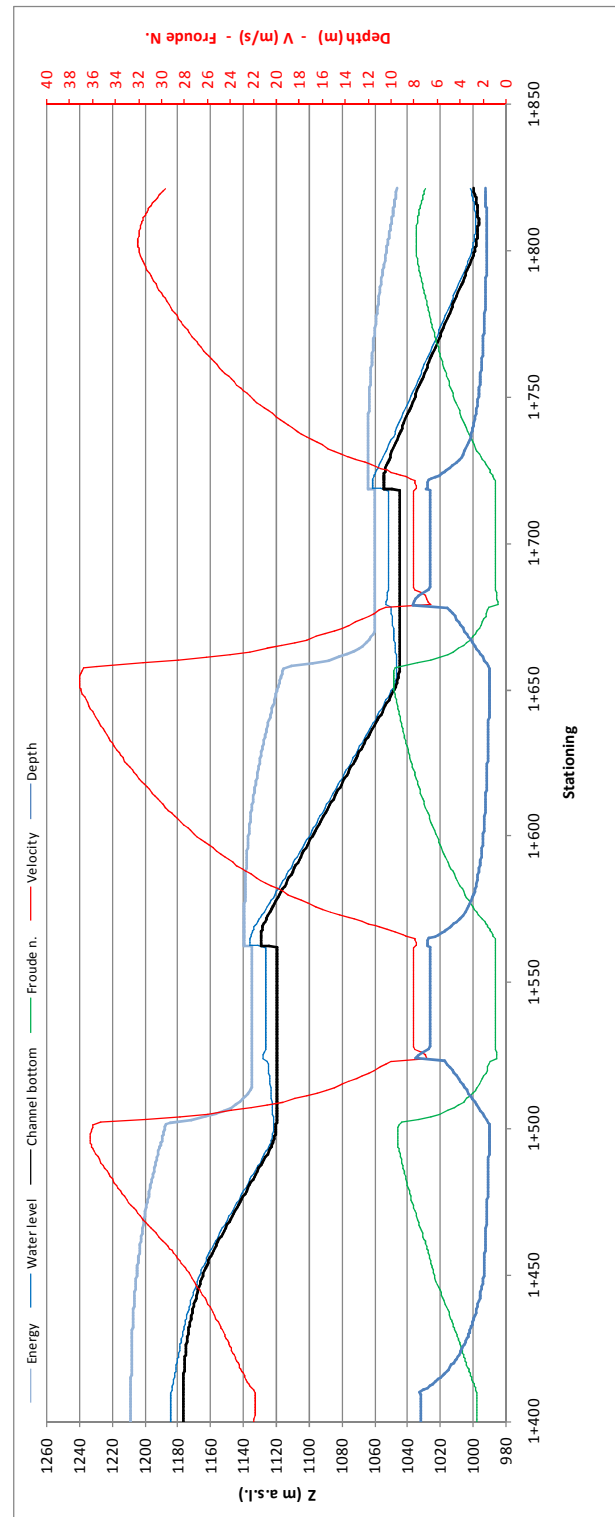


Figure 27. Water profile and hydraulic characteristics for High level tunnel spillway 2, FSL elevation 1290 m

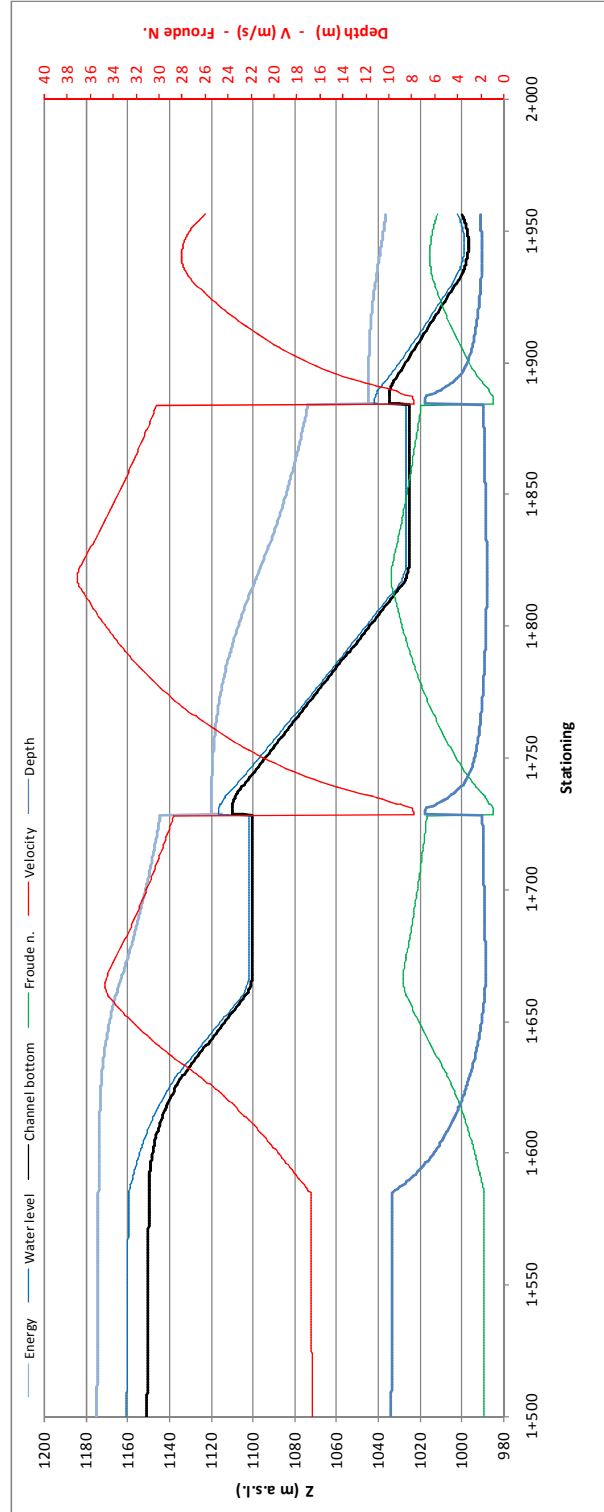


Figure 28. Water profile and hydraulic characteristics for High level tunnel spillway 3, FSL elevation 1255 m

4.3 Flip bucket

4.3.1 Jet trajectories

This section analyses the jet trajectories taking into account a 30° take-off angle for three scenarios: High level tunnel spillways 1 and 2 for FSL elevation 1290 m, and High level tunnel spillway 3 for FSL elevation 1255 m.

The distribution of the dynamic pressures on the plunge pool bottom is examined and compared with the impact pressure applying the Hartung and Häusler method [11] that is indirectly based on the specific stream power of plunging jet transmitted to the bed.

As in the case of the middle level outlets, the profile is calculated by applying the USBR formula [2] that gives the trajectory of the lower nappe of the jet (the origin of the coordinates is taken at the end of the lip).

$$y = x \cdot \tan(\alpha) - \frac{x^2}{K[4 \cdot (d + h_v) \cdot \cos^2(\alpha)]}$$

where:

x = horizontal distance

y = vertical distance

α = angle of the edge of the lip with the horizontal

K = coefficient allowing for the effects of air resistance on the jet trajectory

d = thickness of the jet

$h_v = V_i^2 / (2g)$

g = acceleration due to gravity

The results are summarized in the next table:

| Z_{ip} [m a.s.l.] | Take off angle [°] | Impingement distance form lip [m] | Impingement angle $\left(\frac{dy}{dx} \Big _{X=X_0} \right)$ [°] | Trajectory length $\left(\int_0^{x_0} \sqrt{1 + \left(\frac{dy}{dx} \right)^2} dx \right)$ [m] |
|---------------------|--------------------|-----------------------------------|--|--|
| 1000.0 (HLTS 1) | 30 | 91 | 45 | 102 |
| 1000.0 (HLTS 2) | 30 | 90 | 46 | 101 |
| 1000.0 (HLTS 3) | 30 | 74 | 48 | 84 |

Table 9 – Summary Results of jet trajectories for the three calculated scenarios - see par. 4.2.5

The computation has been performed for the discharge of 1610 m³/s.

Possible need for the plunge pool pre-excavation and its depth will be defined according to the impact pressure at the surface.

4.3.2 Plunge Pool

As described for Middle Level Outlets and Diversion Tunnel n°3, the depth of erosion is evaluated making use of the same methodology explained in Paragraph 2.3.4.

The following values are adopted:

For HLTS1 and 2 FSL 1290:

- $q = 1,570 \text{ m}^3/\text{s} / 30 \text{ m} = 52.4 \text{ m}^3/\text{s}/\text{m}$
- $H = 67.6 \text{ m}$
- $d = 1 \text{ m}$

| Author | D (m) 1570 m ³ /s | D (m) 1000 m ³ /s | K | x | y | w | z |
|---------------|---------------------------------|---------------------------------|-------|------|-------|------|------|
| Veronese (B) | 41.6 | 32.5 | 1.9 | 0.54 | 0.225 | 0 | 0 |
| Veronese mod. | 32.9 | 25.7 | 1.9 | 0.54 | 0.225 | 0 | 0 |
| Damle (A) | 38.8 | 30.8 | 0.652 | 0.5 | 0.5 | 0 | 0 |
| Damle (B) | 32.3 | 25.7 | 0.543 | 0.5 | 0.5 | 0 | 0 |
| Damle (C) | 21.5 | 17.1 | 0.362 | 0.5 | 0.5 | 0 | 0 |
| Martins (A) | 31.1 | 23.7 | 1.9 | 0.6 | 0.1 | 0 | 0 |
| Martins (B) | 24.6 | 18.7 | 1.5 | 0.6 | 0.1 | 0 | 0 |
| Mason | 32.8 | 25.0 | 3.27 | 0.6 | 0.05 | 0.15 | -0.1 |
| Taraimovich | 25.7 | 19.0 | 0.633 | 0.67 | 0.25 | 0 | 0 |
| INCYTH | 29.3 | 23.3 | 1.413 | 0.5 | 0.25 | 0 | 0 |
| Pinto | 26.2 | 20.5 | 1.2 | 0.54 | 0.225 | 0 | 0 |
| Chee and Kung | 41.5 | 31.6 | 1.663 | 0.6 | 0.2 | 0 | -0.1 |

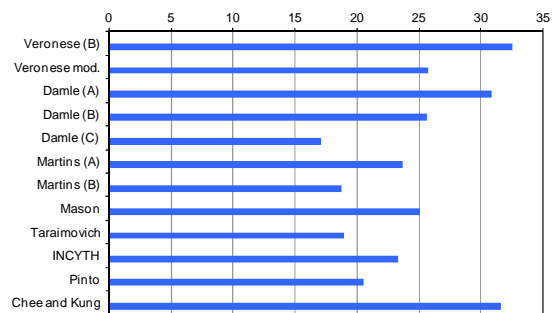
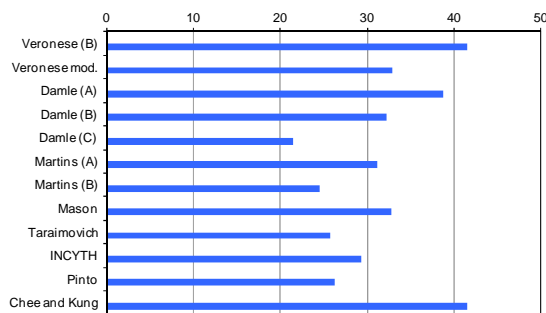


Figure 29 Scour depths (m) calculated by using different empirical formulae for 1570 m³/s and 1000 m³/s.

The same considerations made for DT-3 are applicable in the case of the High Level Tunnel Spillways; in fact, by applying the pressure bulb theory to the case of HLTS 1 and 2 for the discharges of 1570 m³/s and 1000 m³/s and HLTS3 for the discharge of 1490 m³/s we can observe:

In the case of HLTS 1 and 2, the take-off angle is 30°. The take-off velocities are of approximately 30 m/s for both cases (without considering the head losses). The elevations corresponding to the energy at the flip bucket are 1047.6 and 1047.0 m a.s.l. while the tailwater elevation is 980 m a.s.l.

The horizontal distance of the point of impact of the jet with respect to the flip bucket is 91 m for the discharge 1570 m³/s and 90 m for 1000 m³/s.

Figure 30 shows, for the discharge 1570 m³/s, the pressure bulb with respect to the point of impact where the impact pressure is $P_u = 68.5 \text{ T/m}^2$ (6.85 kg/cm²) with an impingement angle of 45°, while the Figure 31 shows, for the discharge of 1000 m³/s, the pressure bulb with respect to the point of impact, where the impact pressure is $P_u = 67.5 \text{ T/m}^2$ (6.75 kg/cm²) with an impingement angle of 45°. In fact, there is no difference in the trajectories, since the energy at the take-off is basically the same in both scenarios, head losses can be considered negligible given the simplified approach adopted in the calculation of the impact dynamic pressures. Nevertheless, the pressure bulbs are different, due to the different specific discharges.

Considering, also in this case, a pressure value of 15 T/m² (1.5 kg/cm²) as an erodibility threshold, we can see from Figure 30 and Figure 31 that this value is reached at a distance of 13 m along the axis of the bulb for the 1570 m³/s case, while for the 1000 m³/s case this happens at 8 m.

In this situation, given the head and the specific discharge, the plunge pool pre-excavation would not be strictly necessary. However, since the falling jet is impacting on the right bank of the river, measures to protect the same bank and avoid instability of the outlet structures are proposed.

Those measures consist in pre-excavating the possible scouring area down to el 970 m a.s.l. for a width equal to 1.5 times the flip bucket and to protect the bank with a concrete structure constituted by a grid of beams and a slab 1 m thick laying on the excavation slope, anchored to the rock by tendons. A terminal cut-off some 8 m deep is foreseen at the lower end of the protection structure, reaching a depth of almost 25 m below the original ground surface.

Anyway, experimental tests are necessary in order to more precisely evaluate the local scouring over the right bank and to more precisely define the extent of the mitigation structures.

Figure 32 shows the pressure bulb in the case of HLTS 3. The maximum bulb pressure is 57.3 T/m² in the point of impact and the specific discharge is 49.7 m³/s. The pressure of 1.5 kg/cm², considered as erodibility threshold, is reached at a distance of 11 m.

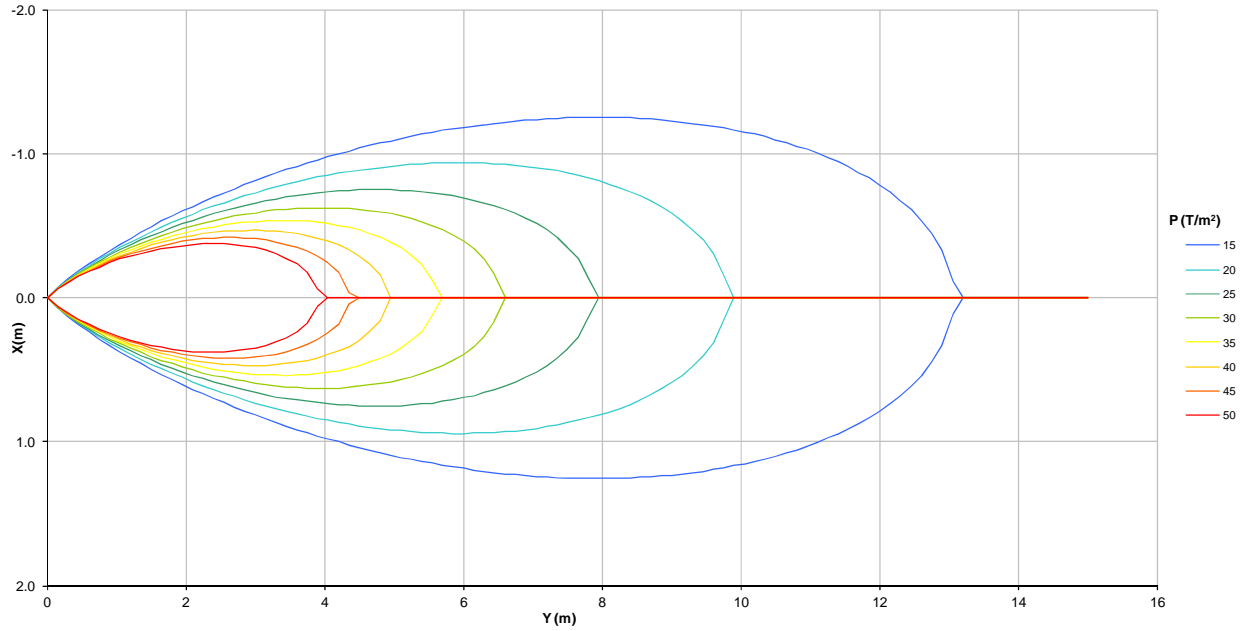


Figure 30 Hydrodynamic pressure bulb: $Q = 1570 \text{ m}^3/\text{s}$. Pressure in the point of impact $P_u(0,0) = 68.5 \text{ T/m}^2$. Angle of impact 45° .

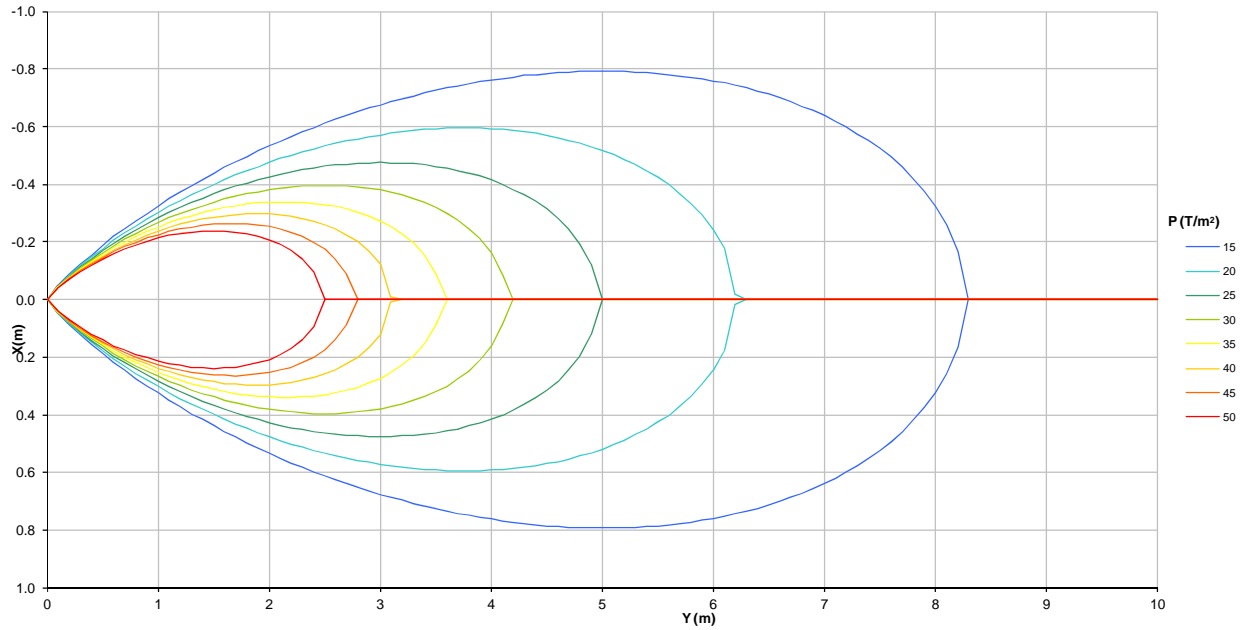


Figure 31 Hydrodynamic pressure bulb: $Q = 1000 \text{ m}^3/\text{s}$. Pressure in the point of impact $P_u(0,0) = 67.5 \text{ T/m}^2$. Angle of impact 45° .

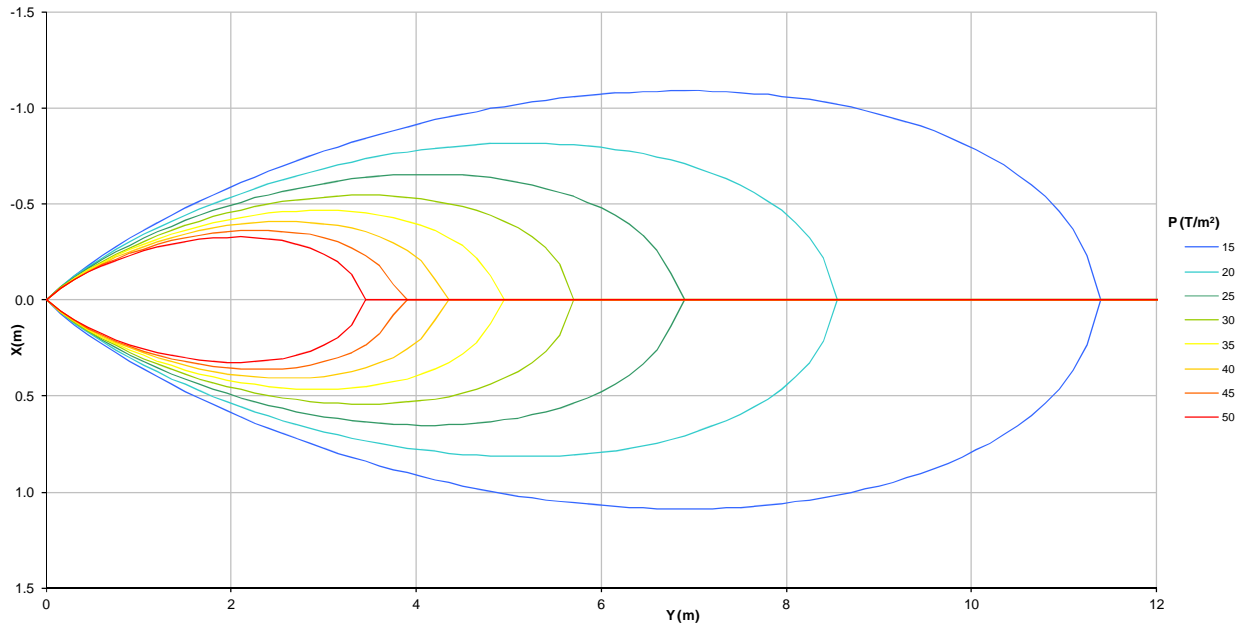


Figure 32. Hydrodynamic pressure bulb: $Q = 1490 \text{ m}^3/\text{s}$. Pressure in the point of impact $P_u(0,0) = 57.3 \text{ T/m}^2$. Angle of impact 48° .

Figure 33 shows the jet trajectory and pressure bulb for HLTS 1 and 2, while Figure 34 show the same for HLTS 3, $Q = 1490 \text{ m}^3/\text{s}$.

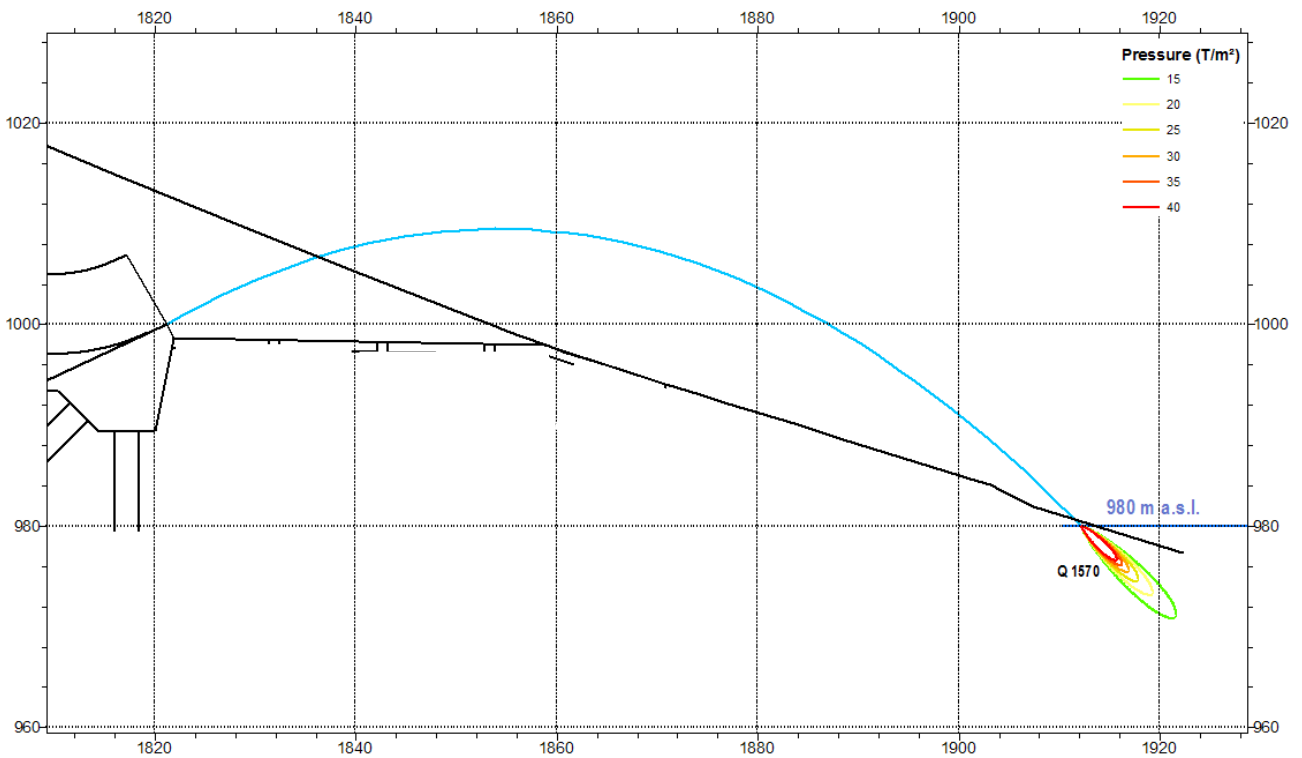


Figure 33. Jet trajectories for High level tunnel spillway 1 and 2 (FSL EL. 1290 m), with a flip bucket angle of 30° ; $Q = 1570 \text{ m}^3/\text{s}$

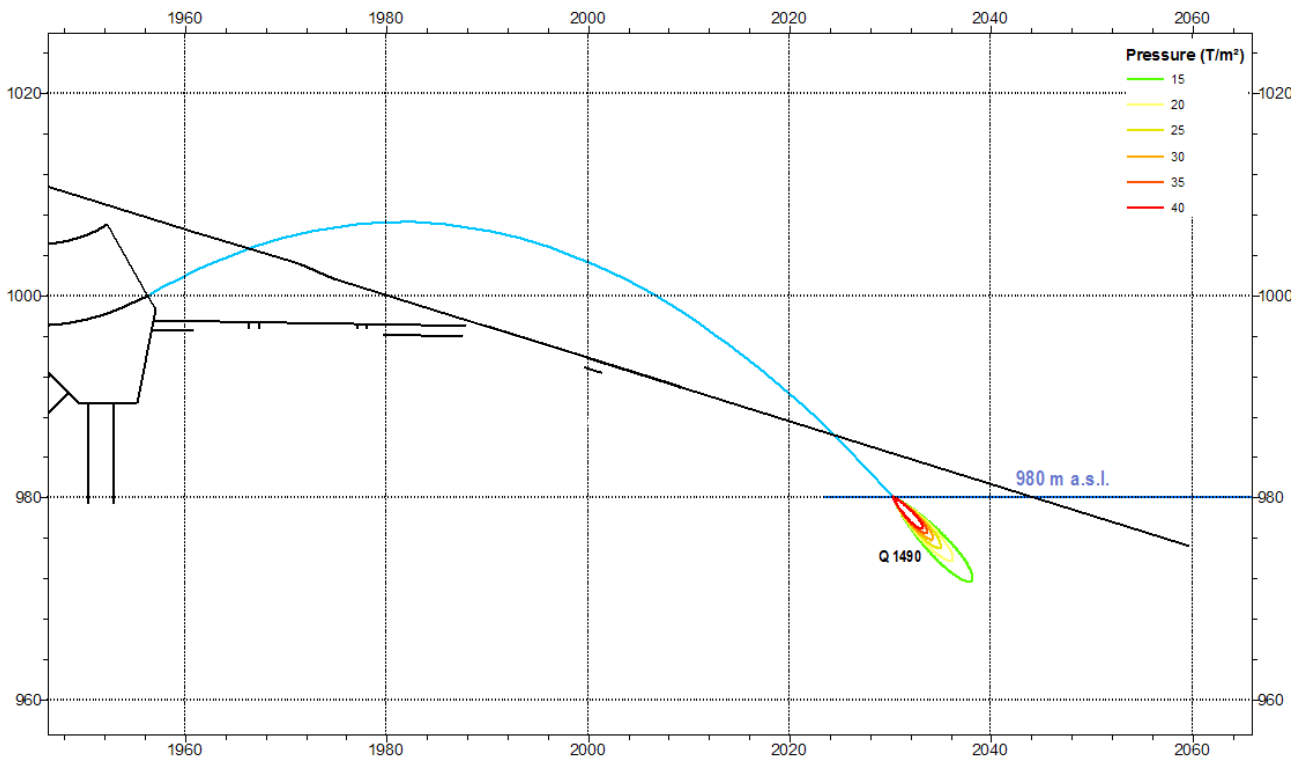


Figure 34. Jet trajectories for High level tunnel spillway 3 (FSL EL. 1255 m), with a flip bucket angle of 30° and $Q = 1490 \text{ m}^3/\text{s}$

5 SURFACE SPILLWAY

5.1 Design Criteria

In this paragraph only the design criteria and data related to the specific function of the surface spillway are listed. Detailed design procedures and criteria are given in the next chapter (“Calculations”) where the design is developed.

The surface spillway, as an ultimate stage flood evacuation facility, should replace in the long term the flood evacuation facilities planned for the beginning of the useful life of the project (first stage evacuation facilities).

Its discharge capacity must be, accordingly, equal to the peak discharge of the Probable Maximum Flood (PMF). See probability of floods in table 1, below.

It is supposed to be partially or fully operational when the sediment load in the reservoir affects the discharge capacity of tunnels having lower level intakes.

Because of the sediment load, the future surface spillway is to be designed and built in such a way that erosion damages caused by sediments running along it can be easily repaired by isolating part of the spillway.

Other design criteria as location and alignment, specific discharge, cavitation index, number of bays, sill efficiency, energy dissipation, geotechnical aspects of tunnel excavation, etc. are given in the next paragraph as the design progresses.

| VAKHSH River at the ROGUN H.P.P. | | | |
|----------------------------------|---|--------------|--------------|
| Flood Probability | | | |
| TMR (yr) | Peak Discharge (daily; m ³ /s) | | |
| | Lower* | Calc. | Upper* |
| 2 | 2 200 | 2 300 | 2 300 |
| 5 | 2 600 | 2 700 | 2 800 |
| 10 | 2 900 | 3 000 | 3 100 |
| 20 | 3 100 | 3 300 | 3 400 |
| 50 | 3 400 | 3 600 | 3 800 |
| 100 | 3 700 | 3 900 | 4 100 |
| 200 | 3 900 | 4 200 | 4 400 |
| 500 | 4 200 | 4 500 | 4 800 |
| 1 000 | 4 500 | 4 800 | 5 100 |
| 2 000 | 4 700 | 5 100 | 5 400 |
| 5 000 | 5 000 | 5 400 | 5 800 |
| 10 000 | 5 300 | 5 700 | 6 100 |
| PMF | 6 100 | 7 000 | 7 800 |

* : Conf. Interval of 95% (99%)

Table 5.1: Probability of Floods

5.2 Calculations

5.2.1 Pre-analysis

The simplest configuration of a surface spillway evacuating large floods in the Rogun HPP consists of a series of gated sills followed by a sub-horizontal channel and then a chute channel “copying” the local topography and then returning the flow into the river through a ski-jump-type end structure.

Such a configuration is shown in figures 5.1 (longitudinal section) and 5.2 (plan view).

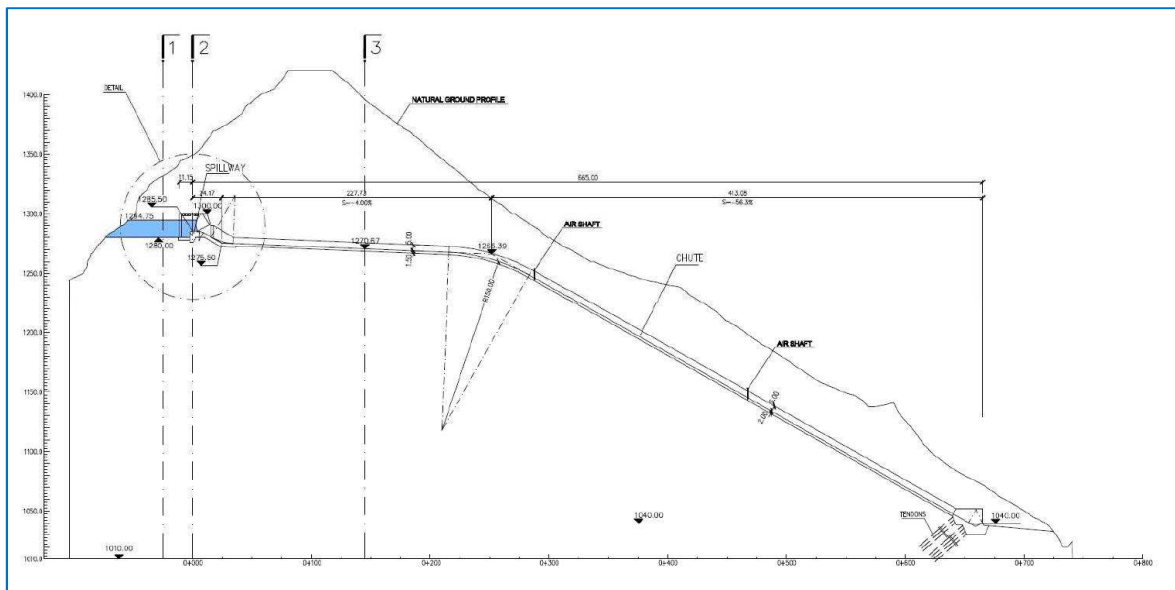


Figure 5.1: First approach spillway configuration (longitudinal section)

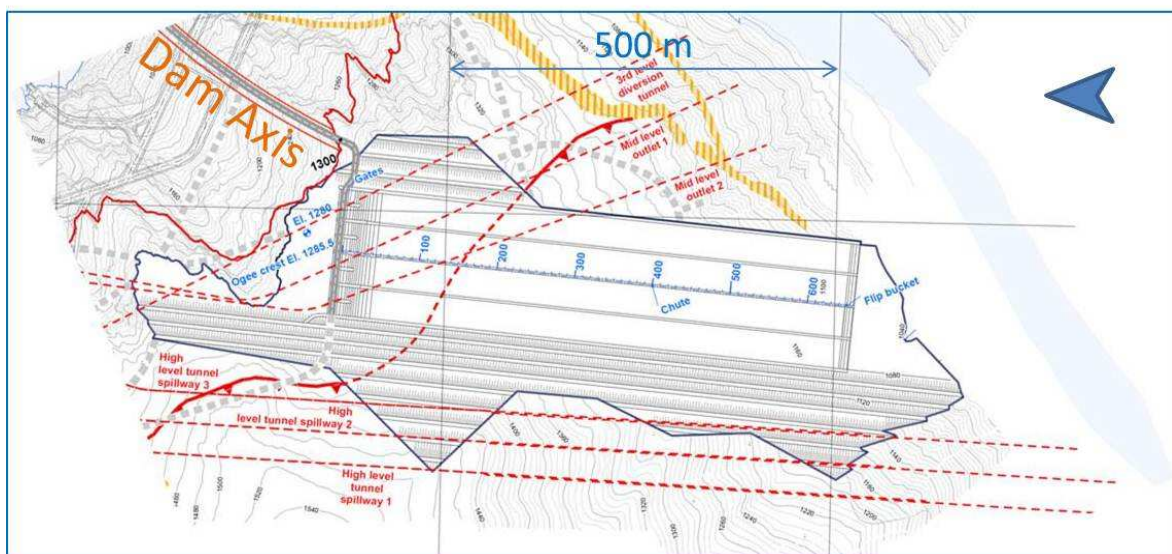


Figure 5.2: First approach spillway configuration (plan view, schematic)

In this first approach configuration the head above the spillway sill is of approximately 10 m. Difference in elevation between the sill and the beginning of the sub-horizontal channel (4% slope) is again approximately 10 m, as well as between this latter and the vertical bend prior to the chute channel (56%). The total difference in head along the chute channel is about 210 m and the head difference between the ski jump and the river is about 80 m for the PMF. The total vertical distance between the reservoir level and the river is then about 320 m when the PMF is being evacuated.

The specific discharge along the channels adopted for this preliminary analysis is close to $50 \text{ m}^3/\text{s}/\text{m}$ (four 40 m wide channels to evacuate the PMF of $7,800 \text{ m}^3/\text{s}$).

The main hydraulic parameters of this configuration, when evacuating the PMF, are shown in figure 5.3.

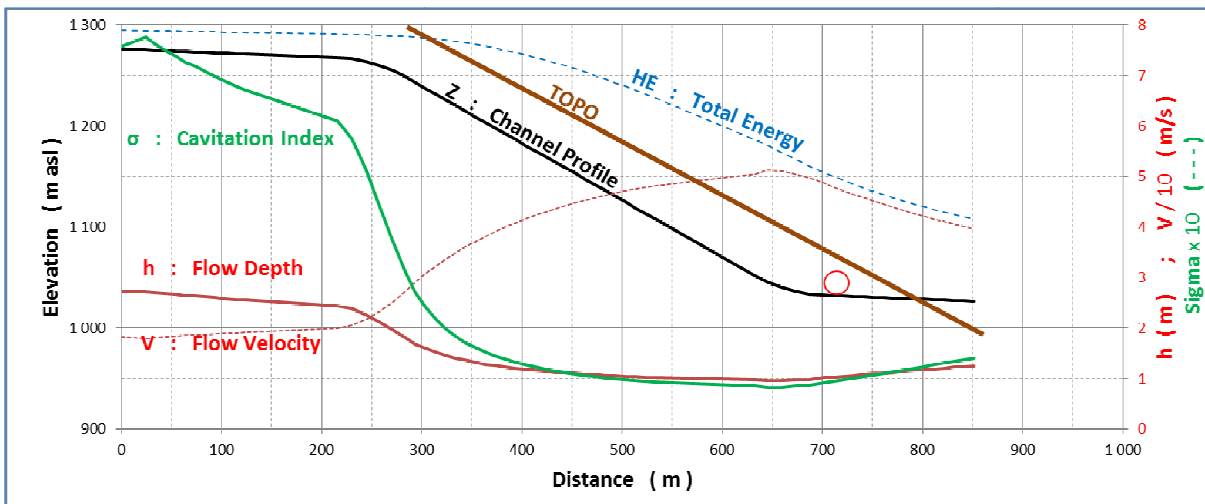


Figure 5.3: First approach spillway configuration (main hydraulic parameters for PMF)

The hydraulic “picture” of the first approach configuration shows the following characteristics:

- in the sub-horizontal stretch the water depth and the flow velocity reach the values of 2.5 m and 20 m/s, respectively, while the cavitation index takes a value of approximately $\sigma = 0.6$ just before the vertical bend.
- in the high slope reach the water depth rapidly decreases down to 0.9 m just before the next sub-horizontal reach where the ski jump (red circle) is located.
flow velocity rapidly increases up to some 50 m/s while the cavitation index gets down to $\sigma = 0.1$ and even a little less.
- at the end of the chute channel the total head (water depth plus kinematic head) is about 130 m.

Let us recall that the cavitation index is defined as:

$$\sigma = \frac{(p_a/\gamma + h_F - h_v)}{v^2/2g}$$

where:

- p_a : atmospheric pressure, with γ : specific gravity of water
- h_F : depth of flow
- h_v : vapor pressure, when cavities start getting formed.
- v : flow velocity.

The cavitation index characterizes the potential for a flow to produce cavitation and cavitation damages. The larger the cavitation index, the smaller the risk of cavitation damages to occur. The cavitation index of a given flow should be larger than the cavitation index of geometrical irregularities in the channel surface if cavitation is to be avoided.

Design practice ⁽¹⁾ recommends the following limits for cavitation indices of flow:

- $\sigma < 0.1$: risk of cavitation is too high, change the design
- $0.1 < \sigma < 0.2$: acceptable only under tough preventive measures (aeration, fine surface finishing) and short operation time.
- $0.2 < \sigma$: design scheme may go on. Preventive measures as flow aeration, fine surface finishing may be helpful.

At the light of these design standards and recommendations, the first approach configuration for the surface spillway had to be rejected and a new design scheme to be proposed.

A second configuration was then proposed in which three sets of sub-horizontal and high slope channels are chained as indicated in figure 5.4. The total height of each set is about 70 m.

In order to minimize the excavation, the slope of the chute channels was made as steep as 0.8H:1V, as in the spillways of typical concrete gravity dams.

The reason for selecting a height of 70 m is two-fold:

- at the end of the first step of the cascade a high but still acceptable flow velocity of 40 m/s has been reached and specially the cavitation index, with a value $\sigma \approx 0.2$, falls within the recommended limits.
- the difference in height between the highest and the smallest dam alternatives is 70 m (FSL = 1290 m a.s.l. – 1220 m a.s.l.). This allows for adopting in both cases the same scheme, just eliminating one step in the cascade of the lowest dam.

In this alternative spillway configuration, the flow velocity reaches a value of some 40 m/s at the end of the first chute channel and does not increase along the sub-horizontal reach. But it increases again in the second and third chutes. The final head (at the level of the end structure) is

⁽¹⁾ *Cavitation in Chutes and Spillways / Henry T. FALVEY / USBR-1990*

even larger than in the former case. This is indeed explained by the fact that energy losses along the sub-horizontal reaches are less than in the former high slope reach.

Cavitation indices are also as low as in the former case, leading (according to the standard design recommendations) to rejection of the design scheme.

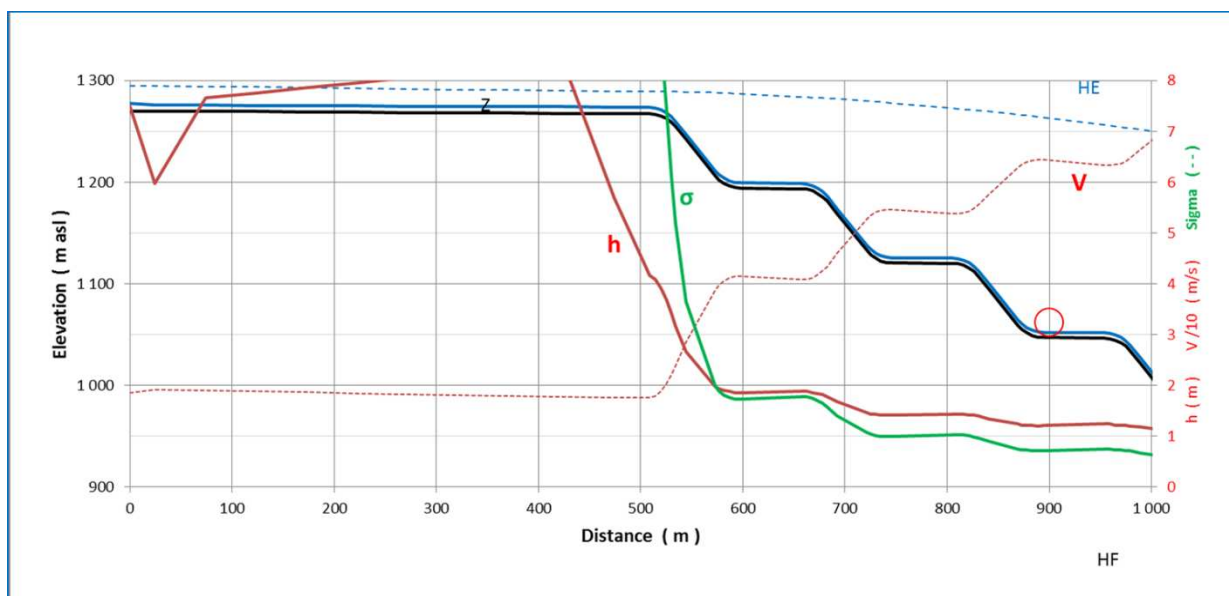


Figure 5.4: Second configuration (cascade), hydraulic main parameters

The conclusion is that if cavitation indices are to be raised up to a value of 0.2, the flow velocity is to be lowered. The only way of reaching this objective is by dissipating energy every time that the velocity reaches a given, tolerable limit value.

This is done by introducing a stilling basin in the two first sub-horizontal channel reaches.

The third scheme consists then of a three step cascade with intermediate energy dissipation, ending (as in the former configurations) with a ski jump.

The next paragraphs will describe the hydraulic solutions proposed for each component of the surface spillway.

5.2.2 Analysis of the adopted configuration

5.2.2.1 General Alignment

The next figure shows the possibilities for location of the surface spillway in the right bank.

Other hydraulic structures (tunnels) are also indicated together with the elevation of their outlets: the Diversion Tunnels (DTs), the Mid-Level Outlets (MLs) and the High-Level Outlets (HLs).

For the easiness of reading the sketch also shows the main level curves in a simplified way.

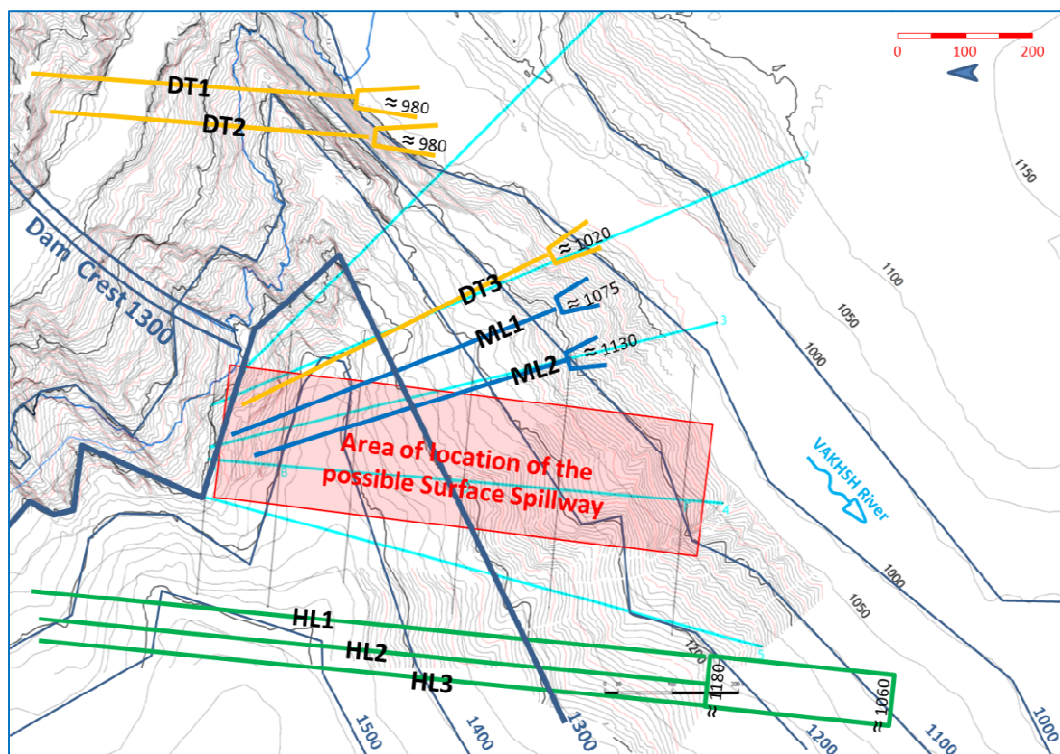


Figure 5.5: Constraints for location of the Surface Spillway

The area where the surface spillway could be placed is not aligned with the gradient (maximum slope) of that bank, which varies in the area from 1V:1H to 1V:1.3H. This fact will increase the volume of excavation on the one side, but on the other side will allow for placing the intermediate energy dissipators announced in the former paragraphs.

Two other topics related with the topographical conditions are to be observed in the sketch:

- The topography along the potential flow alignment reaches El. 1430-1440, while the reservoir elevation is about 1290 or lower. This topographical condition can be solved either with a full excavation of the rock heights or crossing it with tunnels.
- The access of flow from the reservoir into that area is confined between the dam crest and a salient rock overhang. At elevation 1300 the corresponding width is close to 250 m.

The first subject will be more cheaply handled by crossing the rock heights with tunnels: this is the result of a preliminary cost estimate of both alternatives for the highest dam alternative, with Full Supply Level (FSL) at 1290 m asl. For the two other dam alternatives with lower FSLs (namely 1255 and 1220) the tunnel solution will be, a fortiori, the best solution. Tunnels will then be adopted as the design solution for crossing the above mentioned rock heights in the three dam height alternatives.

The second topic (flow access to the spillway channels/tunnels) will be treated in the next paragraph: approach bay.

5.2.2.2 Approach Bay

The flow approaching from the reservoir into the spillway area should not affect the rip-rap blocks in the nearby standing upstream face of the dam. Indeed, an approach bay too close to the dam crest may produce block instability because of tangential flow velocities along the upstream face of the dam.

In order to avoid that effect, a minimum distance of some 50 m will be left between the axis of the dam crest and the closer side of the approach bay. This design criterion leaves some 200 m available for the approach bay out of the 250 m mentioned in the former paragraph.

Should this scheme be adopted, the specific discharge in the approach bay would be $q = Q / b = 7800 \text{ m}^3/\text{s} / 200 \text{ m} = 39 \text{ m}^3/\text{s}/\text{m}$. Together with a water depth slightly below 20 m it will generate an average approach velocity of some 2 m/s, comfortable enough for a safe design.

Should the approach bay lead to four conduits, the characteristic dimensions of the main structures will be approximately those indicated in figure 5.6, as the available room is $\approx 200 \text{ m} / 4 \approx 50 \text{ m}$. In the sketch below four bays with a width of 51 m have been adopted. The conduits mentioned above are a tunnel, first, to cross the rock heights between the reservoir and the river and a chute channel then to lead water back to the river.

With that width it becomes possible to lodge $2 \times 4 = 8$ spillway bays having a discharge capacity of nearly $1,000 \text{ m}^3/\text{s}$ each when the PMF ($7,800 \text{ m}^3/\text{s}$) is discharged. The same width allows also for excavating tunnels with their axis separated to each other by as much as three tunnel widths.

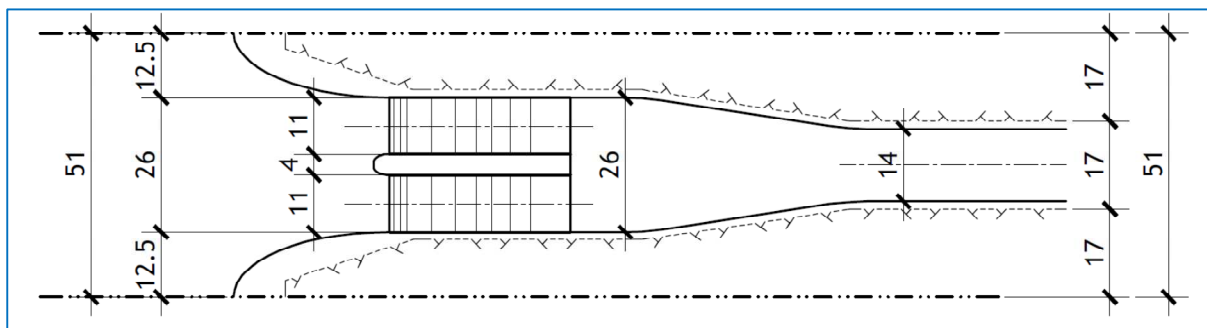


Figure 5.6: Scheme of works (plan view) in case of four bays

In case of selecting only three conduits, the width available for each section will be $\approx 200 \text{ m} / 3 \approx 67 \text{ m}$. In the sketch below three bays with a width of 68 m each have been adopted. In these conditions, a total of $3 \times 4 = 12$ spillway bays will exist with a discharge capacity of nearly $675 \text{ m}^3/\text{s}$ each. The same rules as before are applied for the selection of the tunnel width.

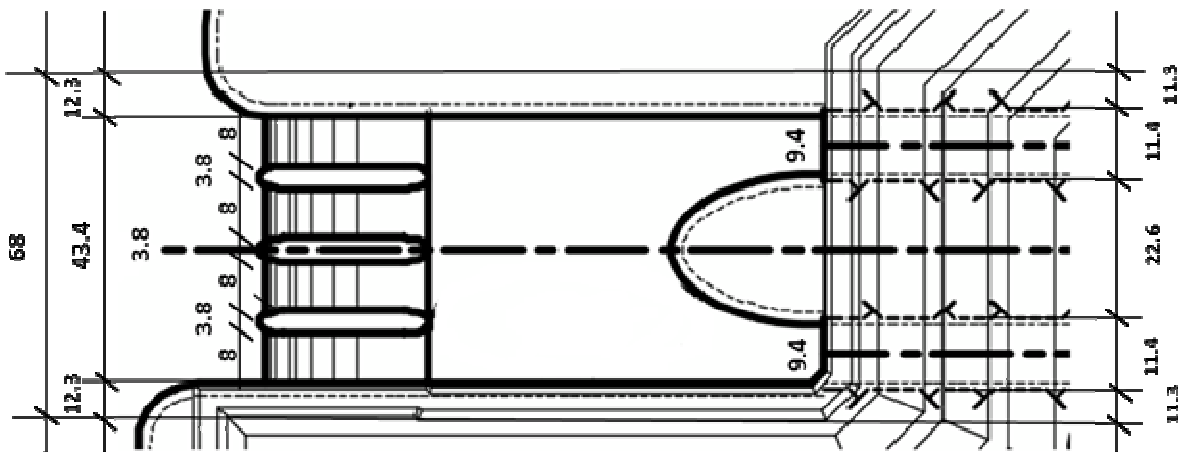


Figure 5.7: Scheme of works (plan view) in case of three approach bays. Two tunnels per bay.

It will be shown below that the volume of excavation for the alternative with four “conduits” is significantly larger than in the case of three. The alternative with three conduits is then preferred. It supposes three, 68 m wide approach bays with four spillway bays each. This scheme will be further developed in the next paragraphs.

5.2.2.3 Gated Sills

The evaluation of the discharge capacity of the surface spillway followed the methodology proposed by the USBR (Bureau of Reclamation), described below.

$$Q = m_0 \cdot r_1 \cdot r_2 \cdot r_3 \cdot r_4 \cdot \sqrt{2g} \cdot N \cdot b \cdot (H - H_0)^{1.5}$$

where (see figure 6.8):

- Q : total spillway discharge
- m_0 : discharge coefficient due to vertical contraction of a standard Creager profile
- r_1 : adjustment due to operation for heads other than the design head
- r_2 : adjustment for u/s face slope other than vertical
- r_3 : adjustment for drawn flow
- r_4 : adjustment for abutment and pier conditions
- N : number of spillway (gated) bays
- b : width of those bays
- h : head over the spillway sill: $h = H - H_0$
- H : water surface elevation in the approach area
- H_0 : elevation of the spillway sill.

The corresponding design graphs and formulae are given in Annex 2.

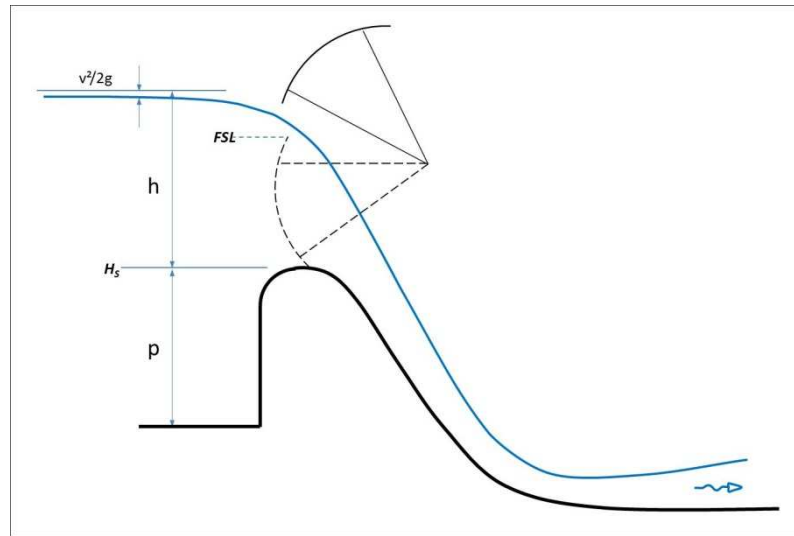


Figure 5.8: Vertical section of the spillway sill, definitions

Taking into account that this spillway is to be designed for the long term future conditions, when the reservoir has lost its regulating capacity, the design discharge is to be adopted equal to the peak of the Probable Maximum Flood (PMF). No peak dumping due to reservoir routing is then considered. The peak discharge of the PMF (in daily terms) equals $7770 \text{ m}^3/\text{s}$ (we use the value $7800 \text{ m}^3/\text{s}$). The instantaneous value of the PMF has been estimated to be 5% higher than the daily average, namely $8160 \text{ m}^3/\text{s}$ (say $8200 \text{ m}^3/\text{s}$).

The design discharge is also to take into account the “N-1” or “N-2” condition: i.e., the necessity of being able to discharge the flood with a mean period of return of 10,000 years assuming that one (or two, if $N > 6$) out of the “N” existing gates cannot be opened. The daily discharge at the peak of the one-in-10,000-year flood (without any dumping effect due to reservoir routing) has been estimated at $5690 \text{ m}^3/\text{s}$. The instantaneous value of the PMF has been estimated to be 5% higher than the daily average, namely $5970 \text{ m}^3/\text{s}$ (say $6000 \text{ m}^3/\text{s}$).

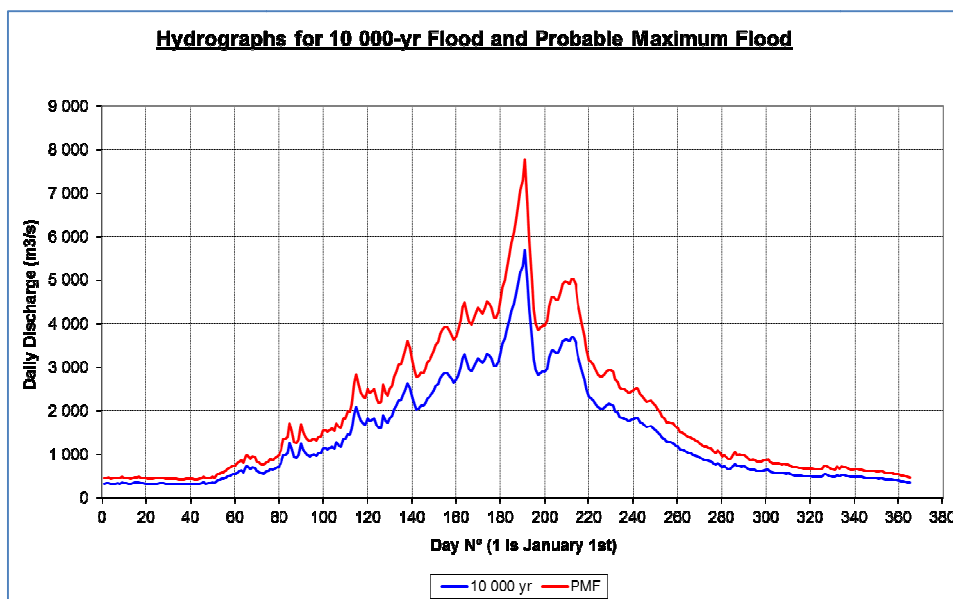


Figure 5.9: Hydrographs of the design and check floods

These floods are to be discharged under the elevation of the top of the dam core. Dam core top elevation is placed 3.75 m below the dam crest elevation for all the three alternatives of full supply level.

That condition is indeed the governing condition, because:

- Wind waves concomitant with the PMF and the one-in-10,000-year flood are not significant. Indeed, assuming a low combined probability of occurrence of floods and winds, winds supposed to occur simultaneously with high floods are frequent winds thus generating small waves.
- Long term dam settlement is supposed to have been compensated with an equivalent dam crest chamfer.
- GLOFs (glacial lake outburst floods) are unlike to happen simultaneously with the peak of the design floods. Indeed, the volume of glacial lakes may be related to persistent high temperatures (as in the case of high floods) but the outburst triggering causes are to be related also with mass movements and seismicity. Mitigation measures can also be envisaged.

Looking for an efficient compromise between volume of excavation and discharge capacity, the coefficient of vertical contraction has been selected with a value close to $p/h_D = 0.5$. This coefficient measures the ratio between “p”, height of the sill (vertical distance between the sill crest and the bottom of the approach channel), and the design head “ h_D ”. Values of p/h_D lower than 0.5 induce a rapid loss of efficiency (discharge coefficient) and values high than 0.5 produce only marginal gains of efficiency.

The design head “ h_D ” is the value of the head over the spillway sill for which the geometry of the Creager profile is fixed. For values of operating head higher than the design head ($h > h_D$) the discharge coefficient gets higher but the risk of cavitation also increases. Taking into account that

on the long term the spillway will need to pass sediments producing concrete surface irregularities, the design discharge will be defined as the head corresponding to the PMF. By this means additional erosion produced by cavitation will be avoided or delayed.

The upstream face of the sill is adopted as vertical also in order to minimize surface erosion.

The adopted pier and abutment coefficients are $k_P = 0.005$ and $k_A = 0.02$, respectively. These values correspond to typical, rounded piers and abutments according to experimental results.

Let us recall that three independent approach bays and “conduits” have been adopted ($N_C=3$). Within each one of them, four spillway bays ($N_B=4$) having a width of 8 m have been adopted.

Taking into account the above mentioned concepts and the corresponding adopted dimensions, the resulting discharge curve was calculated. The discharge curve is shown in figure 5.10.

With the above mentioned spillway characteristics the instantaneous peak discharge of the PMF (8200 m³/s) is evacuated under a head of 11.96 m (say 12.0 m). The crest of the spillway sills are then placed at 1284.0 m a.s.l., 1249.0 m a.s.l. and 1214.0 m a.s.l. for the three alternative dam heights with FSLs of 1290, 1255 and 1220, respectively.

With respect to the top of the dam core the maximum water level during evacuation of the PMF still leaves a margin of 0.25 m.

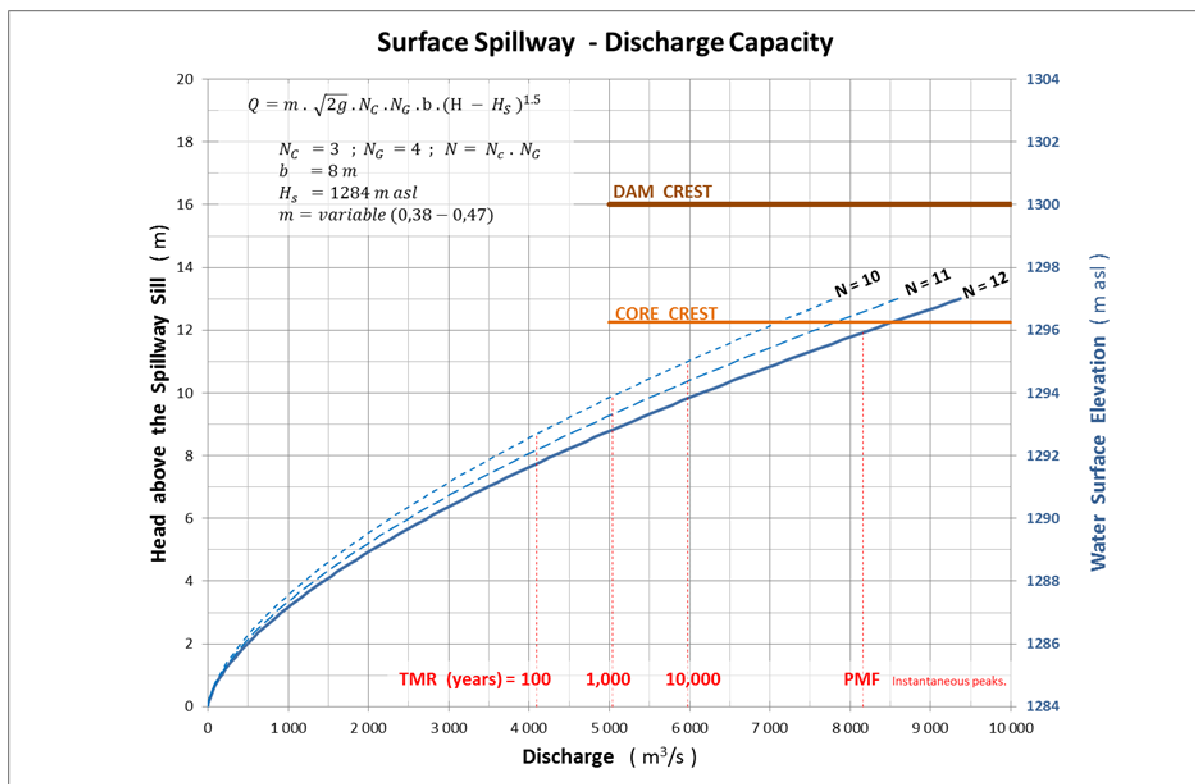


Figure 5.10: Spillway discharge capacity

5.2.2.4 Tunnel Reach

Each one of the three “conduits” includes a tunnel reach. Flow in this reach is a free surface flow.

In order to provide a safe design from the geotechnical point of view, a minimum separation between neighboring tunnels is required. At this level of the studies it is assumed that the separation between contiguous tunnel axes will be three times the equivalent tunnel diameter.

Keeping in mind the analysis presented in # 5.2.2 and in figure 5.7, a total width of 68 m is available for each “conduit”. Within that width, the geotechnical condition indicated above can be satisfied with different numbers of tunnels (1 through 3 in the table below). Critical water depth, critical slope and depth of flow for a slope of 1% are also indicated in the table below.

With $N_{TNL}=1$ the tunnel width is excessive for ordinary technological and economic conditions. Still with a single tunnel, smaller channel widths could be adopted, but in that case high specific discharges would result together with high velocities and increased cavitation risks.

For $N_{TNL}=3$ the critical slope has increased significantly and the Froude number for a reference slope of 1% becomes close to unity, which indicates a risk of losing flow control and stability.

Finally, with $N_{TNL}=2$ the geometrical (geotechnical) and hydraulic dimensions appear acceptable. The exact calculation of the hydraulic profile confirms this preliminary analysis. Please note that in this design scheme the slope of the tunnel reach becomes the adjusting variable as tunnel lengths change, because of the topography, for each “conduit” and for each dam height alternative.

| $Q (m^3/s) = 2733 = 8200 / 3$ $B (m) = 68$: total available width (tunnel + rock) $e (m) = 0,9$: width of lining | | | | | | | | | | |
|--|-------------|------------|---------|-----------|-------|-------|-------|-------------|-------------|-------------|
| N_{TNL} | b_{EXCAV} | b_{CHNL} | Q_1 | q | h_c | i_c | v_c | $h_{n-1\%}$ | $v_{n-1\%}$ | $F_{n-1\%}$ |
| --- | m | m | m^3/s | $m^3/s/m$ | m | % | m/s | m | m/s | --- |
| 1 | 22,7 | 20,9 | 2733 | 131 | 12,0 | 0,20 | 10,9 | 6,7 | 19,6 | 2,4 |
| 2 | 11,3 | 9,5 | 1367 | 143 | 12,8 | 0,40 | 11,2 | 8,8 | 16,3 | 1,8 |
| 3 | 7,6 | 5,8 | 911 | 158 | 13,7 | 0,72 | 11,6 | 11,8 | 13,4 | 1,3 |

Table 5.2: Tunnel characteristics as a function of tunnel number

5.2.2.5 Chute and intermediate energy dissipation

The chute channel leads water from the sub-horizontal channel reach (tunnels with free surface flow) to the ski-jump structure and eventually back to the river. The total head differential along this channel is about 200 m.

It has been shown in # 5.2.1 that the water velocity along the chute channel rises up to more than 50 m/s. This condition (that happens with a single slope chute or with a stepped channel) leads to cavitation indices below 0.1, indicating a non-acceptable design condition.

The only way of avoiding that situation is to let the flow dissipate energy every time that velocity goes beyond an acceptable limit. Figures 5.3 and 5.4 indicate that the flow velocity goes above 40 m/s (and cavitation index below 0.2) after a chute of about 70 m.

Introducing a sub-horizontal reach where a stilling basin is placed after every 70 m of chute should fulfill the desired objectives. Figure 5.11 shows the main parameters associated to that stilling basin: entering Froude number, necessary end sill height, remaining energy and theoretical length of the hydraulic jump. Equations and graphs used for the pre-design of the stilling basin are shown in Annex 2.

In order to reduce as much as possible the volume of excavation, the slope of each one of the three chutes has been adopted equal to 0.8H:1V, which is the typical slope of spillways in concrete gravity dams. Also, the effective length of the basin has been adopted as two thirds of the theoretical length of the hydraulic jump. This condition aims at reducing the volume (and cost) of the structures and takes into account the fact that the strongest rate of energy dissipation occurs in the first half of the length of the hydraulic jump.

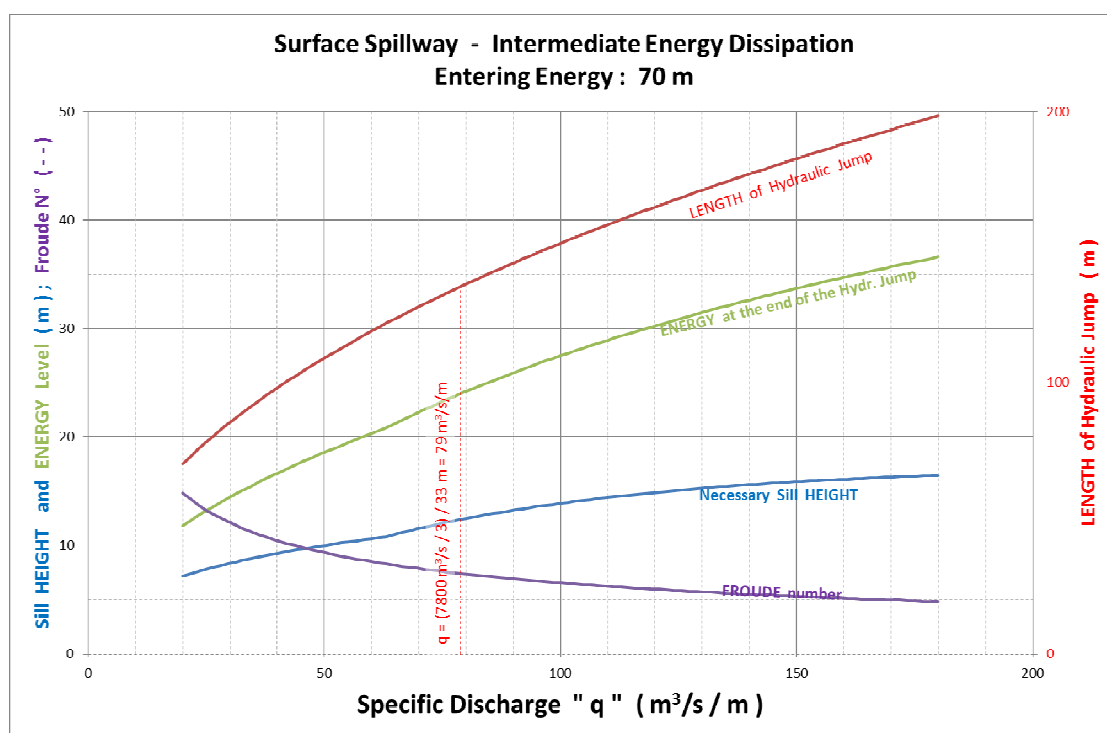


Figure 5.11: Hydraulic parameters in a stilling basin

As a result of the design, the following spillway configuration was adopted: see longitudinal section in figure 5.12 and the transversal sections in figure 5.13.

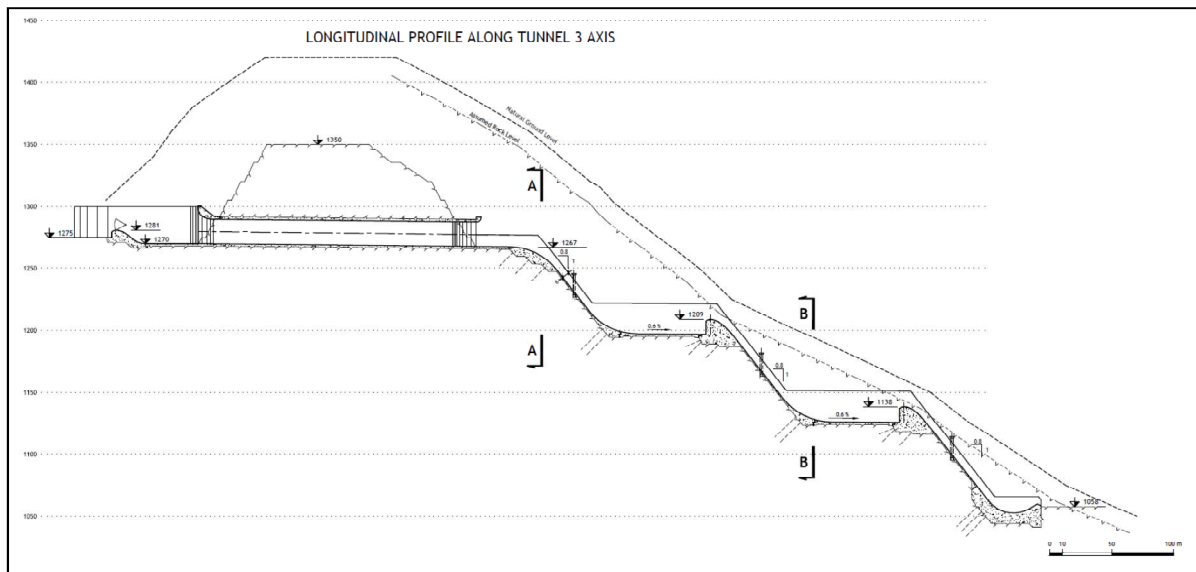


Figure 5.12: Longitudinal section of the stepped spillway

Aerators have been included in the intermediate chutes in order to minimize cavitation damages induced by the high velocities.

The dam alternative with FSL = 1220 has a total head 70 m smaller than in the case of the highest dam alternative (FSL=1290). In that case only two of the three, 70 m high steps will be used for the chute section of the spillway.

The intermediate dam alternative (FSL=1255) has a total head just 35 m smaller than in the case of the chute channel developed above for the dam alternative with FSL=1290. In that case, the same design principles will be adopted but reducing the height of each one of the three steps by 12 m, 12 m and 11 m, respectively.

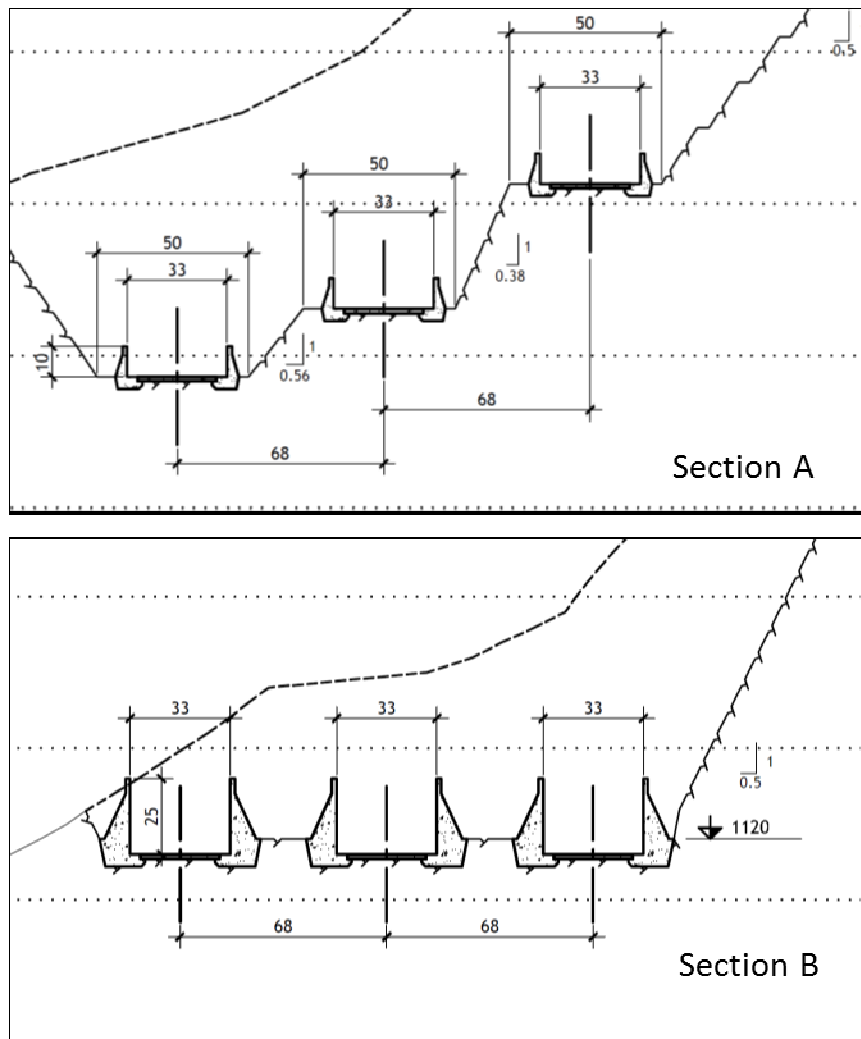


Figure 5.13: Transversal sections of the stepped spillway

5.2.2.6 Ski Jump and Plunge Pool

The last structure in the stepped spillway with intermediate energy dissipation is a ski-jump deflector. Its role is to redirect the spillway flow into the river.

The next picture illustrates the calculation performed to evaluate the area of impact of the jet. The basic equation as well as the sensitivity studies have been indicated in it.

The results of the study indicate that there is some margin to adjust the ski-jump design parameters in order to optimize the energy dissipation and the formation of the plunge pool.

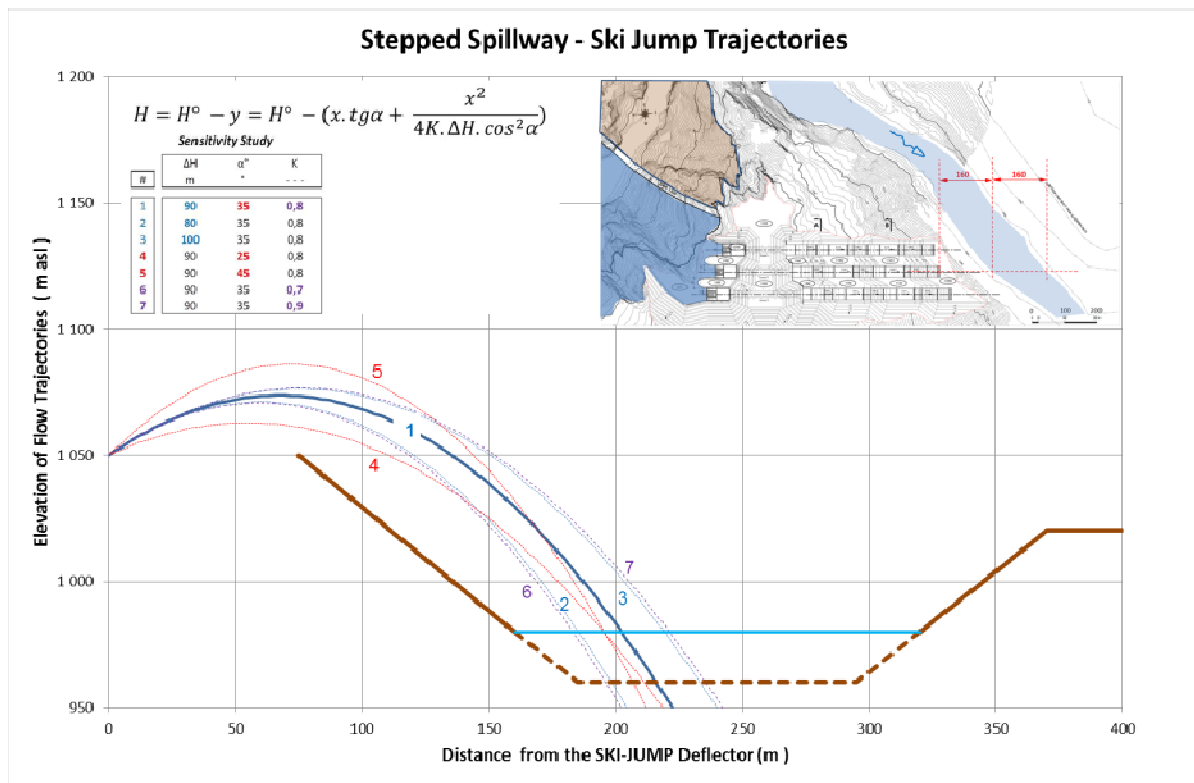


Figure 5.14: Flow trajectories from the Ski-jump end structure

The calculation of the trajectories aims at evaluating the viability of the ski-jump solution, by checking if the jet falls in the desired area (generally the river bed), as well as evaluating its main hydraulic parameters (specific discharge, angle of incidence, head, etc.) in order to verify also the viability of the plunge pool.

$$H = H^{\circ} - y = H^{\circ} - \left(x \cdot \tan \varphi + \frac{x^2}{4K \cdot H \cdot \cos^2 \varphi} \right)$$

where:

- x and y : co-ordinates of the jet trajectory measured from the jump lip,
- H° : elevation of the departure point at the jump lip,
- φ : angle of issue from the jump lip,
- H : hydraulic head over the jump deflector,
- K : dumping factor with $K = 0.7 \rightarrow 0.9$.

The baseline calculation as well as the sensitivity analyses confirm the correct location of the plunging jet with respect to the stability of the banks and the potential development of the plunge pool.

The following favourable circumstances deserve a comment (see figure 5.15):

- The falling jet enters obliquely in the river bed with a horizontal angle of some 45° with respect of the axis of the river bed in that location. Adjusting the geometry of the terminal structure (angle of departure, oblique section, re-direction) of the three ski-jump structures, the impact area can be extended in order to reduce the specific discharge and consequently the depth of scour in the plunge pool.
- The opposite bank shows a flat platform (El. 1080-1130) over some 700 m aligned with the spillway axis, before the steep, structural slopes re-start. This fact provides additional margin for the development of the plunge pool without endangering the stability of the left bank.

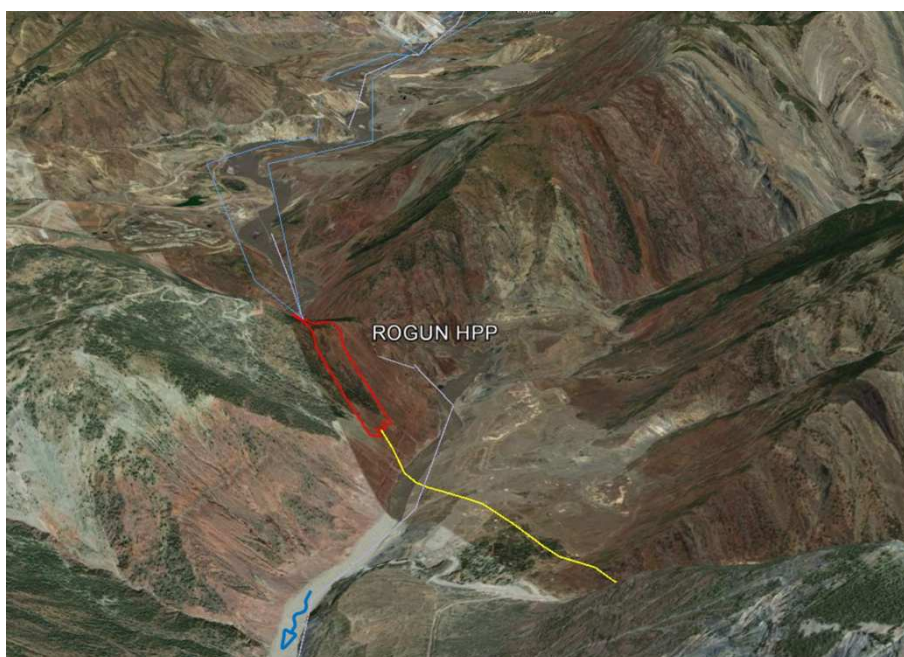


Figure 5.15: Downstream view of the impact zone (Google Earth)

The basic parameter to check the resulting plunge pool is the scour depth. Several empirical formulae furnish an estimate of that depth as described in paragraph 2.3.4.

The following values are adopted in the case of the surface spillway, for the application of the empirical formulae:

- $q = (7800 \text{ m}^3/\text{s} / 3) / 33 \text{ m} = 79 \text{ m}^3/\text{s}/\text{m}$, together with a $\pm 5\%$ variation,
- $H = 90 \text{ m}$,
- $h = 20 \text{ m}$,
- $d = 1 \text{ m}$.

The coefficients and power factors used in the adopted equations and results are:

| Author | D (m) | K | x | y | w | z |
|---------------|-------|-------|------|-------|------|------|
| Veronese (B) | 62.9 | 1.9 | 0.54 | 0.225 | 0 | 0 |
| Veronese mod. | 56.1 | 1.9 | 0.54 | 0.225 | 0 | 0 |
| Damle (A) | 73.2 | 0.652 | 0.5 | 0.5 | 0 | 0 |
| Damle (B) | 61.0 | 0.543 | 0.5 | 0.5 | 0 | 0 |
| Damle (C) | 40.6 | 0.362 | 0.5 | 0.5 | 0 | 0 |
| Martins (A) | 43.4 | 1.9 | 0.6 | 0.1 | 0 | 0 |
| Martins (B) | 34.2 | 1.5 | 0.6 | 0.1 | 0 | 0 |
| Mason | 45.7 | 3.27 | 0.6 | 0.05 | 0.15 | -0,1 |
| Taraimovich | 42.0 | 0.633 | 0.67 | 0.25 | 0 | 0 |
| INCYTH | 44.6 | 1.413 | 0.5 | 0.25 | 0 | 0 |
| Pinto | 39.7 | 1.2 | 0.54 | 0.225 | 0 | 0 |
| Chee and Kung | 63.0 | 1.663 | 0.6 | 0.2 | 0 | -0.1 |

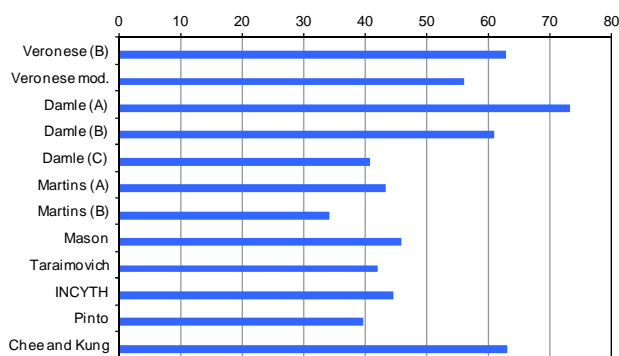


Figure 5.16 Scour depth (m) calculated by using different empirical formulae.

The field of variation of the scour depth $D = t + h$ obtained by application of empirical formulae, is between 34.2 and 73.2 m, while the average value is 51 m. This value is for a single chute.

It is to be noticed that this is the value resulting from the use of the peak discharge of the PMF as a permanent value. Taking into account the short duration of the peak of the PMF and using the persistent value of $4,000 \text{ m}^3/\text{s}$ (see hydrograph in figure 5.9), a new global average of 35 m (minimum 22.9 and maximum 52.4 m) is found. This value is to be read as $h=20 \text{ m}$ of water cushion plus $t=15 \text{ m}$ of true scour.

Together with the scour there is also the deposition of the scoured material in the form of a dune. The dune raises the water level producing the inundation of the structures upstream of it (tailrace tunnels and powerhouse).

As the surface spillway in its final configuration is to be used at the long term when the powerhouse will be no longer in operation, the scour, the dune and the inundation then would not a problem. However, since at least part of the surface spillway will be built and operated at an earlier stage of the project, it is envisaged to pre-excavate a part of the plunge pool in order to avoid the dune formation that raises water levels. A rapid estimate of the volume of rock to excavate yields: 200 m (the distance between the extreme sides of the three chute channels plus a margin corresponding to their width) times 160 m (length along the plunging jet equivalent to the chute width) times 15 m (net scour according to the precedent estimate) equals $0.55 \times 10^6 \text{ m}^3$. This

value is a reduced part of the total amount of the excavation associated with the surface spillway. The solution then is viable from this point of view.

The methodological approach based on the assessment of the hydrodynamic pressure of the underwater jet, described in paragraph 2.3.4, was applied for the discharge 7800 m³/s concerning the PMF with specific discharge of 79 m³/s/m corresponding to a single chute. The footprint of the impact area for three chutes is about 200 m.

The take-off velocities are of 40 m/s. The maximum pressure at the point of impact is $P_u = 160.9$ T/m². The angle of impact is 45°.

Considering also in this case a pressure value of 15 T/m² (1.5 kg/cm²) as an erodibility threshold, we can see from Figure 5.16 that this value is reached at a distance of 30 m along the axis of the bulb. In this situation, a pre-excavation of the above cited dimensions, see empirical equations, is compatible with the dynamic pressures identified along the axis of the bulb adopting the method proposed by Hartung and Häusler [14].

Experimental tests are necessary in order to more exactly define the local scouring over the left bank and the possible further mitigation structures, whenever required.

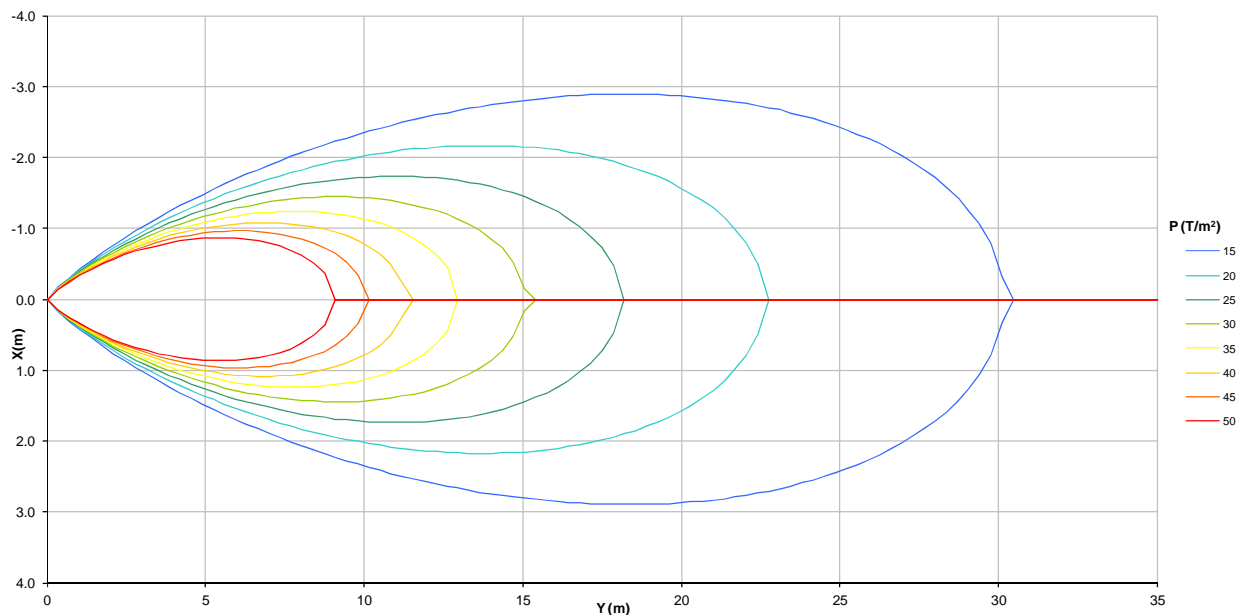


Figure 5.17. Hydrodynamic pressure bulb: $Q = 7800$ m³/s. Pressure in the point of impact $P_u(0,0) = 160.9$ T/m². Angle of impact 45°.

5.3 Resulting Design

The resulting design of the surface spillway for the three dam height alternatives is shown in the relevant drawings.

5.4 Conclusions and Recommendations

The analyses conducted in this section have proved the feasibility of a surface spillway for each one of the three dam height alternatives, having a discharge capacity equal to the peak of the Probable Maximum Flood, to be implemented in the long term on the right bank of the reservoir, close to the dam.

This surface spillway is to replace the other flood evacuating facilities once when the sediments in the reservoir make them useless or reduces their discharge capacities.

Without the possibility of a surface spillway the entire project should be dismantled in a mid-term future or simply not constructed at all.

The spillway structure consists of three independent modules having the following components:

- an approach bay,
- a control sill with four gated bays (the total number of gated bays is $3 \times 4 = 12$),
- a sub-horizontal free surface flow channel along tunnels excavated through the high hill on the right bank,
- an open air stepped chute channel with intermediate energy dissipation. Each step is 70 m high and consists of a steep chute (0.8H:1V) followed by a sub-horizontal reach where a stilling basin dissipates part of the energy. There are three steps in the two higher dam alternatives and just two steps in the smallest one.
- a ski-jump end structure in the last step of the chute,
- a plunge pool in the river bed.

All these components have been designed and dimensioned on the basis of the state of the art and have proved to be feasible. Model tests are recommended anyhow.

As mentioned in paragraph 1.1.6, according to the conclusions of Volume 3 – Chapter 3 – Appendix 5 “PMF Management”, only one “module” will be required in the initial stage of the project operation for alternatives with FSL 1290 and 1255, whilst two modules are adopted for the alternative with FSL 1220. For the two highest alternatives, this is a consequence of the need of keeping the flow discharged from Rogun within values which assure that the safety of Nurek is not impaired.

The final complete configuration, constituted by three modules, each composed by an intake/approach bay, a tunnel and a stepped chute discharging to the river, will be needed in the

long term, once the reservoir sedimentation will prevent the discharge of the floods through other hydraulic facilities, in particular the high level spillway tunnels.

6 OPERATION OF THE HYDRAULIC FACILITIES

During the construction stage of the project and subsequently during the operation of the plant different hydraulic facilities are required to provide the discharge capacity needed for protecting the works under construction and the dam completed up to the final elevation.

As described in Volume 3 – Chapter 3 – Appendix 3 “Flood Management during Construction” and Volume 3 – Chapter 3 – Appendix 5 “PMF Management”, safety cannot be assured by a single hydraulic facility but at different stages it is necessary to operate simultaneously up to 3 of them to achieve the discharge capacity required by the criteria set up in the mentioned documents.

In fact the safety of the works must not depend on one single hydraulic structure, since its failure would unavoidably lead to very serious consequences.

Here in after the sequences by which the various hydraulic facilities are operated in order to provide the discharge capacities determined for the various construction stages and in the long term are summarized, providing where necessary comments about the possible interferences among them or impact on the construction and operation of the plant.

It is noted that only the alternative FSL 1290 is described in detail here in after. In fact other alternatives exhibit a lower number of outlets.

It is recalled that MLO2 is present only in the alternative with FSL 1290 (two outlets), while two HLTs are envisaged for alt. FSL 1290, three for alt. FSL 1255 and only one HLT is present in alt. FSL 1220.

Therefore, at least one additional point of impact is present for the higher dam alternative with respect to the intermediate one.

The fact that MLO2 is not implemented in the intermediate and lower dam height, substantially improves the situation, being in these layouts the distance between the surface spillway and the DT3 in the order of 500 m.

6.1 Cofferdam

At the very beginning of the activities, the cofferdam for passing the river flows through the diversion tunnels will be constructed. As discussed in Volume 3 – Chapter 3 – Appendix 3 “Flood Management during Construction”, besides Diversion Tunnels n. 1 and n. 2 (DT1 and DT2), also Diversion Tunnel n. 3 (DT3) is required for providing the required protection to the cofferdam until stage 1 dam will be raised above its elevation.

During this phase those three facilities could discharge contemporaneously.

In the following figure 6.1, the locations where the discharges occur are shown by positions A' (DT1 and DT2) and A (DT3). The distance between the points of discharge into the river is more than 200 m, measured from the outlet of DT2 to the area of impact of DT3.

Thus no interference problems are envisaged.

6.2 Stage 1

This stage corresponds to the construction of the dam with the configuration which allows starting the energy generation with the first two units U6 and U5.

During this phase, the same hydraulic facilities above indicated are used for managing the floods, thus the scheme of the discharges is the same above mentioned.

It is to be noted that the next hydraulic facilities which will start operating is the Middle Level Outlet 1 (MLO1) which intake is set at el. 1,085 m a.s.l.

When the FSL of Stage 1 configuration at 1,100 is taken into account, it can be noted that MLO1 will be already constructed while DT1 and DT2 are still operative. At this elevation, the discharge capacity of MLO1 would be in the order of 1,000 m³/s.

The points of impact into the river of MLO1 are marked with B', and correspond to the same area of the surface spillway channels. Those impact points (marks B') are about 500 m downstream from that of DT3 (mark A).

6.3 Dam Construction

Following the scheme of Volume 3 – Chapter 3 – Appendix 3 “Flood Management During Construction”, this phase has been divided into different steps, which correspond to a different utilization of the hydraulic facilities.

6.3.1 Step A

During this step, floods management is assured by Diversion Tunnel n. 3 (DT3) and Middle Level Outlet n. 1 (MLO1), while DT1 and DT2 are no longer operated. In the figure 6.1 which follows, for this step the points of discharge-impact into the riverbed have been marked with B and B' respectively.

As already above noted, the distance between the points of impact (marks B and B') is about 500 m.

Depending upon the FSL alternative, the elevation at which DT3 would be “switched off” is between 1,160 (FSL 1290) and 1,170 m a.s.l. (FSL 1255).

It is to be noted that the next hydraulic facility which will start operating is the Middle Level Outlet n. 2 (MLO2) for the case of FSL 1290, which intake is set at el. 1,140 m a.s.l.

If the water level of 1,170 is considered, it can be noted that MLO2 will be already constructed and ready to operate while DT3 will go out of service. At this elevation, the discharge capacity of MLO2 would be in the order of 1,700 m³/s.

The points of impact into the river of MLO2 are marked with C' and are about 150 m downstream from that of DT3 (mark B), and about 200 m upstream from those of MLO1 (marks B').

6.3.2 Step B

During this step, in the alternative with FSL 1290 the floods management is assured by Middle Level Outlet n. 1 (MLO1) and Middle Level Outlet n. 2 (MLO2), while DT3 is no longer operated.

In the figure 6.1 which follows, the points of discharge-impact into the riverbed for this step have been marked with C and C' for MLO1 and MLO2 respectively.

As already above noted, the distance between the points of impact is about 200 m. Given the alignment of the tailrace tunnels of MLO2, the distance between their points of impact is about 100 m.

In this alternative, the elevation at which MLO1 would be “switched off” is 1,215 m a.s.l.

The next hydraulic facilities which will start operating are the two High Level Tunnel Spillways (HLTS) which intakes are set at el. 1,190 m a.s.l.

The two HLTS will be constructed and ready to operate when MLO1 will go out of service. At the elevation above indicated, the discharge capacity of the two HLTSs would be in the order of 800 m³/s each.

The points of impact into the river of HLTSs (marks D') are about 400 m downstream from that of MLO1 (mark C).

6.3.3 Step C

During this step, in the alternative with FSL 1290 the floods management is assured by Middle Level Outlet n. 2 (MLO2) and the two High Level Tunnel Spillways (HLTS), while MLO1 is no longer operated.

In the figure 6.1 which follows, for this step the points of discharge-impact into the riverbed have been marked with D and D' respectively.

The distance between the respective points of impact is more than 700 m. Given the alignment of the tailrace tunnels of MLO2, the distance between their points of impact is about 100 m.

In this alternative, the elevation at which MLO2 in principle would be no longer required for management of floods related to the construction phase is 1,270 m a.s.l.

However, it will remain available and would be used during the operation phase for managing high floods, according to the conclusions of Volume 3 – Chapter 3 – Appendix 5 “PMF Management”.

6.4 Operation Phase

Once the dam is completed and the project operates normally, the floods management is assured by the two High Level Tunnel Spillways (HLTS) and by the Middle Level Outlet n. 2 (MLO2). The points of their impacts have been already indicated above.

It is foreseen that also one channel of the Surface Spillway (SS) will be constructed, to be used in case of unavailability of part of the tunnels.

The points of impact related with this phase have been marked with E, E' and E'' for the MLO2, HLTs and the Surface Spillway SS respectively.

The distance between the points of impact are of almost 300 m between MLO2 and SS (marks E and E'') and about 400 m between SS and HLTs (marks E'' and E').

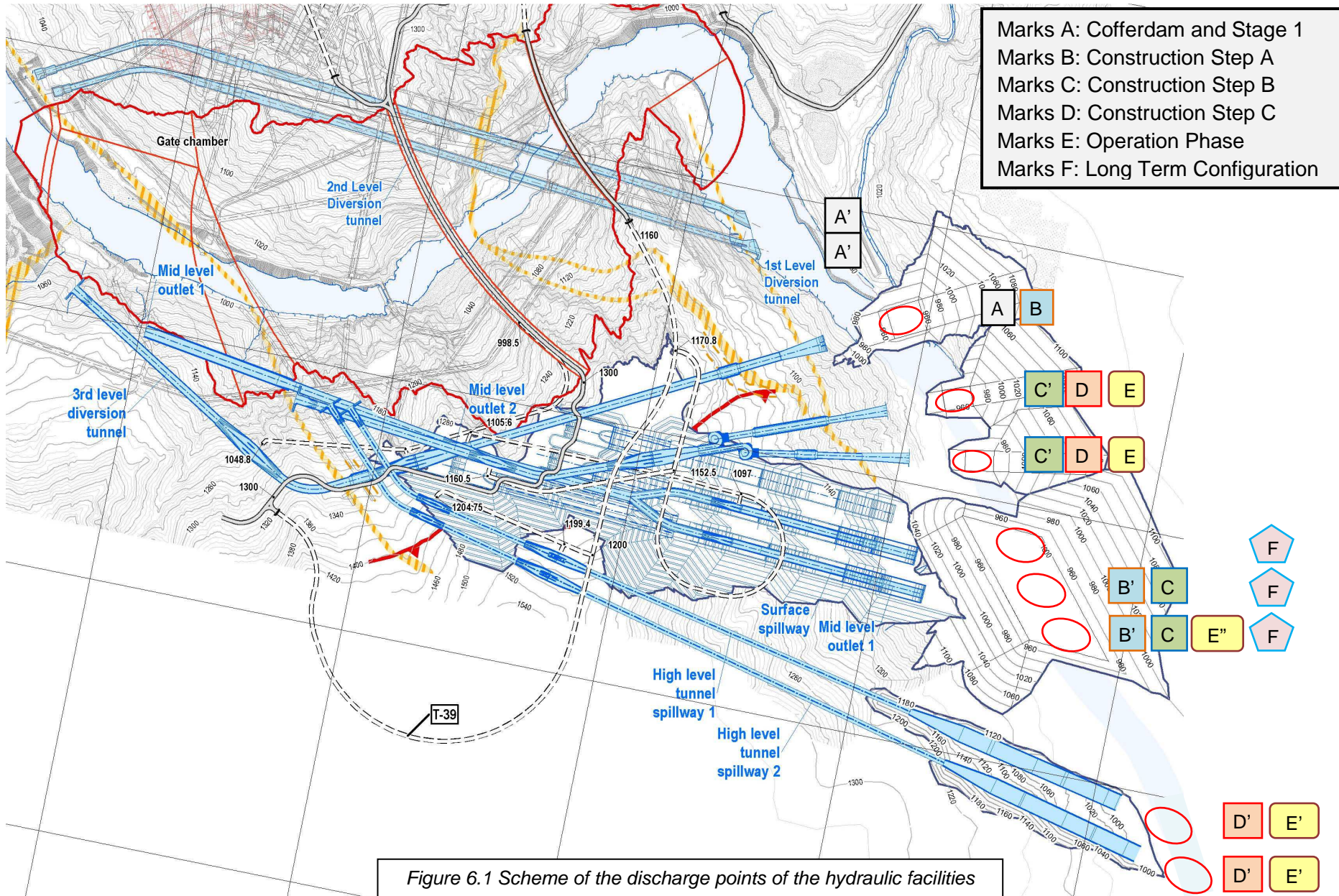
6.5 Long-term Operation Phase

As mentioned in paragraph 1.1.3, in the long term MLO2 will be out of operation due to the silting in the reservoir. At that point, at least one further channel of the Surface Spillway will have to be constructed. Finally, once the sediments will have reached the intakes of the HLTs, there will be the need for availing of the full discharge capacity of the Surface Spillway, which construction will have to be completed including the third channel.

At that point, this facility will be the only way to evacuate whatever flood.

In this situation the only area of discharge to the river will be that corresponding to the points marked with F in the layout of the figure 6.1, which are at a distance from the tailrace tunnels outlets of about 600 m as a minimum.

In consideration of the above indicated relevant to the location of the points of discharge during the various steps and phases of the project, no interferences are envisaged between the operation of the various discharge facilities.



7 PHYSICAL MODELS

The need for physical or mathematical modeling has been several times mentioned in the report, in consideration of the complexity of the hydraulic phenomena involved in the design of the facilities of the project. The considerable heads resulting from the dam heights, which are responsible for high water velocity in most of the discharge facilities, and the peculiarity of the solutions proposed, bring to the necessity of testing through models the various components involved, in order to validate first of all the solutions proposed and then to optimize both technically and economically the hydraulic structures.

It is however noted that some of the hydraulic facilities are based on very similar solutions, being possible to perform tests addressed to define the behavior of an aspect or component which is common to various of them.

Therefore, the following possible components could be separately tested, applying then the results to different facilities.

Hydraulic Model Test Program

In order to study the hydraulic performance regarding the main hydraulic structures, five hydraulic models are proposed:

1. Pressure tunnel and free flow headrace tunnel;
2. Vortex Spillway;
3. Surface Spillway and cascade system of chutes and stilling basin;
4. HLTS with cascade system of chutes and stilling basin;
5. Plunge pools along the river.

In principle the hydraulic models should be as large as possible, but upper limitations are given by the possibilities of the laboratory; in any case, they shall be sufficiently large to respect the similarity condition.

From the perspective of the similarity laws, physical modeling with fixed bed condition must be based on the criteria of gravitational Froude Law. The problem connected with sediment transport must be analyzed considering the densimetric Froude model law and the Froude grain number in order to define the size of the material for the representation of the complicated processes at the starting of sediment motion in the flushing phenomenon. The scouring problems in the plunge pool must be simulated with movable bed using grain size in geometric scale and adopting the gravitational Froude law.

In the physical models the criteria to be used are the gravitational Froude number and the geometrical similarity in model and prototype.

In the case of model with movable bed and motion in suspension the time scale for sediment transport processes will be quasi-qualitative in the model; therefore, in order to find a suitable time scale for morphological developments, one has to run a so-called hypothetical morphological scenario with proper model adaptation. In this case, the temporal scale can be deduced by the gravitational Froude law.

The Pressure tunnels and free flow headrace tunnel

The hydraulic model has to be built at a scale of at least 1:40 in order to have sufficient reliability concerning reproduction of air entrainment problems. The following problems related to the tunnel structure must be investigated with the hydraulic model tests:

- Discharge capacity;
- Overall hydraulic behavior of the structure including pressure measurements in the pressurized zone of the gates chamber and along the bottom of the tunnel, water level measurements and determination of particular flow conditions;
- Air demand;
- Necessity of air slots;
- Confirmation of the mathematical model using the test results;
- The sluice gates in principle have to operate fully open. Various combinations of gates fully open shall be tested.

Vortex spillway

The hydraulic model has to be built to a scale of approximately 1:30, in order to assess the negative pressures along the discharge shaft and the hydraulic performance in the transition between the vertical shaft and the tailrace tunnel.

The helicoidal flow in the headrace tunnel and the efficiency of the flip bucket must be examined.

The main aspects to be investigated are:

- Discharge capacity;
- Overall hydraulic behavior of the structure including pressure measurements in the vertical shaft and in the tailrace tunnel;
- Evaluation of the behavior of the approach chamber;
- Air demand;
- Necessity of air slots in the tailrace tunnel;
- Evaluation of dissipation due to helicoidal flow generated by the transition between the shaft and the tailrace tunnel;
- Confirmation of the mathematical model using the test results;
- Confirmation of the design of the chute and flip bucket structure.

Surface Spillway and HLTS and relevant cascade systems of chutes and stilling basins

The physical model has to be built at a scale of 1:100 or larger on fixed bed. The main topics to be assessed are:

- Shape of channel transitions at the entrance to the cascade;
- Efficiency and optimization of the stilling basins;
- Air demand;
- Necessity of air slots on the spillway chutes;
- Channels/basins walls height;
- Behavior of the cascade system with low discharges;

- Flow in the outlet channel at flip bucket;
- Jets Trajectories.

Plunge pools along of the river

The model has to be built at a scale of 1:100 at least. The main topics to be assessed are:

- Maximum scouring;
- Definition of pre-excavation pools;
- Optimization of the flip bucket of the outflow structure in order to reduce scouring;
- Evaluation of the impact pressures in order to define mitigation structures.

There may be the need for preparing more than one model for the case of the tunnels and the plunge pools, since the conditions may be quite different from one facility to another.

In fact, besides of the tunnel dimensions, the number of gates may vary from two to four, thus the shape of the chambers may vary considerably and the flow behavior also.

Also for the plunge pools there are several situations related with the specific discharge and the jets trajectory.

Once the TEAS activities will be concluded, a program tailored on the selected alternative may be prepared with higher detail.

It should be noted, and it has been recalled in the document at hands, that model studies are being conducted in respect to the various diversion tunnels at the Hydraulic Laboratory in Moscow.

Therefore, the results of those tests can be used anyway for those tunnels which have been modeled and for a first evaluation of the solutions proposed for other similar works.

As for the specific models above indicated, they have to be programmed keeping in mind that after the finalization of the tests some time shall be allowed for performing the final design, in advance with respect to the construction starting date.

Even in an optimistic perspective, the models needed in order to define the design of a certain structure shall be implemented at least 12/15 months before the relevant construction starting date.

8 BIBLIOGRAPHY

- [1]. Abramovich G.: Angewandite gasdynamik. - Verlag Technik, Berlin - 1958
- [2]. Annandale, G.W., Scour Technology, 2006
- [3]. Air Entrainment in free surface flows, Hydraulic structures design manual Ian R. Wood Editor. 1991.
- [4]. Blaisdell, F. Development of hydraulic design, Saint Anthony Falls Stilling Basin, Transactions ASCE, 113, 1948, P.483.
- [5]. Bollaert E., Schleiss A., Scour rock due to impact of plunging high velocity jets. Part 1. A state of the art review. Journal of Hydraulic Research, 2003
- [6]. Dong, X. and Gao, J., "Report on model study of retrofitting a diversion tunnel into a vortex dropshaft spillway in Shapai Power Station", IWHR Research Rep., China Institute of Water Resources and Hydropower Research, China (in Chinese), 1995. (in Chinese) Reported by Zhao, C.H, Zhu, D.Z. , Sun, S.K. and Liu, Z.P. "Experimental study of flow in a vortex drop shaft", Journal of Hydraulic Engineering, ASCE, January 2006.
- [7]. ELC Electroconsult S.p.A., Proyecto Hidroeléctrico Coca Codo Sinclair, Estudio de factibilidad para 1500 MW, June 2009, Milán, Italy.
- [8]. Ervin, D.A., Falvey, H.T., Behaviour of turbulent water jets in the atmosphere and in plunge pools. Proc. Inst.Civ.Engrs., Part 2, v83, 1987
- [9]. Falvey, H. T., 1980. Air-water flow in hydraulic structures. Engineering monograph No. 41. Bureau of Reclamation, Denver, Colorado.
- [10]. Hager, H.: Vortex drop inlet for supercritical approaching flow - Journal of Hydraulic Engineering - Vol. 116 - n. 8 – 1990.
- [11]. Hager, W. H. and Bretz, N. Hydraulic Jump at positive and negative steps, Journal of Hydraulic Research, 24, 4, pp 237-253, 1986.
- [12]. Hager, H.W., Bremen R., Kawagoshi N., 1990. Classical hydraulic jump: length of roller. Journal of Hydraulic Research, 28, 591-608.
- [13]. Hager, W.H. and Sinniger, R. Flow characteristics of the hydraulic jump in a stilling basin with an abrupt bottom rise. Journal of Hydraulic Research, 23, 2, pp. 101-113,1985.
- [14]. Hartung and Häusler, Scours, stilling basins and downstream protection under free overfall jets at dams. Commission Internationale Des Grands Barrages – Onzième Congres des Grands Barrages – Madrid, 1973.
- [15]. Jain, S.C., and Kennedy, J.F., "Vortex-flow dropstructures for the Milwaukee Metropolitan Sewerage District inline storage system." IIHR Rep. No. 264, Univ. of Iowa, Iowa City, Iowa, 1983.
- [16]. Kalinske, AA & Robertson, J M .1943 Closed Conduit Flow. Transactions ASCE 108, 1435-1447.
- [17]. Molinas, Yang, "Generalized water surface profile computations", Journal of Hydraulic Engineering, ASCE, Vol. III, N°3, 1985.
- [18]. Montes S., Hydraulics of Open Channel Flow, ASCE Press, 1998.
- [19]. Pacheco R.: "Sistema de controle automático de vazoês com válvula de vórtice axial." - Dissertação apresentada a Escola Politécnica da Universidade de São Paulo, para obtenção do título de Mestre em engenharia. - São Paulo - 1986.

- [20]. Pacheco R., A. De Souza : "Sistema de Controle Automático de Vazoês com Válvula de Vórtice Axial"- AIPH. Congresso Latinoamericano de Hidráulica 31 ago. - 2 set. – 1986 San Paolo Brasil.
- [21]. Pacheco R., A. Paoletti: "Studio di una valvola troncoconica a vortice assiale ("Hydrobrake")." - Lavoro svolto nell'ambito del contratto di ricerca del 14 novembre 1990 tra il Politecnico di Milano (Dipartimento D.I.I.A.R) e la società del Gres ing. Sala s.p.a. - Milano Ottobre – 1993.
- [22]. Sanfilippo U., R. Pacheco, A. Paoletti: A comparison between physical an mathematical models of vortex amplifiers. - XXVI IAHR Biennale Congress - 1995 London England.
- [23]. Sanfilippo U., R. Pacheco, A. Paoletti: "Caratteristiche teoriche e sperimentali delle bocche a vortice." - XXV Convegno di Idraulica e Costruzioni Idrauliche, Torino, Set. – 1996.
- [24]. Peterka, A, Hydraulic design of stilling basin and energy dissipators. Engineering Monograph 25 U.S. Department of the Interior, Bureau of Reclamation, 1964.
- [25]. USBR United States Bureau Reclamation, Design of small dams.
- [26]. Vischer, D. L., and Hager, W. H., (1995). "Vortex drops." Energy dissipators: Hydraulic structures design manual, No. 9, Balkema, Rotterdam, The Netherlands.
- [27]. Zhao C.H., Sun S.K., and Liu, Z.P., "Optimal study on the depth of stilling well for rotation-flow shaft flood-releasing tunnel." Water Power, 2001(5), 30-33 (in Chinese) Reported by Zhao, C.H, Zhu, D.Z. , Sun, S.K. and Liu, Z.P. "Experimental study of flow in a vortex drop shaft", Journal of Hydraulic Engineering, ASCE, January 2006.

Annex 1

Drop Shaft Diameter Theoretical Approach

Abramovich [1] and Vischer & Hager [26], Pacheco & Souza [20], Pacheco & Paoletti [21] and San Filippo & Pacheco [21] carried out a comprehensive model study of tangential vortex intake. ELC Electroconsult S.p.A. (2009) reported a design based on theoretical model for the Coca Codo Sinclair Hydropower Project, Ecuador [4]. The present chapter shows the general guideline adopted for the design of the tangential vortex that can convey the flow smoothly without unstable fluctuations in the drop shaft with sufficiently large air core.

In the drop shaft a whirl is imparted to the stream, which is then contracted. The angular momentum created by the tangential approach of the stream remains approximately constant during the flow through the drop shaft. Consequently, as the stream converges, the whirl velocity component increases considerably and large centrifugal forces develop, which throw the water to the walls, forming a thin film which issues from the drop shaft in a spray. Along the centre line of the drop shaft an air vortex is formed in which the pressure at the surface is close to the atmospheric.

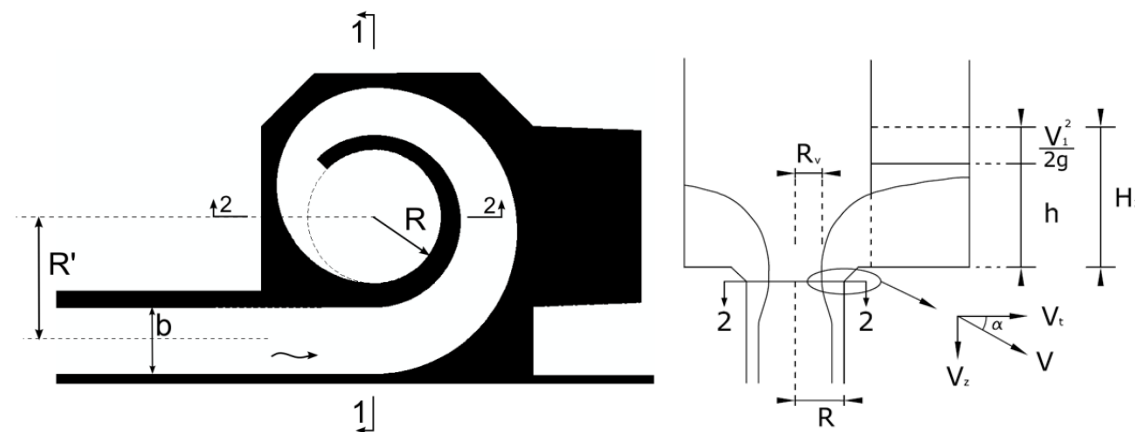


Figure 35: Swirl Shaft, Plan view and side view

Because of this, and also because the resultant velocity of discharge V is directed at an angle to the cross-section of the drop shaft, the tangent of which is equal to the ratio of the whirl component V_t to the axial component V_z , the coefficient of discharge is always much less than unit, varying within broad limits depending upon the geometry and relative dimensions of the drop shaft.

The theoretical approach is based on particular conditions where the annular flow discharges freely into the outlet tunnel and the pressure is atmospheric at the lower end the drop shaft.

Bernoulli's equation between sections 1-2 and 2-2:

$$\frac{P_1}{\gamma} + \frac{V_1^2}{2g} = \frac{P_2}{\gamma} + \frac{V^2}{2g} + \Delta H_{1-2}$$

$$H = \frac{V_z^2 + V_t^2}{2g}$$

where:

$$H = \frac{p_1 - p_2}{\gamma} + \frac{V_1^2}{2g}$$

As above mentioned V_z and V_t are the axial and whirl components of the velocity V at the boundary of the air vortex at section 2-2.

The equation for the conservation of angular momentum of the fluid with respect to the center line between sections 1-1 and 2-2:

$$\rho Q V_1 R' = \rho Q V_t \frac{R + R_v}{2}$$

$$V_t = \frac{V_1 2 R'}{R + R_v}$$

the continuity equation between the sections ²

$$S_1 V_1 = \varepsilon S_2 V_z$$

$$S_1 = bh$$

$\varepsilon = \text{contraction coefficient}$

$$\varepsilon = \frac{S_2 - S_v}{S_2} = 1 - \left(\frac{R_v}{R}\right)^2$$

$$R_v = R\sqrt{1 - \varepsilon}$$

which gives, after substitution into the second equation:

$$V_1 = \frac{\varepsilon S_2 V_z}{S_1}$$

$$V_t = 2 \frac{\varepsilon R' S_2 V_z}{(1 + \sqrt{1 - \varepsilon}) R S_1}$$

Where:

$$A = \frac{S_2 R'}{R S_1}$$

is a parameter characterizing the geometry of the "spillway vortex", then the angle of divergence of the "spray" is equal to:

² Assuming a uniform distribution of the axial velocities about the annular cross-section at the outlet

$$\arctan\left(\frac{1 + \sqrt{1 - \varepsilon}}{2 \varepsilon A}\right) = \alpha = \frac{V_z}{V_t}$$

Substitution in the above expression:

$$\frac{V_z^2}{2g} \left[1 + \frac{4 A^2 \varepsilon^2}{(1 + \sqrt{1 - \varepsilon})^2} \right] = H$$

hence, the velocity coefficient

$$C_V = \frac{1}{\sqrt{1 + \frac{4 A^2 \varepsilon^2}{(1 + \sqrt{1 - \varepsilon})^2}}}$$

Thus, the discharge coefficient is

$$\mu = \varepsilon C_V = \frac{\varepsilon}{\sqrt{1 + \frac{4 A^2 \varepsilon^2}{(1 + \sqrt{1 - \varepsilon})^2}}}$$

Finally, the rate of discharge is:

$$Q = \frac{\varepsilon}{\sqrt{1 + \frac{4 A^2 \varepsilon^2}{(1 + \sqrt{1 - \varepsilon})^2}}} S_2 \sqrt{2gH}$$

The contraction coefficient ε , as well as the dimensions of the air vortex (the radius R_v , for a given R and A), are not known a priori. To determine them, the following additional assumption must be introduced: *"The flow regime is such that a given discharge is produced by the least possible head"* (minimum energy criteria). In other words, the vortex would be of such size as to ensure a maximum rate of discharge Q for a given head H . Hence it is necessary to find the value of ε corresponding to the maximum coefficient of discharge μ . The hypothesis of minimum energy allows obtaining the maximum value of μ . The expression under the radical of the equation of the discharge coefficient is:

$$\frac{\partial V}{\partial \varepsilon} = 0$$

$$\mu = \frac{\varepsilon}{\sqrt{1 + \frac{4 A^2 \varepsilon^2}{(1 + \sqrt{1 - \varepsilon})^2}}} = \frac{1}{\sqrt{\frac{1}{\varepsilon} + \frac{4 A^2}{(1 + \sqrt{1 - \varepsilon})^2}}}$$

$$A = \sqrt{\frac{1}{2\varepsilon^3} (1 + \sqrt{1 - \varepsilon})^3 (1 - \varepsilon)^{\frac{1}{2}}}$$

This equation can be used to plot ε as a function of A . The curve can be used together with the above equation to compute values of μ for a series of values of A and to plot a graph of μ as a function of A .

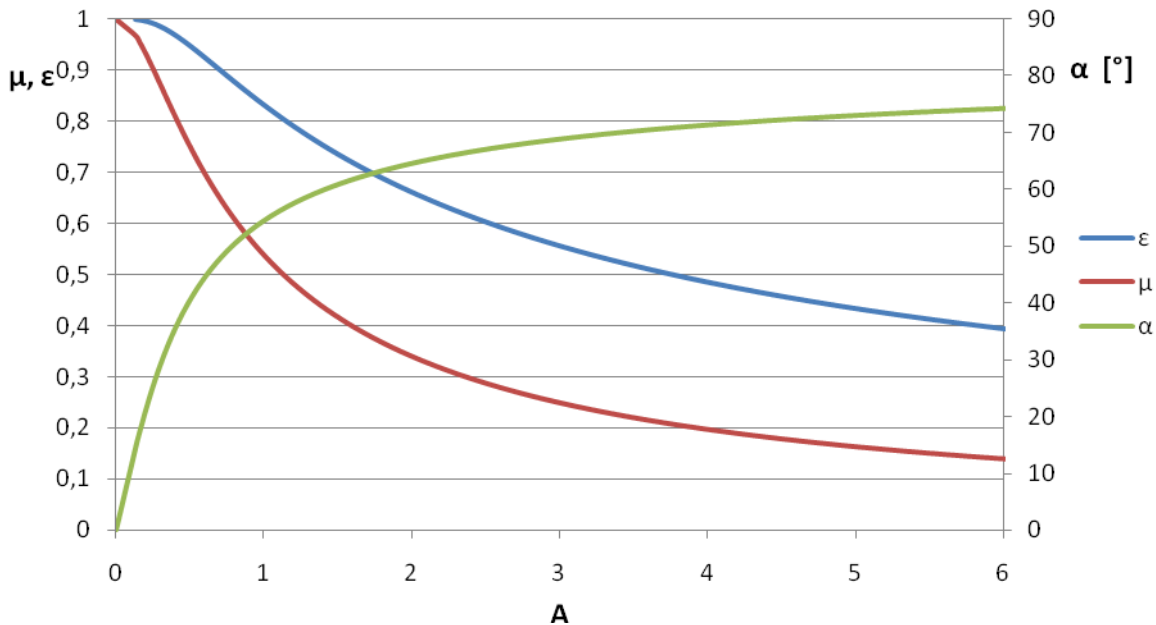


Figure 36. Plot of ε , μ and α versus A for a drop shaft.

The diagram shows that while A increases the coefficient μ decreases. Physically this is explained by the fact that A increase means a higher whirl velocity V_z and, consequently, a more intensive whirl of the fluid. This leads to a vortex of larger diameters and a smaller cross-section area of the stream, which means that more and more of the available energy H is dissipated on building up the whirl velocity. At $A = 0$ ($R=0$), $\mu = 1$, i.e., there is no whirl and the drop shaft works as an ordinary pressure tunnel.

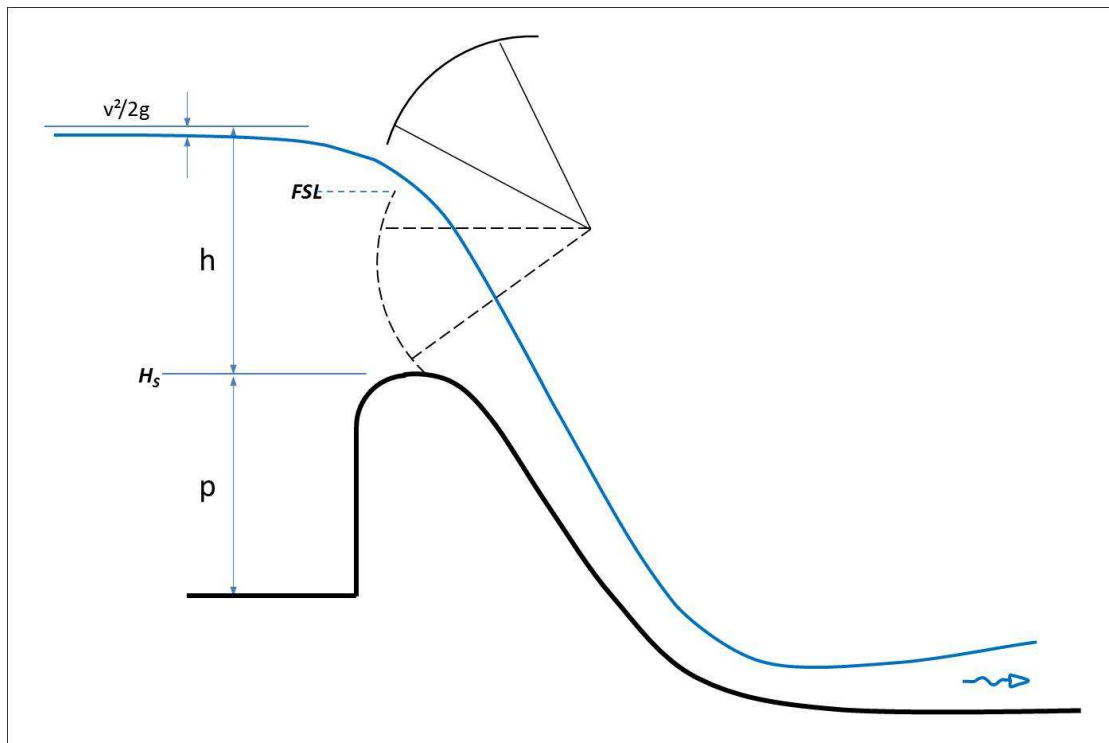
Annex 2

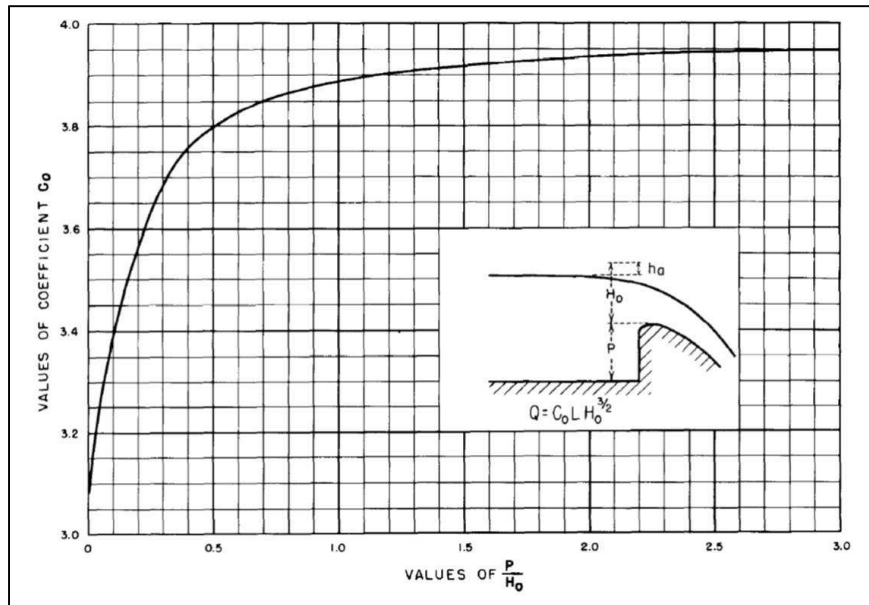
Spillway Discharge Capacity

$$Q = m_0 \cdot r_1 \cdot r_2 \cdot r_3 \cdot r_4 \cdot \sqrt{2g} \cdot N \cdot b \cdot (H - H_0)^{1.5}$$

where :

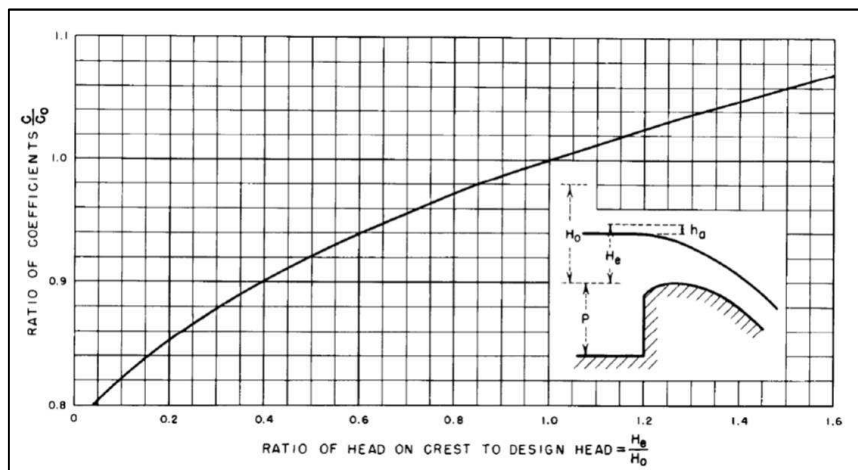
- Q : total spillway discharge
- m_0 : discharge coefficient due to vertical contraction of a standard Creager profile
- r_1 : adjustment due to operation for heads other than the design head
- r_2 : adjustment for u/s face slope other than vertical
- r_3 : adjustment for drawn flow
- r_4 : adjustment for abutment and pier conditions
- N : number of spillway (gated) bays
- b : width of those bays
- h : head over the spillway sill: $h = H - H_0$
- H : water surface elevation in the approach area
- H_0 : elevation of the spillway sill.



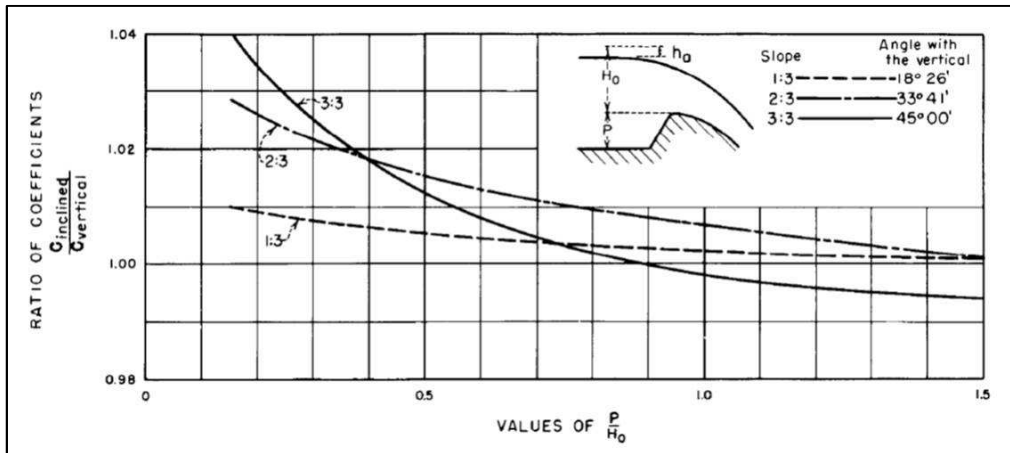


Discharge coefficient m° (divide by 8.0 to obtain metric units)

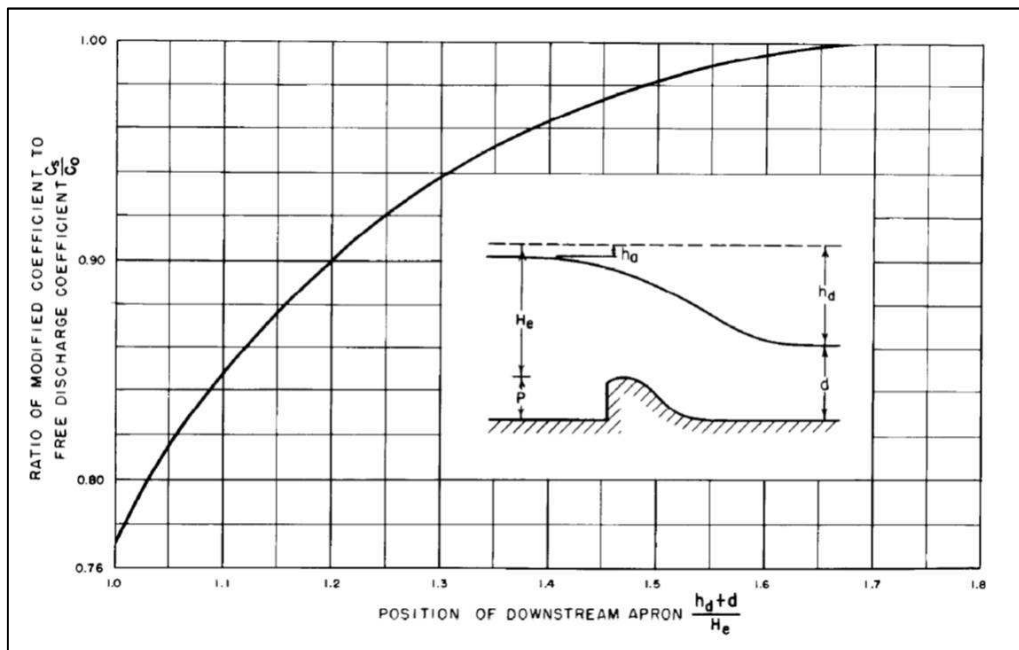
Source : U.S. Bureau of Reclamation



coefficient r_1 : adjustment for operation for heads other than the design head



Coefficient r_2 : adjustment for u/s face slope other than vertical



Coefficient r_3 : adjustment for drawn flow

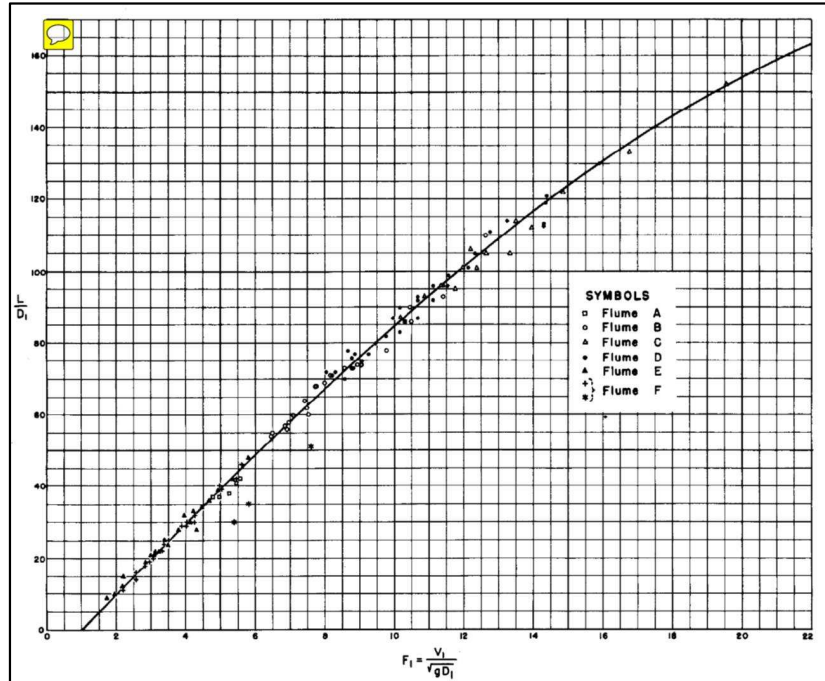
r_4 : adjustment for abutment and pier conditions

$$r_4 = 1 - 2 \cdot (N \cdot K_P + K_A) \cdot h / (N \cdot b)$$

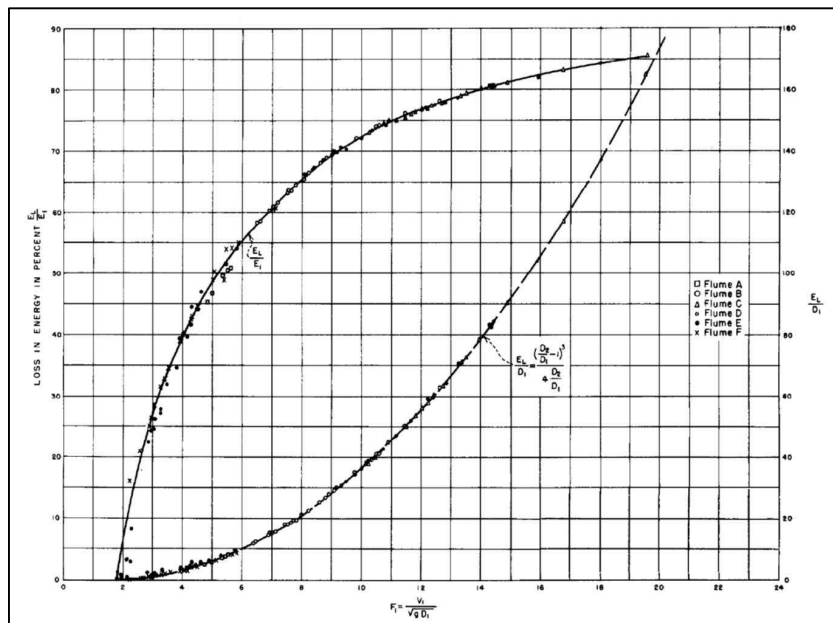
Annex 3

Stilling Basins: Design Charts

Source: Engineering Monograph N°25 – U.S. Bureau of Reclamation



Theoretical Length of the Hydraulic Jump



Loss of Energy in the Hydraulic Jump

Annex 4

STEFLOW User's Manual (abstract)



Laboratoire d'Hydraulique de France-

CGFRHYG

ENEL

Direzione Studi e Ricerche

CENTRO DI RICERCA IDRAULICA
E STRUTTURALE

STEFLO

*

STEADY FLOW COMPUTATION IN RIVERS

*

USER'S MANUAL

*

COPA ORIGINALE MARZO 83
CON L'AGGIUNTA DELLE
INDICAZIONI DEI FORMATI
DEI FILES "DATEAL" E "SINGUL"

March 1989

CONTENTS



| | |
|--|------------|
| <i>Chapter 1 - INTRODUCTION</i> | <i>1.1</i> |
| <i>Chapter2 -- THEORIES AND METHOD DESCRIPTION</i> | <i>2.1</i> |
| <i>2.1 Program operation.....</i> | <i>2.2</i> |
| <i>2.2 Gradually varied flow.....</i> | <i>2.2</i> |
| <i>2.3 Critical, normal and sequent depth computation.....</i> | <i>2.3</i> |
| <i>2.4 Interpolation of the cross-sections.....</i> | <i>2.5</i> |
| <i>2.5 Singularities.....</i> | <i>2.5</i> |
| <i>2.5.1 Sill.....</i> | <i>2.6</i> |
| <i>2.5.2 Orifice.....</i> | <i>2.7</i> |
| <i>2.5.3 Combination of sills and gates</i> | <i>2.8</i> |
| <i>2.5.4 Contraction, expansion, steps</i> | <i>2.8</i> |
| <i>2.5.5 Constriction</i> | <i>2.8</i> |
| <i>2.5.6 Culvert</i> | <i>2.9</i> |

Chapter 3 - Files 3.1

3.1 *Input files*..... 3.1

3.2 *Output files*..... 3.3

3.2.1 *STAMPA*..... 3.3

3.2.2 *RISUL*..... 3.3

Chapter 4 - SINGUL FILES 4.1

Chapter 5 - DATCAL FILES 5.1

Chapter 6 - ERROR MESSAGES 6.1

APPENDIX - EXAMPLES

STEFLO is a computer program for the computation of permanent flow profile in non-branched river models.

The computation of both supercritical and subcritical flow regimes are allowed. Hydraulic jumps may occur and are located.

Man made structures or natural singularities may disturb the flow.

The program uses pre-processor TABSEZ and post-processor DIAGRA1.

The language used in the source code is FORTRAN 77.

This user manual contains all the informations necessary for the user to run the program STEFLO. Informations necessary for the maintenance of the code are in the maintenance manual. Especially the flow charts and the description of the particular features in each Fortran subroutine.

REFERENCES

BAKHMETEFF. *'Hydraulics of open channels'* McGrawHil, 1932.

BLANCHET. *'Sur le problème des remous et des pertes de charge produits par les singularités dans les canaux et rivières'*- La Houille Blanche, N°1, Nov.1945.

DE GERLONI, MOLINARO, PIAZZARDI, VEZZULI. *'Modello matematico di un ramo del delta del Po Utilizzo in parallelo con un modello Pisico'*. Congresso di Idraulica e Costruzioni Idrauliche, Pavia, 1984

HENDERSON. *'Open Channel Flow'*. McMillan, 1966.

KISELEV. *'Formulaires des calculs hydrauliques'*. Gosenergoizat, Moscow.

MOLINAS, YANG. *'Generalized Water Surface Profile Computations'*. Journal of Hydraulic Eng., ASCE, Vol.III, N°3, 1985.

VEN TE CHOW. *'Open Channel Hydraulics'*. McGraw Hill, 1959-1981.

Chapter 2

**THEORIES AND METHOD
DESCRIPTION**

2.1 PROGRAM OPERATION

The central algorithm used to compute the flow-line in the network is based on the elementary principles stated by MOLINAS and YANG.

The program operation may be described by the following breakdown :

Preparation of the computation

- lecture of the general data;
- lecture of the tables describing the cross-sections (from program TABSEZ);
- lecture of the file containing the description of the singularities;
- construction of the computational grid according to the computational space interval demand;
- lecture of the flow conditions (discharge, limit conditions).

Central algorithm:

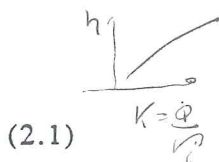
- computation of the critical depth and the normal depth for all the computational points;
- detection of a-priori control sections (where a subcritical normal depth line crosses the critical depth line);
- loop on the different cross sections to compute the flow line down to the next control section.

Edition of the results on a printer file and a result file for post-processing.

2.2 GRADUALLY VARIED FLOW

Balance of mass and of momentum in steady flow lead to the following equation for flow profile :

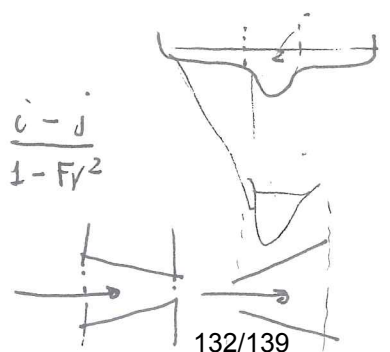
$$\frac{dh}{dx} = \frac{\beta \frac{Q^2}{gA^3} \frac{\partial A}{\partial x} + S_0 - S_f - \left(2\beta \frac{Q}{A} - U_L \right) \frac{q}{gA} - \frac{Q^2}{gA^2} \frac{\partial \beta}{\partial x}}{1 - Fr^2}$$



$PQV = \frac{\rho Q^2}{A} \left(\frac{1}{gA^2} \right)$

$\frac{\partial Q}{\partial t} + \frac{\partial}{\partial x} \left(\frac{Q^2}{A} \right) \frac{1}{gA}$

$\frac{dh}{dx} = \frac{i - j}{1 - Fr^2}$



h water depth
 x longitudinal abscissa
 Q discharge
 β momentum correction factor = $\beta(x,h)$
 A wetted cross-section area = $A(x,h)$
 g gravity acceleration
 S_0 bottom slope = $-dz_f/dx$
 z_f bottom elevation
 S_f friction slope
 Fr Froude number
 q lateral inflow = dQ/dx
 U_L velocity component along x of lateral inflow (neglected by the program)

The Froude number is defined as :

$$Fr^2 = \frac{\beta BQ^2}{gA^3} - \frac{Q^2}{gA^2} \frac{\partial \beta}{\partial h} \quad (2.2)$$

It is of current use in modelling applications to calculate S_f by a uniform flow formula :

$$S_f = Q^2/K^2$$

where :

$$K = K(h,x) = \text{conveyance}$$

Equation (2.1) is an ordinary differential equation of the first order. It is integrated by using either a fourth order Runge-Kutta method or a parabola approximation on successive space intervals Δx .

2.3 CRITICAL, NORMAL, AND SEQUENT DEPTH COMPUTATION

The critical depth is defined as h_c such that $Fr^2 = 1$.

The normal depth is h_n such that the friction slope is equal to the bottom slope. In a practical manner, the program searches for the water depth h_n for which :

$$K(x, h_n) = \frac{Q(x)}{\sqrt{S_0(x)}} \quad (2.3)$$

In the case of an adverse slope, $S_0 < 0$, the normal depth cannot be defined and the program adopts a very large value for h_n .

Let us consider U and D the two cross-sections immediately upstream and downstream a hydraulic jump. U and D are chosen close enough to neglect friction losses and motion forces due to the bed slope. However they are far enough to consider that the velocities V_U and V_D are constant and parallel.

Between sections U and D, the change of momentum discharge is equal to the arithmetic difference of the pressure forces on the cross-sections U and D :

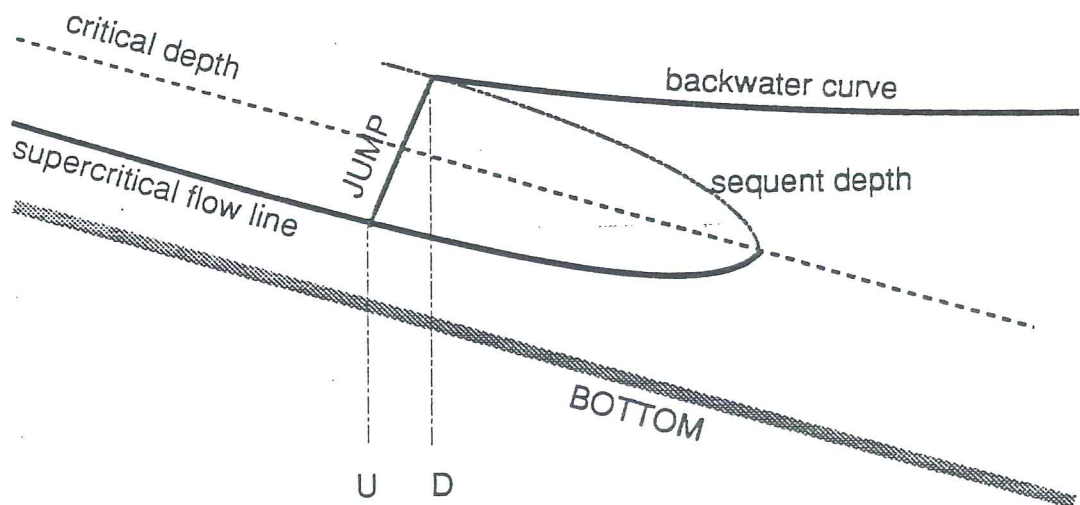
$$\rho \beta_D A_D V_D^2 - \rho \beta_U A_U V_U^2 = \rho g (I_U - I_D) \tag{2.4}$$

where :

$$I = \int_0^h (h - \eta) B(\eta) d(\eta) \tag{2.5}$$

$B(\eta)$: width of the cross-section for depth η

An hydraulic jump will stop a supercritical flow line when the sequent depth line will become lower to the backwater depth line coming from the next downstream cross section (see figure).



Note that the flow line is computed in a discrete manner on the computational grid. As a consequence, neither the control-sections, nor the hydraulic jumps are located more precisely between two successive computational points. In the case when more precision is desired, the user must ask for smaller space intervals.

The length of the jump is neglected. We remember here and empirical estimation of the length of the jump : $L \cong 6.(h_D - h_U)$ and the value of the head loss through a jump in a rectangular channel :

$$\Delta H = \frac{(h_D - h_U)^3}{4 h_U h_D} \quad (2.6)$$

2.4. INTERPOLATION OF THE CROSS-SECTIONS

The river is described by the cross-sections that have been treated by the program TABSEZ.

RISTAB file, which is the output file from TABSEZ, contains the bottom line and for each cross section tables giving geometric data (area, surface, width...) or hydraulic data (conveyance, Boussinesq coefficient...) as functions of the water depth.

For abscissa x and for water depth h , the values of those geometrical or hydraulical data are interpolated from the tables and the two nearest cross sections on each side of abscissa x .

Three options are available for that interpolation:

- according to the depth,
- according to the elevation,
- according to a weighted depth taking into account the range for h disponible for each cross-section (see the description of the DATCAL file).

2.5 SINGULARITIES

We call singularity a section of the river where the gradually flow equation will not be used. It may be a natural cross-section of the river but more often it will be an artificial structure. The singularities are defined in file SINGUL. The effect of a singularity is expressed in term of an head-loss between the upstream point and the downstream point of a singular reach.

In supercritical flow conditions, the singularity may define a control section and force a backwater curve.

We describe hereafter the different formulations that we use for each structure.

2.5.1 SILL

A sill is a crest across the flow.

A sill is described by a polyline and treated by the program as the sum of elementary horizontal and tilted sills.

① Horizontal elementary broad crested sill

If we call :

- Q_i the discharge through the elementary sill
- B_i the crest width of the elementary sill
- H_U the upstream head (above the crest)
- h_D the downstream water depth (above the crest)

The elementary discharge Q_i will be :

i) In free flowing conditions

$$Q_i = m B_i \sqrt{2g} H_U^{3/2} \quad (2.7)$$

ii) In flooded flow conditions

$$Q_i = \varphi B_i \sqrt{2g} h_D \sqrt{H_U - h_D} \quad (2.8)$$

with :

$$m = \frac{2\varphi^3 (2\varphi^2 - 1)}{[1 + 2\varphi^2 (2\varphi^2 - 1)]^{3/2}} \quad (2.9)$$

φ is a discharge coefficient specified by the user of the program.

Flooded flow occurs if :

$$H_D > \frac{2\varphi^2}{1 + 2\varphi^2 (2\varphi^2 - 1)} H_U \quad (2.10)$$

Free flowing conditions occurs if :

$$H_D < \frac{2\phi^2}{1 + 2\phi(2\phi - 1)} H_U \quad (2.11)$$

There is no discharge if $H_U < z_s$

② Tilted elementary sill

A formula is obtained for Q_i on a tilted sill by integration of the horizontal expressions on the whole width of the sill (flooded part+free flowing part).

The sum of the elementary discharges on the different elementary sill furnishes a relation between the total discharge, the upstream water depth, and the downstream water depth.

2.5.2 ORIFICE

The discharge through a rectangular orifice is expressed in the following form :

$$Q = \sigma \mu b a \sqrt{2gH_U} \quad (2.12)$$

where :

H_U the upstream head

a the heigh of the orifice

b the width of the orifice

μ a discharge coefficient

σ a correction coefficient in the case of flooded conditions (taken from Kiselev-
'Formulaire des calculs hydrauliques')

The orifice may also works in sill mode.

An orifice is defined by the user as a polygon which will be treated by the program as an equivalent rectangular orifice.

2.5.3 COMBINATION OF SILLS AND GATES

In order to describe complex structures, compound singularities may be introduced between two computational points.

In that case, the total discharge is the sum of the discharge that can be computed over each sill or gate with the current upstream and downstream levels.

2.5.4 CONTRACTION, EXPANSION, STEPS

There is a rapid change of the geometry and the user of the program does not want to use the equations of the gradually varied flow.

The upstream section U and the downstream section D must be described in RISTAB.

The local head-loss is represented by a Borda type formula.

$$h_U + z_{fv} + \frac{V_U^2}{2g} = h_D + z_{fD} + \frac{\eta}{2g} (V_U - V_D)^2 \quad (2.13)$$

2.5.5 CONSTRICTION

The current section of the river is locally constricted (bridge, piers, mines, natural constriction...).

There is no head-loss between the upstream section U and the constricted section C.

A Borda type formula expresses the head-loss between the constricted section C and the downstream section D :

$$\Delta H_{C \rightarrow D} = \eta \frac{(V_C - V_D)^2}{2g} \quad (2.14)$$

2.5.6 CULVERT

Pressure flow occurs between sections U and D.

The total head-loss through the culvert is the sum of a linear friction loss (the Manning formulation is used) and a Borda head-loss at the downstream end :

$$\Delta H = \frac{L Q^2}{K^2} + \eta \frac{(V_D - V_C)^2}{2g}$$

where :

- V_C = Q/A = the flow velocity inside the culvert
- A the cross-section area of the culvert
- K conveyance of the culvert
- L length of the culvert
- η the Borda head-loss coefficient